UNIVERSITAT POLITÈCNICA DE CATALUNYA

CONTRIBUTION TO THE IMPROVEMENT OF INTEGRAL EQUATION METHODS FOR PENETRABLE SCATTERERS

Tesi Doctoral

presentada al Departament de Teoria del Senyal i Comunicacions

per a l'obtenció del títol de Doctor Enginyer de Telecomunicació

a càrrec de
Eduard Úbeda Farré

Director de tesi: dr. Juan Manuel Rius i Casals
Barcelona, TSC-UPC, novembre 2000

Chapter 7 RESULTS FOR 3D PEC BODIES

7.1 VERIFICATION OF THE THEORETICAL CONCLUSIONS IN ACCORDANCE WITH THE PLANAR APPROACH

In Chapter 6, there have been presented the conditions to yield the consistent electromagnetic solution over a polyhedron. In regard with the patch-based operators, the conclusions are: (i) PeC-EFIE(*RWG,RWG*) is as well-defined as the condition number low is, (ii) PeC-MFIE(*RWG,unxRWG*) has a low and stable condition number and the electromagnetic requirement is well-accomplished, (iii) PeC-MFIE(*unxRWG,RWG*) has a low and a stable condition number and the electromagnetic requirement is as well-accomplished as $\hat{n}$ uniform is.

Another issue of discussion, which has been out of the scope of the theoretical discussion in Chapter 6, is if the solution of the polyhedron approaches the real solution in the body before the discretization. That is, one has to assess if the polyhedron with a low-order current expansion -*RWG* and *unxRWG*- is a good model for the electromagnetic behaviour of the physical body.

In general terms, as mentioned in Chapter 2, there are two important sources of error when solving the mathematical problem. The expansion of the current and the expansion of the surface interface where the boundary conditions are posed. One must not ever forget that a constraint of the polyhedron is the planar modelling of the geometry. Therefore, in order to check the theoretical conclusions of Chapter 6, it is reasonable to choose objects with no curvature, which correspond to physical polyhedrons. One ensures so that the error is only due to the insufficient low-order expansion of the current. This study is included in 7.4.

In curved objects, the verification of the theoretical study up from the results is not straightforward since the effect of the wrong modelling of the surface also takes part. Of course, the dissimilarity between the results due to the different operators must include the study of the polyhedron properties developed in Chapter 6 but the curvature effects condition the results as well. In any case, some results are commented for spheres, cones and cylinders in section 7.5.

In section 7.6, some corrections to improve the performance of the operators are given. It is provided a heuristic procedure to diminish the inherent error in PeC-MFIE(*unxRWG,RWG*). It is also supplied a way to decrease the effect of the curvature on the operators for small frequencies.

7.2 NUMERICAL COMPUTATION OF THE OPERATORS

In the theoretical reasoning of section 6.5, it has been assumed that the computation of the source and field integrals was carried out accurately for both PeC-EFIE and PeC-MFIE. The PeC-MFIE integrand presents a $1/R^3$-dependence in its highest order term; the PeC-EFIE operator presents a smoother $1/R$-dependence at most. As shown in the first half of this Dissertation Thesis, this has been so critical in the development of the BoR operators that the PeC-MFIE could not be in practice carried out beyond a certain bound. For the 3D-operators, being the patch much more reduced and always restricted to a small portion of the wavelength, this accuracy requirement for the PeC-MFIE must be better managed.

The high-order terms of the PeC-MFIE operator are especially critical for those impedance terms linked to steep transitions of the surface curvature -cubes, cylinders or cones-. In Chapter 6, along the description of the PeC-MFIE operators, it has been reasoned in detail that the integration of these high-order terms tend to zero over smooth-varying surfaces. So as to achieve the maximum accuracy, the high-order terms have been computed analytically in any case.

For the operators PeC-EFIE(*RWG,RWG*) and PeC-MFIE(*unxRWG,RWG*), where it is undertaken firstly the source integration, the low-order source terms and the field integrals have been computed preferably with four gaussian points. The self-terms are obtained with four testing points. Moreover, in the PeC-MFIE(*RWG,unxRWG*), which tackles firstly the field-integration, the low-order field terms are computed with four gaussian points -it is assumed so by the default-. The self-term, which corresponds to the integration of the singularity, is obtained with four testing points too.

7.3 CONDITIONING OF THE MATRICES

In all the examples tested, the condition number is lower for PeC-MFIE(*RWG,unxRWG*) and PeC-MFIE(*unxRWG,RWG*) than for the PeC-EFIE(*RWG,RWG*). Furthermore, the PeC-EFIE(*RWG,RWG*) grows together with the degree of meshing; on the other hand, the PeC-MFIE(*RWG,unxRWG*) keeps a low and stable condition number when yielding the discretization finer. All this confirms the theoretical reasoning in the section 6.5.

In accordance with the computer capabilities, which do not allow the computation of condition numbers of too big matrices, some low-frequency results are shown in Table 7.1 and Table 7.2 to confirm this, respectively for a cube and a sphere.

N. of triangles	Cond. Number - PeC-EFIE(*RWG,RWG*)	Cond. Number - PeC-MFIE(*RWG,unxRWG*)
48	164	9
192	611	11
300	871	11
432	1235	11
588	1700	11
768	2446	13

Table 7.1 Condition number of a cube with side of 0.1λ

N. of triangles	Cond. Number - PeC-EFIE(*RWG,RWG*)	Cond. Number - PeC-MFIE(*RWG,unxRWG*)
48	84	6
120	299	7
360	1984	14
440	2860	17
528	4001	20
624	5458	13
728	7284	26

Table 7.2 Condition number of a sphere with radius of 0.1λ

In view of these tables, the condition number for the PeC-EFIE(*RWG,RWG*) gets to be even two orders of magnitude higher than for the PeC-MFIE(*RWG,unxRWG*), which is very stable in any case. For electrically bigger bodies, although one cannot assess it directly through the tables -the required amount of memory to compute the condition number is too big-, one can accordingly infer that the condition number can grow much. Indeed, it is well-known that the inverting iterative algorithms demand for the PeC-EFIE(*RWG,RWG*) gradually more and more iterations as the dimensions of the object and the degree of discretization grow.

The condition number of PeC-MFIE(*unxRWG,RWG*) has not been presented in the tables above. Anyway, since the PeC-MFIE(*unxRWG,RWG*) matrix is very similar in numerical terms to the matrix resulting from PeC-MFIE(*RWG,unxRWG*) -the impedance terms corresponding to the Cauchy principal value are transposed-[21], the condition numbers of both are alike.

It must be noted that the very advantageous condition numbers of the PeC-MFIE operators rely very much on the accuracy when computing the impedance elements. It is especially important to compute precisely the integration of the singularity, which corresponds to the PeC-MFIE self-terms. As a matter of fact, as shown in Chapter 6, since it is required a power-two field-integration, it can be undertaken exactly. Indeed, in the above-shown tables, four field-integrating points have been imposed, which must be enough.

Some examples have been found where an inaccurate computation of the singularity in the PeC-MFIE has led to high condition numbers. For example, the sphere of radius 0.1λ analysed with the PeC-MFIE(*unxRWG,RWG*) with 48 edges and one testing point has led to condition numbers of about 1e16. Similarly, the cube of side 0.1λ undertaken by the PeC-MFIE(*RWG,unxRWG*) with 72 edges and one testing point has led to condition numbers over 200. Particularly, for the particular case of 6 source-integrating points, the condition number yields 3104. In this case, if the singularity is computed with four testing points and the Principal Cauchy value remains still with one field-integrating point, the condition number declines to 8. In consequence, henceforth, the PeC-MFIE computation will be always assumed with the singularity computed exactly. The change on the number of testing points will thus affect the computation of the Cauchy principal value.

Finally, it is interesting to point out how the condition number is more variable for PeC-MFIE(*RWG,unxRWG*) for the sphere than for the cube. This makes sense if we consider that a change of the discretization for the cube corresponds still to the same physical

[21] The condition number for a given matrix and its transposed is the same

polyhedron. On the other hand, every change on the discretization of the sphere yields a different polyhedron.

7.4 PHYSICAL POLYHEDRONS

Some results are shown for simple polyhedrons such as a cube, a pyramid of square basis or an octahedron. It is the aim of this section to prove the predicted error in PeC-MFIE(*unxRWG,RWG*) when compared with PeC-MFIE(*RWG,unxRWG*). Note than on a physical polyhedron the dissimilarity between the results of both operators must come from the physical edges, since it is the only part of the body where the direction of the normal vectors at both sides is different. It is hence good to present low-frequency objects to assess the error -the influence of the physical edge is comparatively more important-.

In this section, it is also wanted to assess the goodness of PeC-EFIE(*RWG,RWG*) compared to PeC-MFIE(*RWG,unxRWG*). According to Table 7.1, the order of the condition number is 1e3, which does not seem to condition the robustness of the solution. Indeed, one expects that PeC-EFIE(*RWG,RWG*) results can also be taken as reference. It is actually widely assumed that the PeC-EFIE(*RWG,RWG*) results are robust for low-frequency objects; they are often taken as reference.

One must not ever forget that the chosen approach forces an expansion of the current of low-order. Therefore, the solutions for the current due to PeC-EFIE(*RWG,RWG*) and PeC-MFIE(*RWG,unxRWG*) correspond to the low-order part of the current with respectively normal or tangential continuity across the edge. This means that both solutions, even being robustly defined, are not to be coincident. A way to yield a comparatively higher-order expansion is to overdiscretize the body so that at a certain point one expects that the solutions due to both operators will be coincident. Indeed, augmenting the overdiscretization must yield a solution of increasingly higher order so that the whole unique solution of the physical polyhedron would be practically attained by means of both operators.

Four different examples of low-frequency conducting physical polyhedrons are presented right away. The bistatic RCS under an impinging axial wave for several increasingly fine discretizations is presented for each example and for each operator: PeC-EFIE(*RWG,RWG*), PeC-MFIE(*RWG,unxRWG*) and PeC-MFIE(*unxRWG,RWG*). Results are presented for the PeC-MFIE(*unxRWG,RWG*) with one or four testing points (nf=1 or nf=4) regarding the Cauchy principal contribution.

- **Pyramid**:

  Three different discretizations are employed to analyse the pyramid -see Fig. 7.1-: 4 segments per physical edge (128 triangles), 8 segments per physical edge (512 triangles) and 10 segments per physical edge (800 triangles). The corresponding RCS results are presented in Fig. 7.2, Fig. 7.3 and Fig. 7.4.

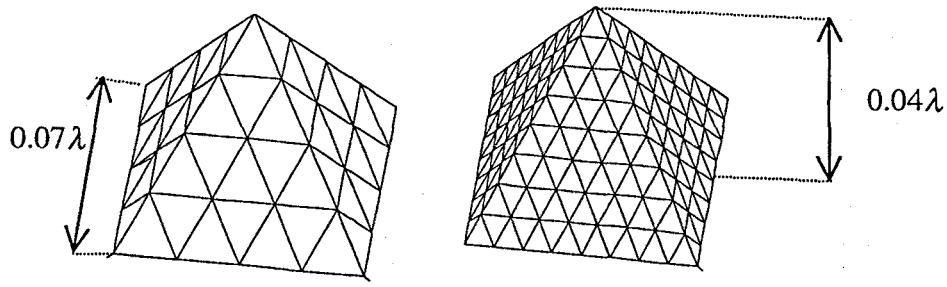

Fig. 7.1 Pyramid with 4 and 8 segments per physical edge

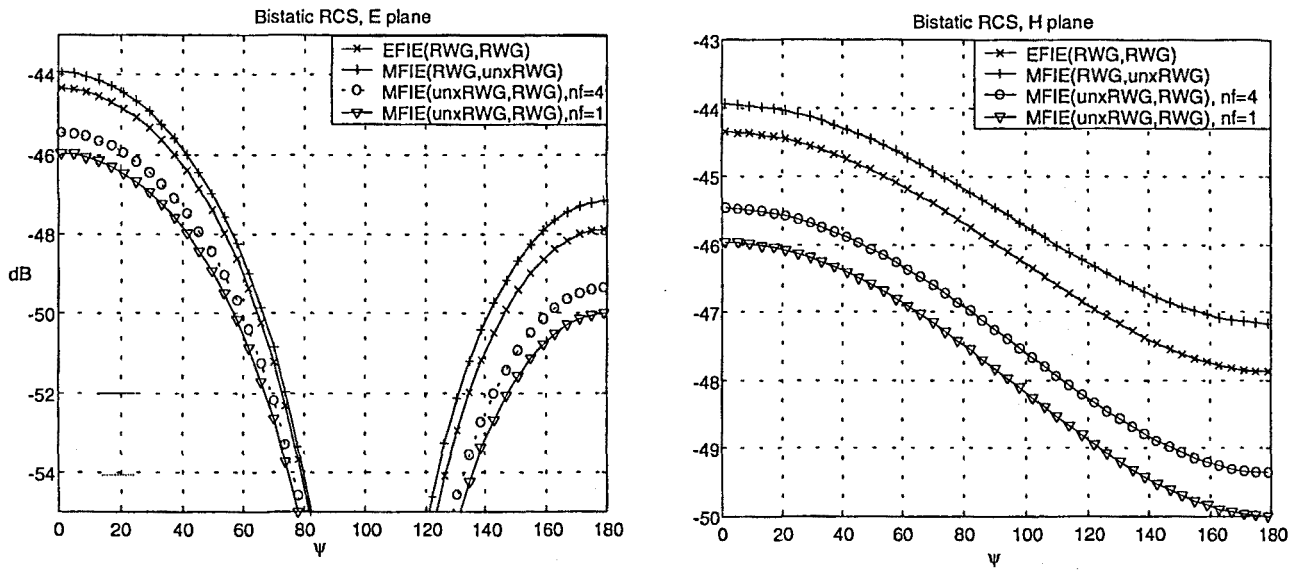

Fig. 7.2 RCS for the pyramid with 128 triangles

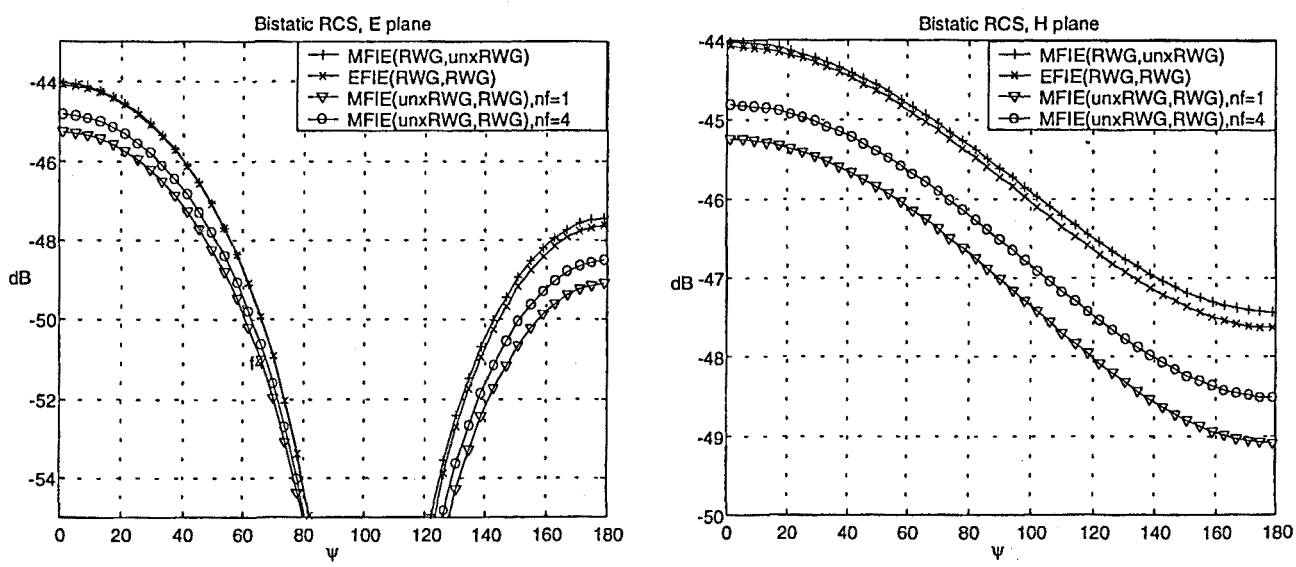

Fig. 7.3 RCS for the pyramid with 512 triangles

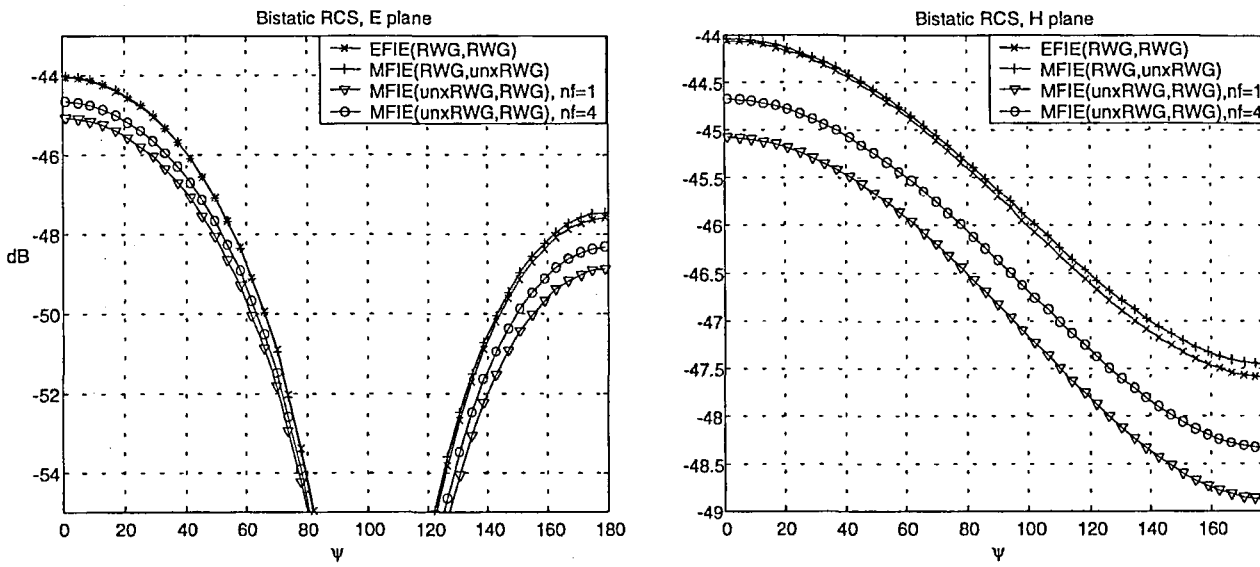

Fig. 7.4 RCS for the pyramid with 800 triangles

♦ Cubes

Four different discretizations are employed to analyse the cube: 2 segments per physical edge (48 triangles), 4 segments per physical edge (192 triangles), 5 segments per physical edge (300 triangles) and 8 segments per physical edge (768 triangles).

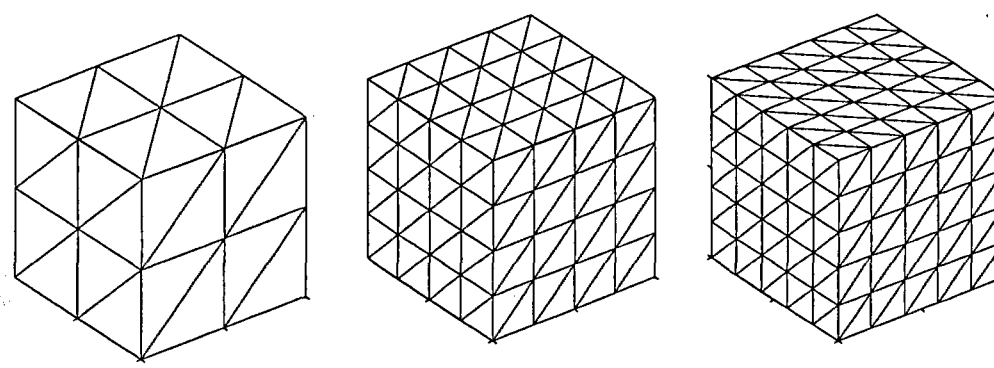

Fig. 7.5 Cube with 2, 4, 5 and 8 segments per physical edge

Firstly, in Fig. 7.6, Fig. 7.7, Fig. 7.8 and Fig. 7.9, results for increasingly finer meshings are shown for a cube with a side of 0.1λ.

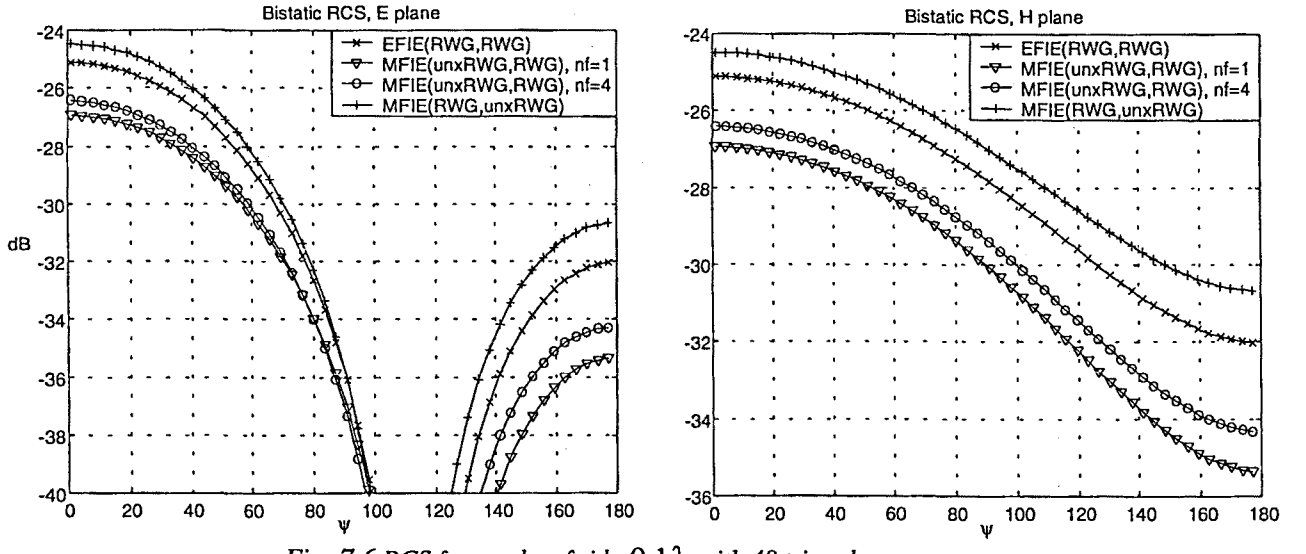

Fig. 7.6 RCS for a cube of side 0.1λ with 48 triangles

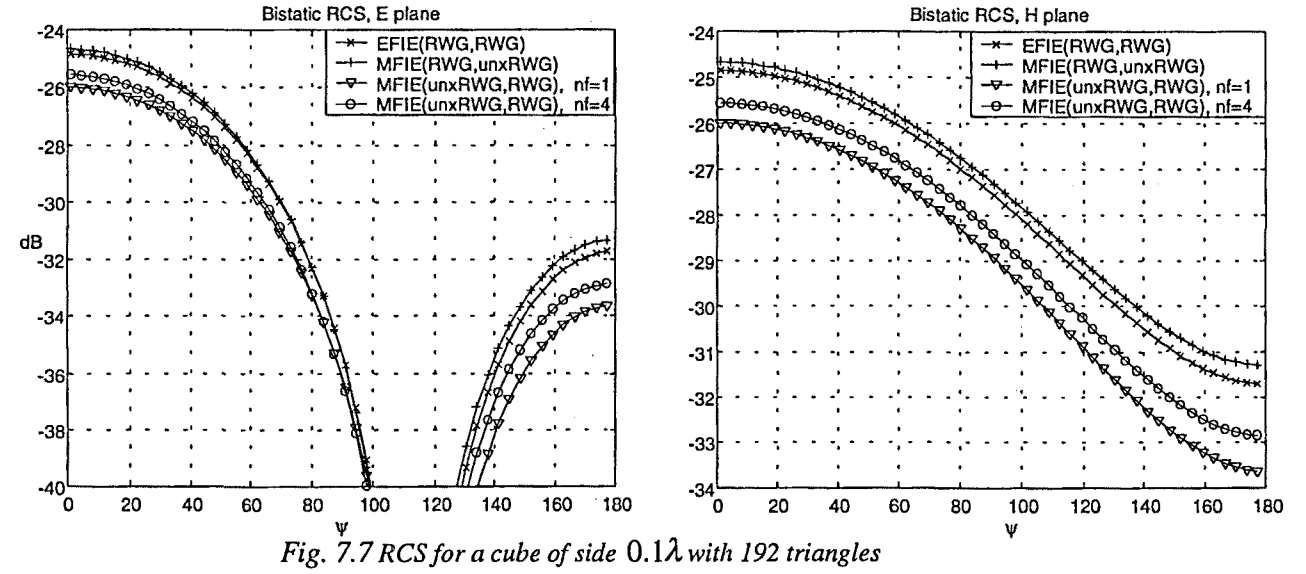

Fig. 7.7 RCS for a cube of side 0.1λ with 192 triangles

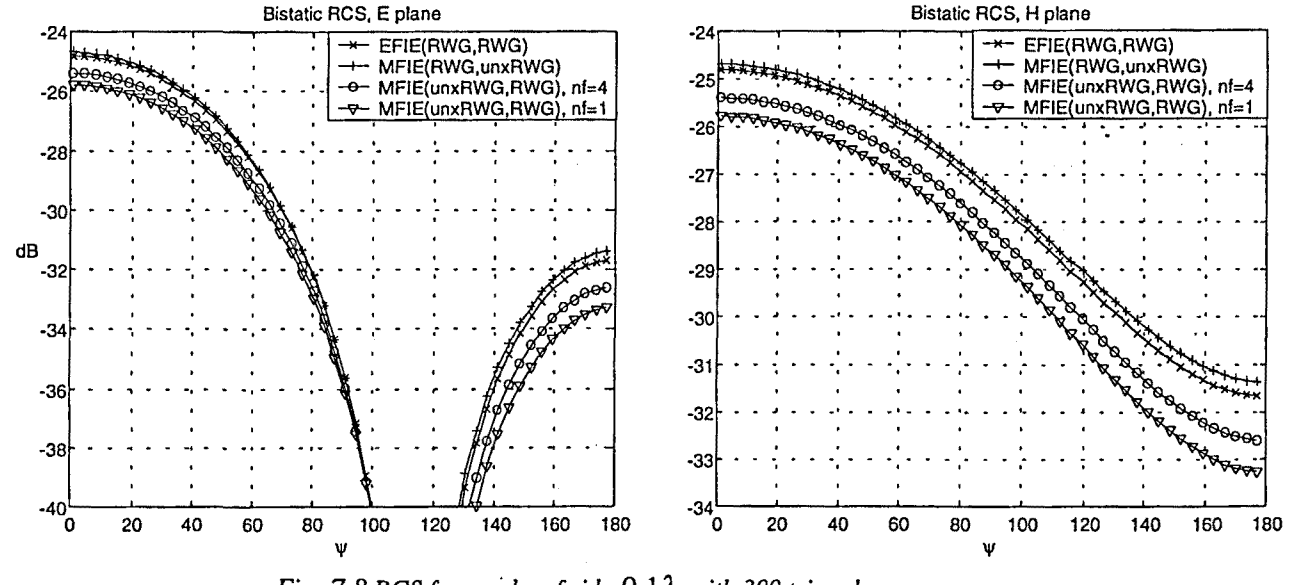

Fig. 7.8 RCS for a cube of side 0.1λ with 300 triangles

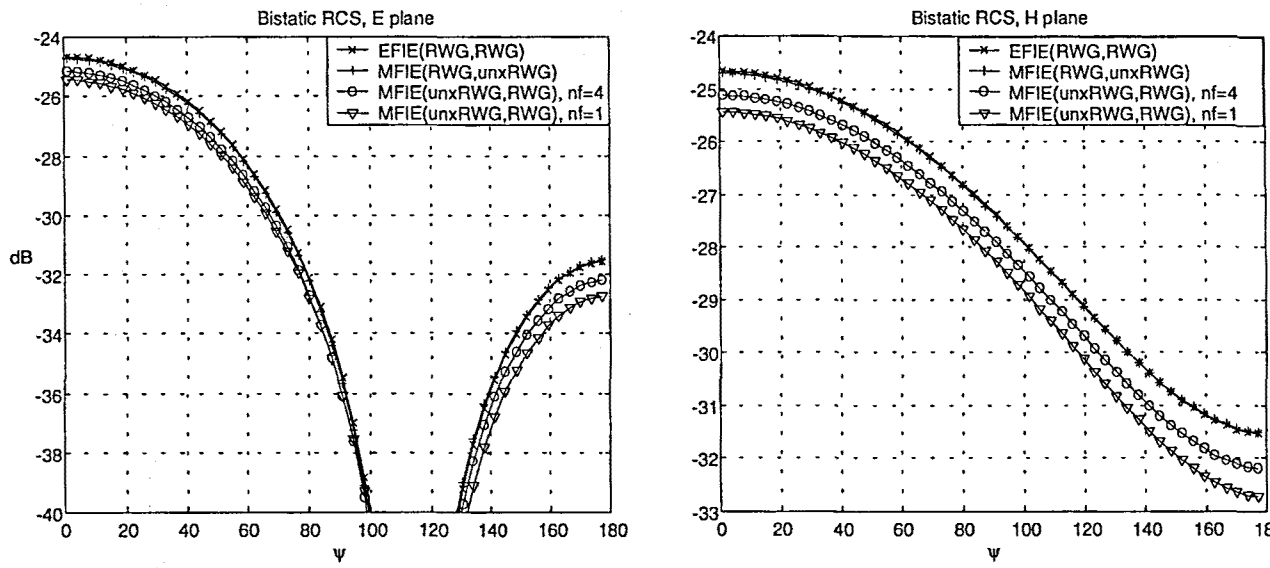

Fig. 7.9 RCS for a cube of side 0.1λ *with 768 triangles*

The evolution of the RCS is analogous for a bigger cube with side of 0.2λ, as it is shown in Fig. 7.10, Fig. 7.11, Fig. 7.12 and Fig. 7.13

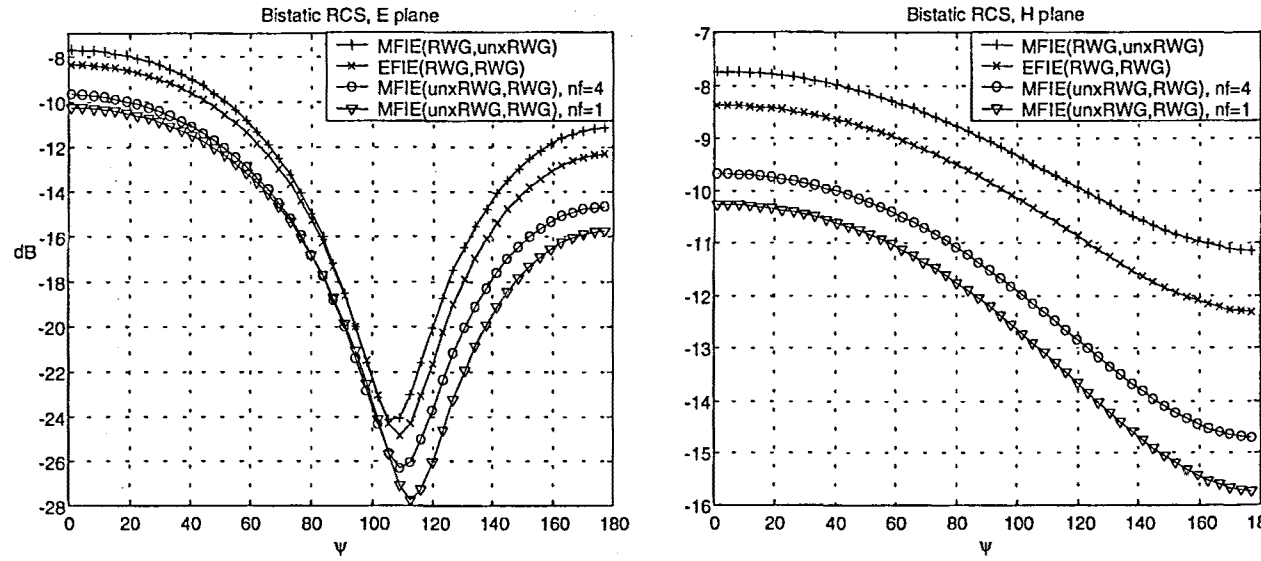

Fig. 7.10 RCS for a cube of side 0.2λ *with 48 triangles*

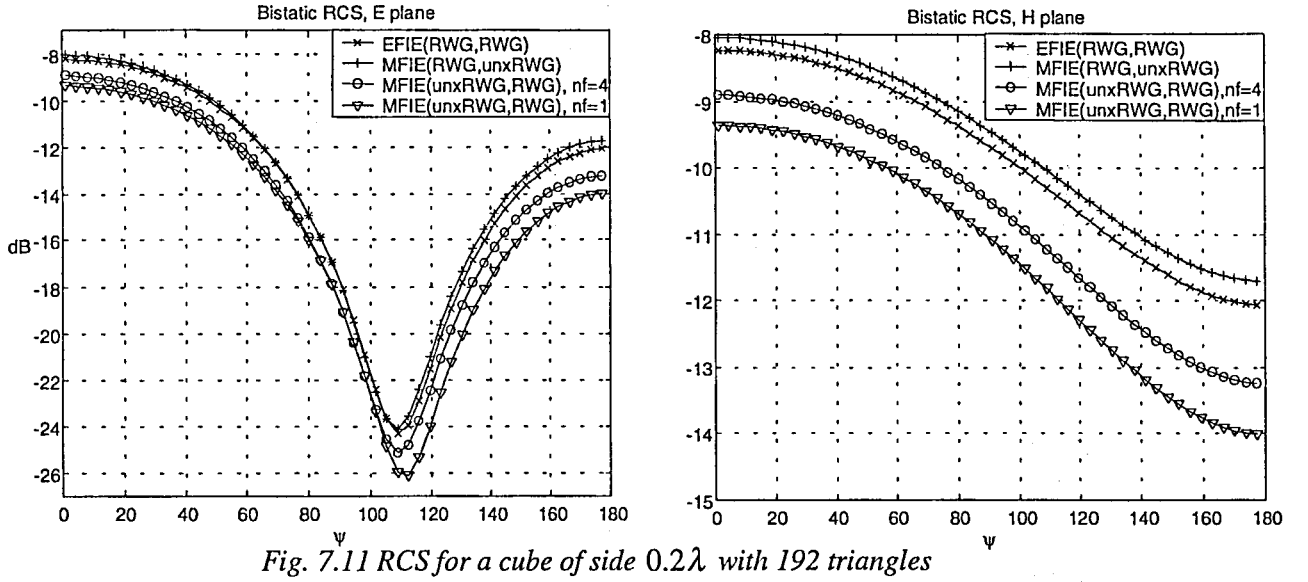

Fig. 7.11 RCS for a cube of side 0.2λ with 192 triangles

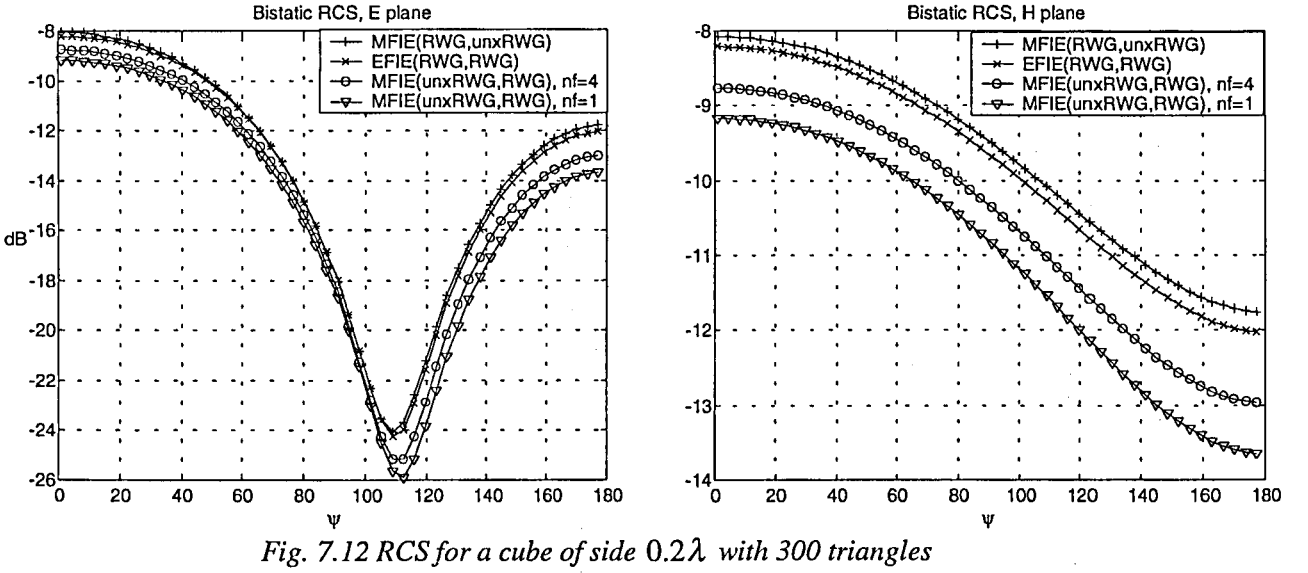

Fig. 7.12 RCS for a cube of side 0.2λ with 300 triangles

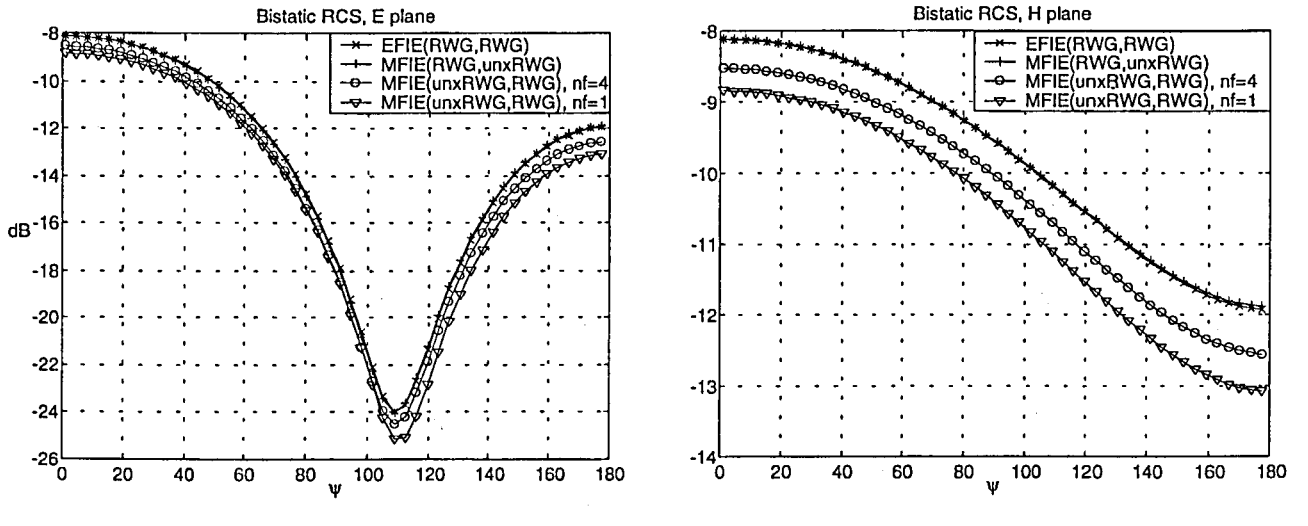

Fig. 7.13 RCS for a cube of side 0.2λ with 768 triangles

♦ Octahedron

Two different discretizations are employed to analyse the regular octahedron in Fig. 7.14: 3 segments per physical edge (72 triangles) and 7 segments per physical edge (392 triangles). The results are respectively presented in Fig. 7.15 and in Fig. 7.16.

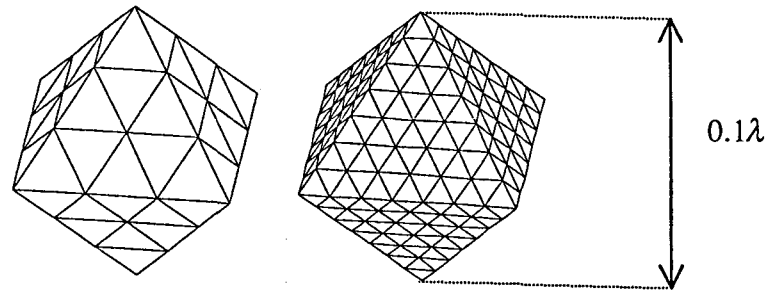

Fig. 7.14 Octahedrons with 3 and 7 segments per physical edge

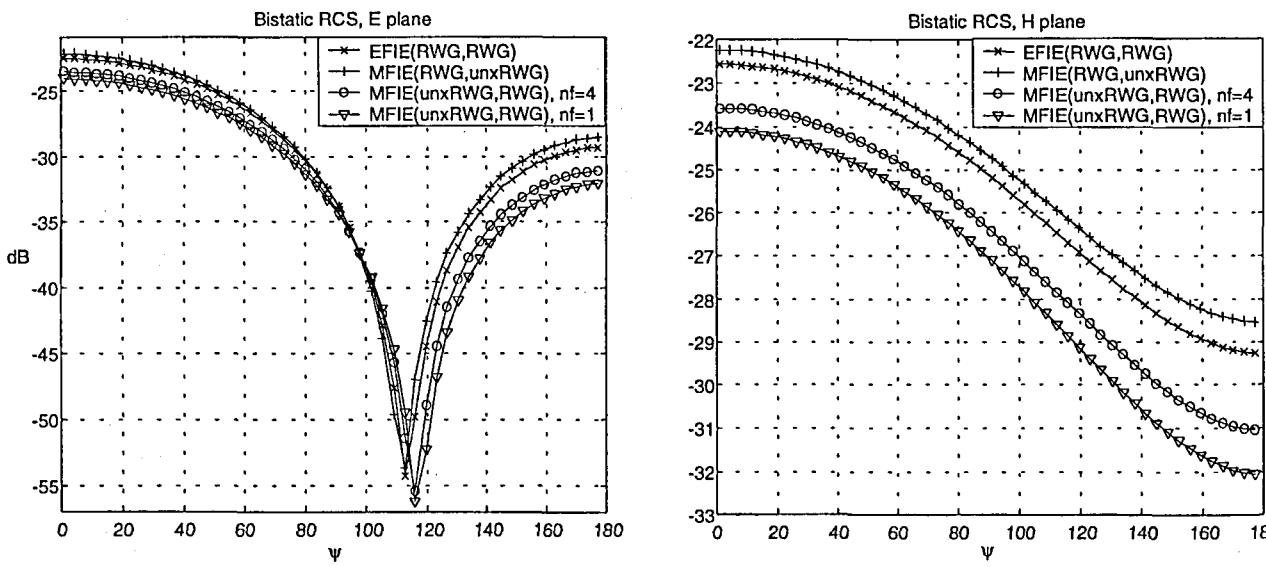

Fig. 7.15 RCS for the octahedron with 72 triangles

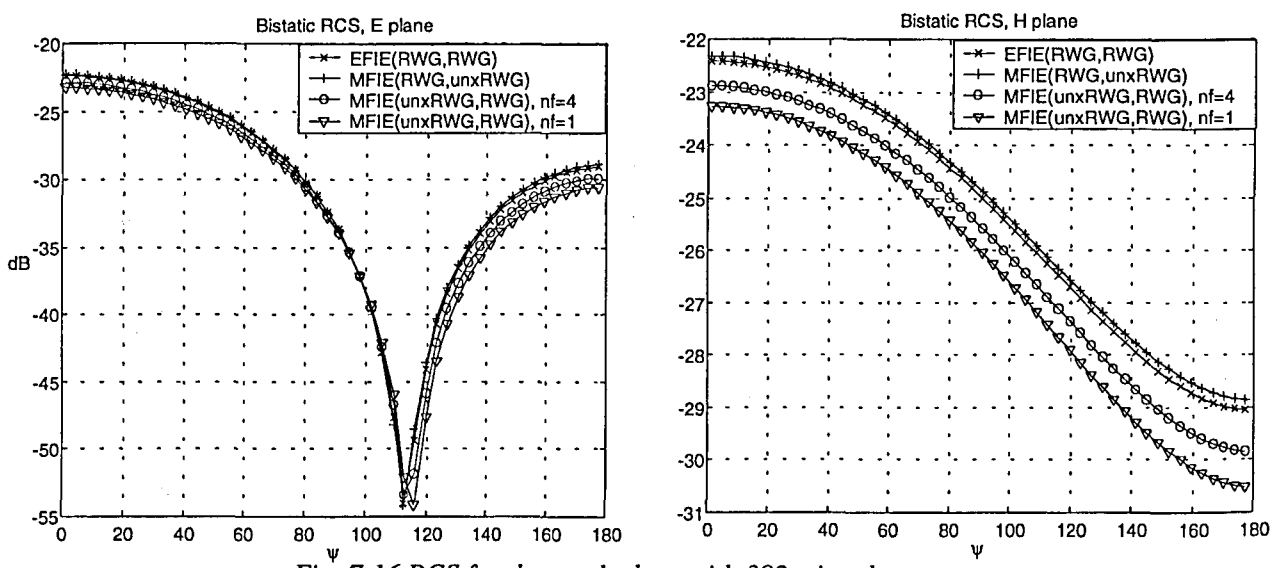

Fig. 7.16 RCS for the octahedron with 392 triangles

For all the different physical polyhedrons presented, the evolution of the results is alike. As the discretization becomes finer, PeC-MFIE(*RWG,unxRWG*) and PeC-EFIE(*RWG,RWG*) yield the same result. The PeC-MFIE(*unxRWG,RWG*) operator, on the other hand, lets a solution that remains at a certain distance of the other two in all the cases. This bias in the solution of PeC-MFIE(*unxRWG,RWG*) must be due to the inherent error of this operator, described in the last section of Chapter 6.

In Fig. 7.4, Fig. 7.9, Fig. 7.13 and Fig. 7.16, the PeC-MFIE(*RWG,unxRWG*) and PeC-EFIE(*RWG,RWG*) results merge. This confirms that for a high-order expansion of the current, which happens for these so overdiscretized polyhedrons, they both lead to the same solution. However, the PeC-MFIE(*unxRWG,RWG*) shows still an appreciable error even for this case of so fine meshing, which, according to the theory in Chapter 6, must be attributed to the effect of the physical edges, where the normal vectors at both sides are not parallel.

These results show also that the increase of testing points of the Principal value contribution in PeC-MFIE(*unxRWG,RWG*) -those contributions corresponding to different field and source triangles- approach the result to the reference results, PeC-EFIE(*RWG,RWG*) and PeC-MFIE(*RWG,unxRWG*); still an error remains though. For PeC-EFIE(*RWG,RWG*) and PeC-MFIE(*RWG,unxRWG*) four testing points for the terms linking different source and field triangles have been taken; in any case, as the discretization becomes finer, taking one or four points makes no difference for the results.

From the observation of the results one can see that for the physical polyhedrons the PeC-EFIE(*RWG,RWG*) results turn out more stable when increasing the degree of discretization than the PeC-MFIE(*RWG,unxRWG*) ones. This means that PeC-EFIE(*RWG,RWG*) reaches a better expansion of the field and current magnitudes for the same number of unknowns than PeC-MFIE(*RWG,unxRWG*). That is, an expansion of higher order is attained through PeC-EFIE(*RWG,RWG*).

7.5 CURVED OBJECTS

The results for curved objects when analysed by the PeC-operators, which assume a planar approach, must include the effect of the wrong modelling of the curved surface. This effect affects differently the PeC-operators.

In any case, the results must allow for the considerations inferred from the study of the conducting polyhedron, which have been proved in the previous section. One cannot expect now that the PeC-EFIE(*RWG,RWG*) and PeC-MFIE(*RWG,unxRWG*) results coincide so well as they did before when the discretization became very fine. Indeed, when yielding an increasingly fine discretization for a curved body, the corresponding physical polyhedron changes accordingly, which did not happen in the examples of section 7.4. Therefore, when analysing a curved body with different degrees of discretization, a relatively low-order solution is obtained for different physical polyhedrons -with different number of edges-. So, the results for PeC-MFIE(*RWG,unxRWG*) and PeC-EFIE(*RWG,RWG*) are not to be identical although they are expected to be similar. Of course, one could yield an increasingly similar performance of both operators by increasing the order of expansion of the current for a given polyhedron derived from the discretization of a curved body. According to the procedure developed in section 7.4, one

should discretize every facet in even more little triangles. Of course, this makes no sense since what it is really wanted to obtain is the results that approach best the performance of the original curved body not of the corresponding polyhedron of work.

Four different examples of low-frequency conducting physical curved bodies are presented below. The bistatic RCS under an impinging axial wave for several increasingly fine discretizations is presented for each example and for each operator: PeC-EFIE(*RWG,RWG*), PeC-MFIE(*RWG,unxRWG*) and PeC-MFIE(*unxRWG,RWG*). To assess the behaviour of the PeC-operators, one must resort to some reference results. For spheres, it is taken the Mie solution; for cones and cylinders, in view of their symmetry of revolution, it is used the PeC-EFIE BoR-operator presented in Chapter 3. All the operators employ now four points -it is assumed so by default- or six points in the numerical integration for the lower-order terms of the inner integral and for the outer integral.

- **Sphere**

  Four examples of electrically small spheres with radius of 0.05λ -Fig. 7.18, Fig. 7.19-, 0.1λ -Fig. 7.20, Fig. 7.21-, 0.2λ -Fig. 7.22 and Fig. 7.23- and 0.25λ -Fig. 7.24- are presented. Both meshes shown in Fig. 7.17 are used for the smallest spheres of radius 0.05λ and 0.1λ. The discretization with 32 triangles cannot be used for the bigger spheres -the edge size is over $\lambda/10$-, whereby the sphere with radius 0.2λ is meshed with 128 and 512 triangles and the sphere with radius 0.25λ, with 128 triangles.

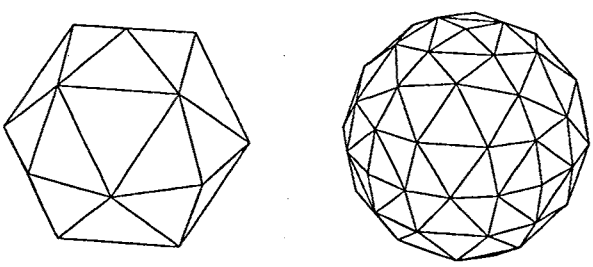

Fig. 7.17 Sphere discretized with 32 and 128 triangles

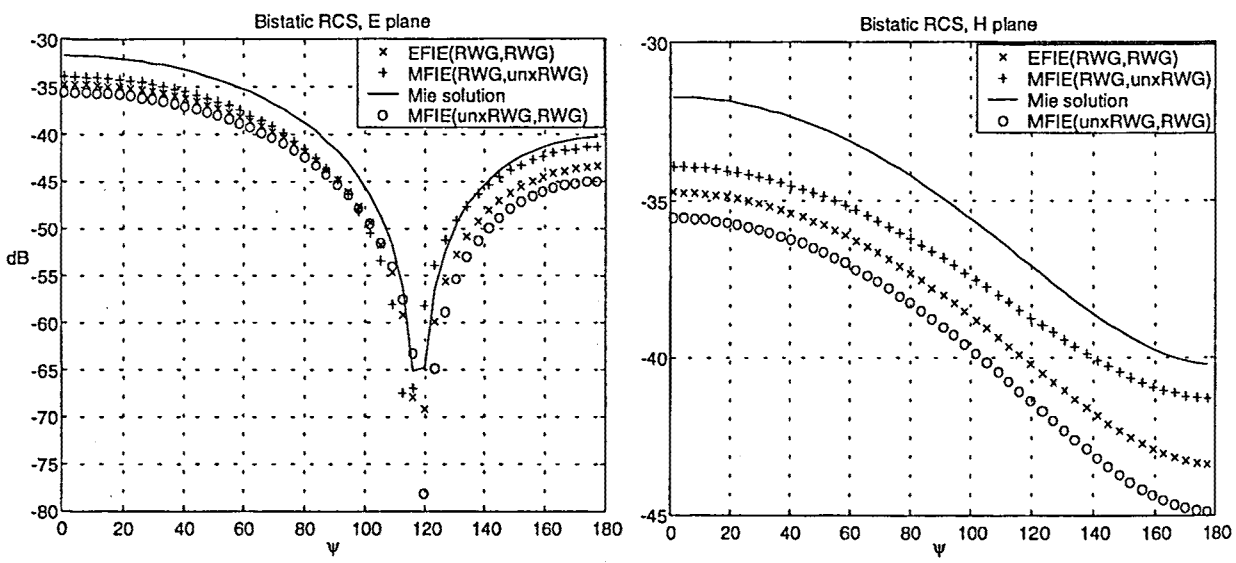

Fig. 7.18 Sphere of radius 0.05λ with 32 triangles

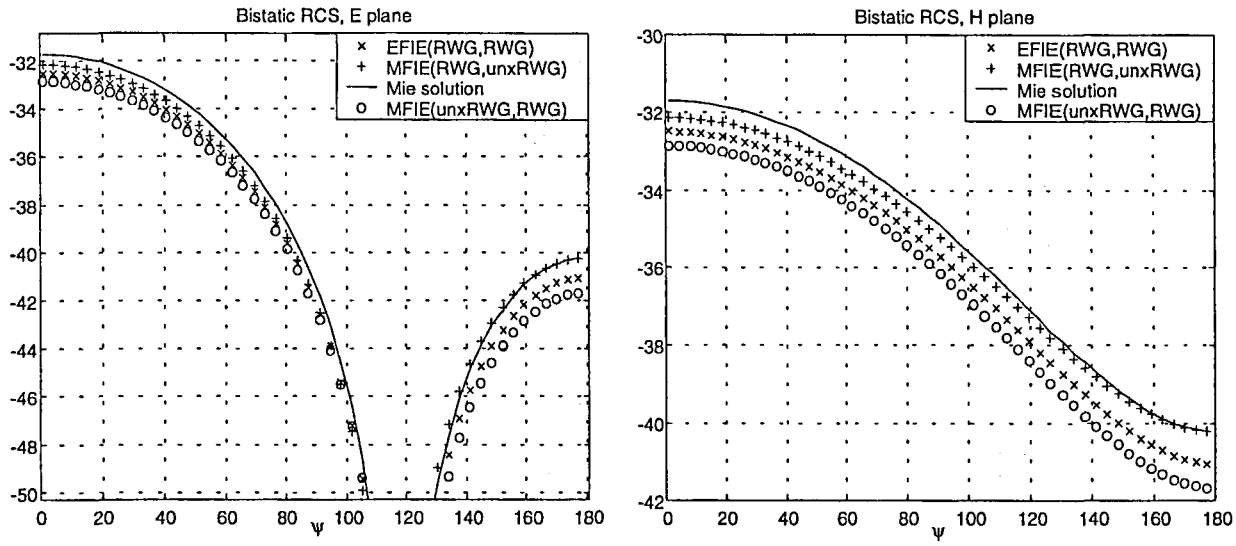

Fig. 7.19 Sphere of radius 0.05λ *with 128 triangles*

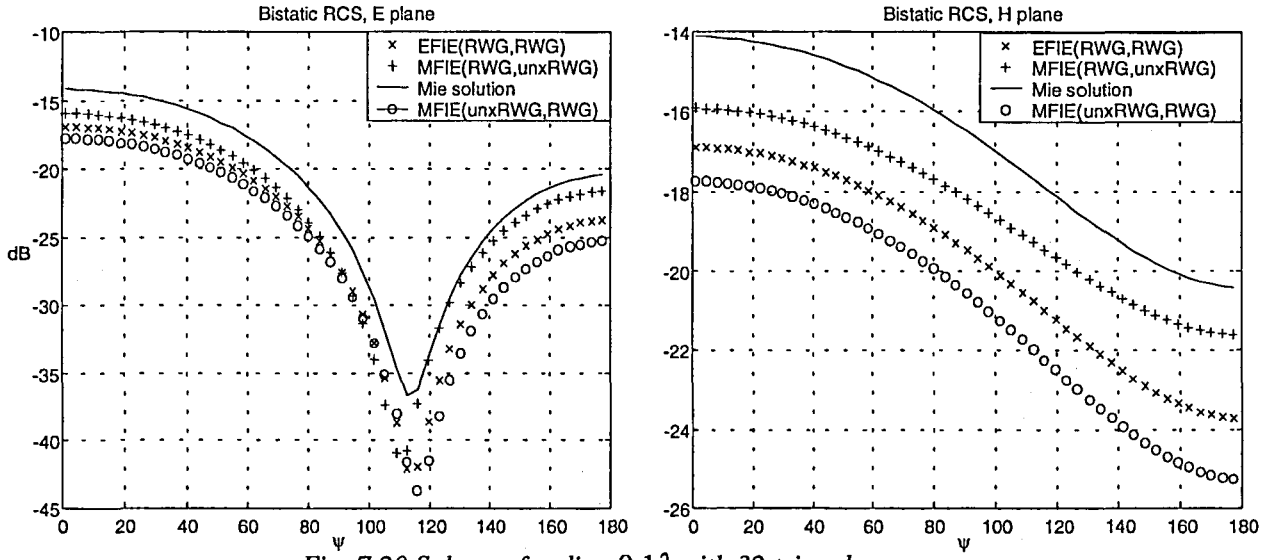

Fig. 7.20 Sphere of radius 0.1λ *with 32 triangles*

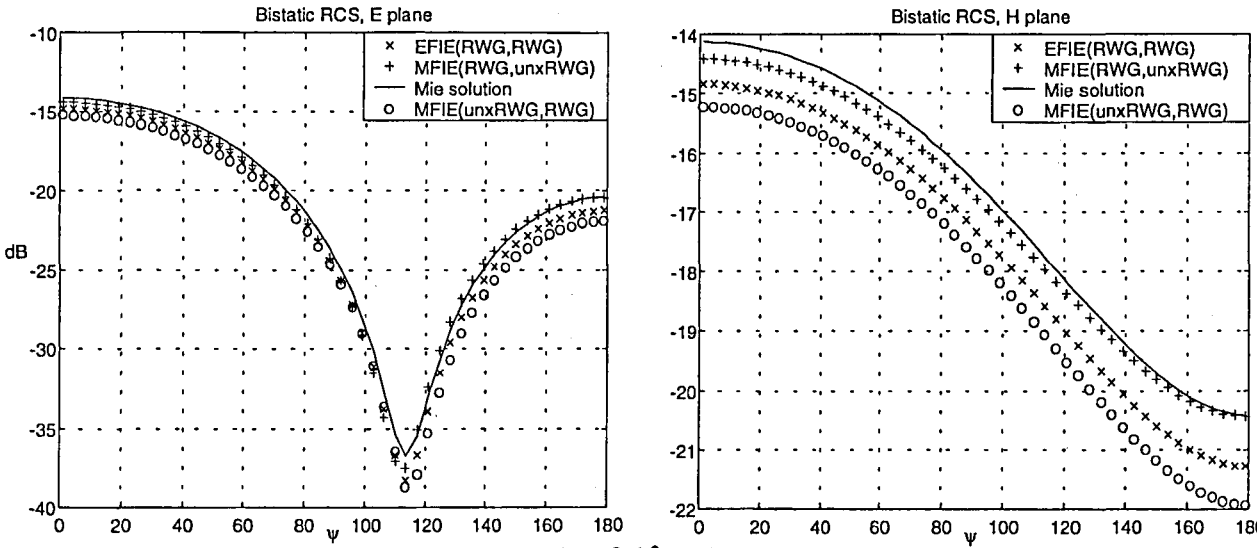

Fig. 7.21 Sphere of radius 0.1λ *with 128 triangles*

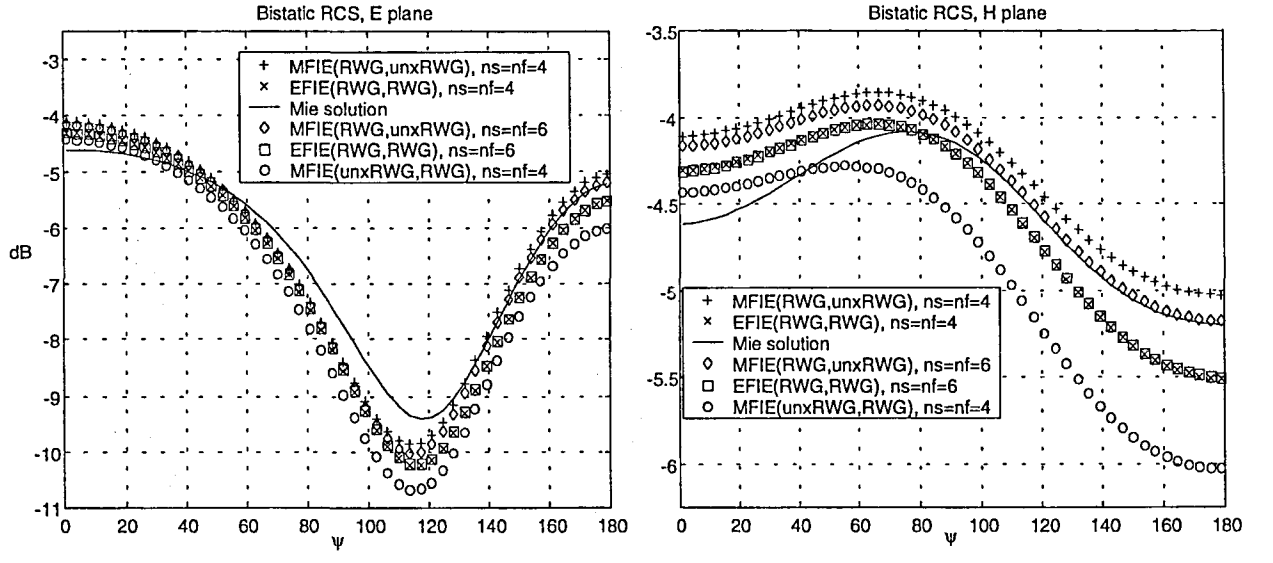

Fig. 7.22 Sphere of radius 0.2λ with 128 triangles

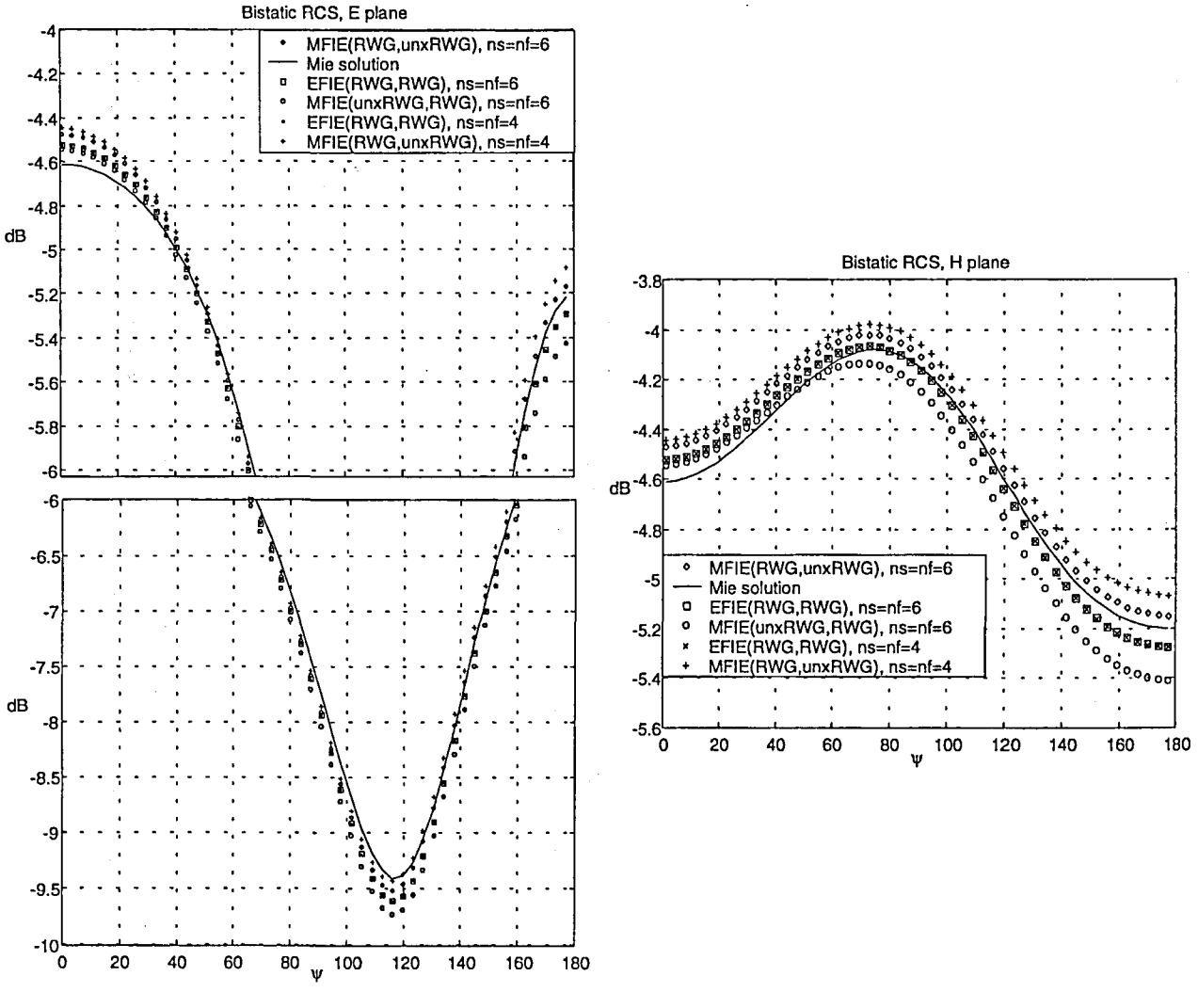

Fig. 7.23 Sphere of radius 0.2λ with 512 triangles

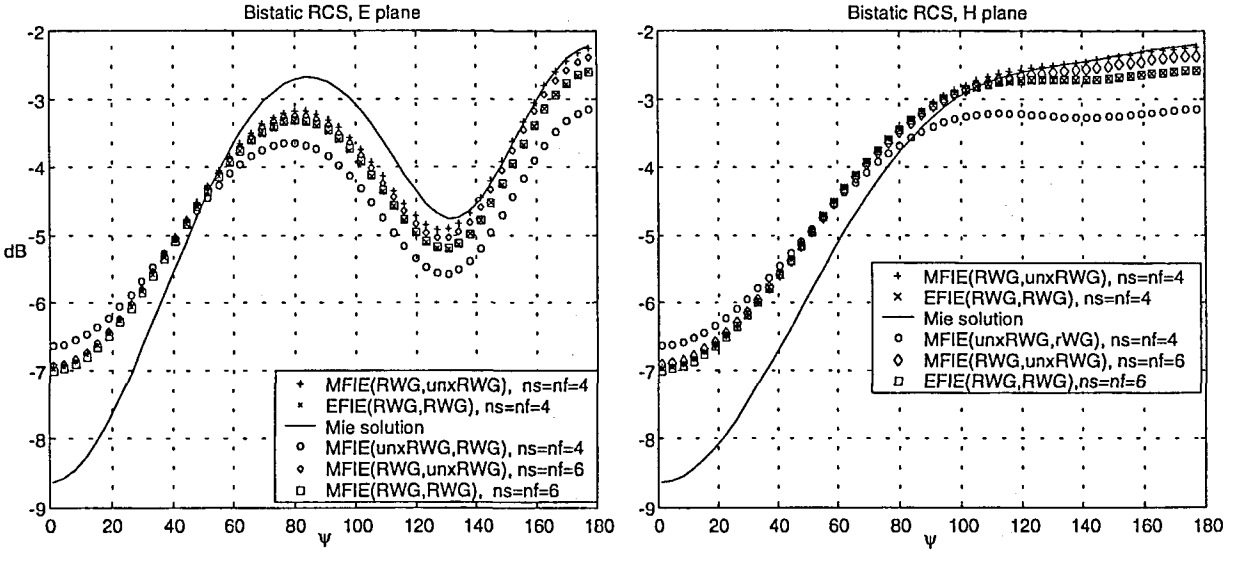

Fig. 7.24 Sphere of radius 0.25λ with 128 triangles

♦ Cone

The RCS results for the cone in Fig. 7.25 under an axially incident plane wave are shown in Fig. 7.26.

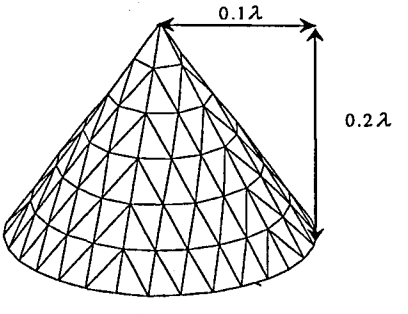

Fig. 7.25 Cone discretized with 360 triangles

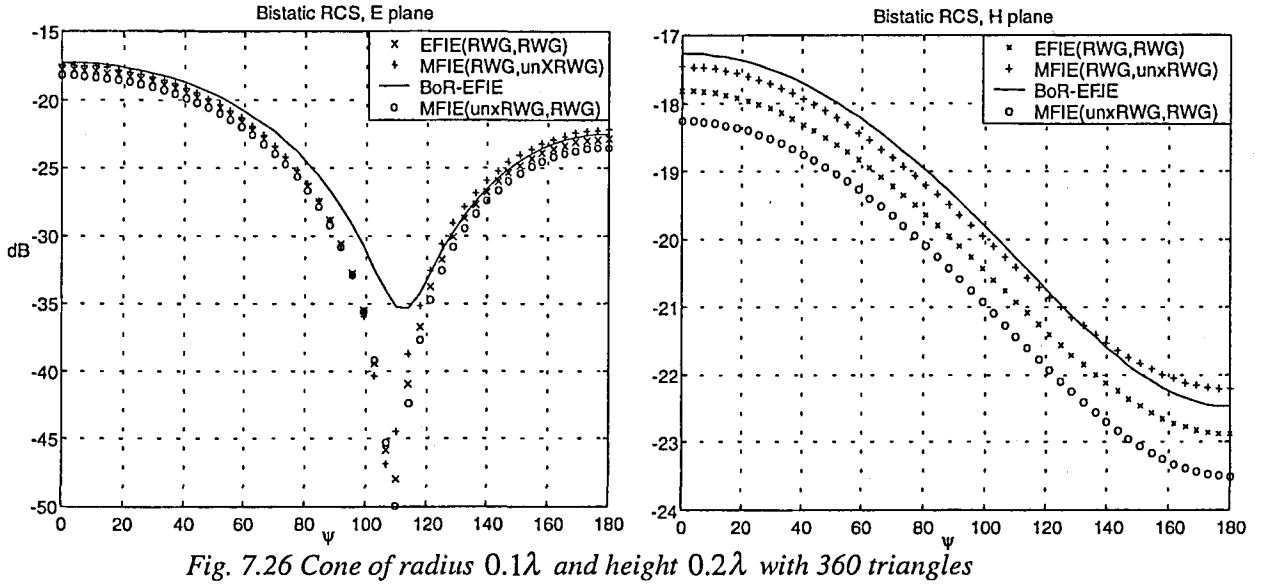

Fig. 7.26 Cone of radius 0.1λ and height 0.2λ with 360 triangles

- **Cylinder**

The RCS results for the cylinder in Fig. 7.27 with radius 0.1λ and height 0.2λ under an axially incident plane wave are shown in Fig. 7.28.

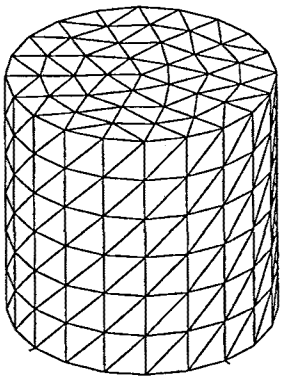

Fig. 7.27 Cylinder discretized with 400 triangles

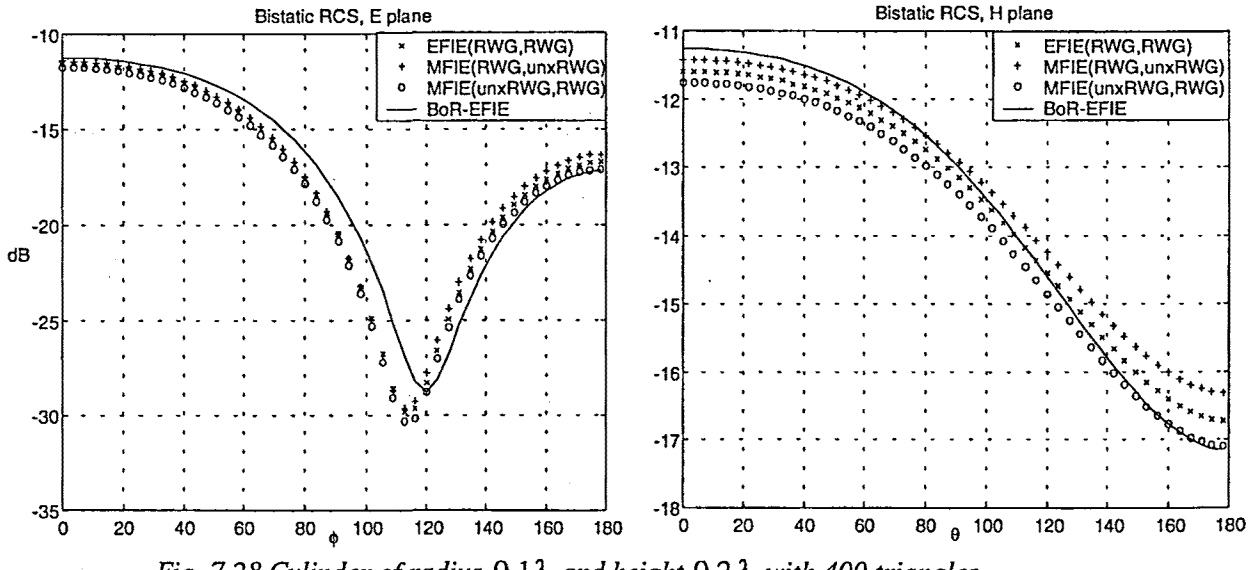

Fig. 7.28 Cylinder of radius 0.1λ and height 0.2λ with 400 triangles

In all the results, the operator PeC-MFIE(*unxRWG,RWG*) shows the worst behaviour, which is in agreement with its inherent bad definition explained in Chapter 6. Note that for the entirely curved objects, the discrepancy with the references is even more evident than for the physical polyhedrons. While the misbehaviour of the PeC-MFIE(*unxRWG,RWG*) for the physical polyhedrons relies on the presence of the physical edges and can be therefore diminished by overdiscretizing the faces, for the objects entirely curved the normal vector is non uniform all over the surface and so keeps being when effectuating the discretization.

The results for the spheres are best to assess the influence of the planar modelling of the curvature on the solution for the well-behaving operators, PeC-EFIE(*RWG,RWG*) and PeC-MFIE(*RWG,unxRWG*). According to the results, above all in the coarse meshings, the performance of PeC-MFIE(*RWG,unxRWG*) is closer to the Mie solution than the solution due to PeC-EFIE(*RWG,RWG*). This can be explained by resorting to the behaviour of both

operators for the physical polyhedrons -section 7.4-. In that case, the PeC-EFIE(*RWG,RWG*) attains a solution closer to the complete solution for a given degree of discretization. In consequence, resulting the planar modelling of the sphere in a polyhedron, it is reasonable that the PeC-EFIE(*RWG,RWG*) yields the solution that approaches more accurately the solution of the polyhedron. Unfortunately, this is not the solution towards which one wants to head; indeed, one wants to obtain the solution of the original body, before being discretized.

Furthermore, the fact of PeC-EFIE(*RWG,RWG*) expanding better the solution of the polyhedron implies that it is able to carry out a higher-order expansion of the solution. One can understand -at least intuitively- that the physical edges represent space discontinuities and therefore demand a higher-order behaviour of the magnitudes -current and field-. However, the PeC-MFIE(*RWG,unxRWG*) showed in the previous section a slower approach to the complete solution, which implies effectively a lower-order expansion of the current. That is why its performance turns out more accurate for modelling the behaviour over a curved surface; indeed, it yields a low-order solution. That is, it remarks less than the PeC-EFIE(*RWG,RWG*) on the high-order constraints of the physical edges, which, as a matter of fact, only appear in the curved objects because of the planar modelling of the curvature. More comments are given about this issue in 7.5.1, where it is given a genuine explanation that accounts for the different sensitivity of PeC-EFIE(*RWG,RWG*) and PeC-MFIE(*RWG,unxRWG*) with regard to the physical edges.

In all the results presented -either physical polyhedrons or curved bodies-, the PeC-EFIE(*RWG,RWG*) results are very consistent. For the case of the physical polyhedrons, the results turn out in general more accurate for a given discretization than those due to PeC-MFIE(*RWG,unxRWG*), which provides a better condition number. This means that the worse condition number of the matrix does not affect in practice the uniqueness of the solution. In other words, the range of ambiguity of the PeC-EFIE(*RWG,RWG*) for these problems is so low that it is not even noticed.

Finally, it must be pointed out that in the results due to the PeC-MFIE(*RWG,unxRWG*) more precision in computing the results is demanded. One can see in Fig. 7.22, Fig. 7.23 and Fig. 7.24 how an increase in the number of gaussian points when numerically integrating either the outer integral or the low-order terms of the inner integral yields a clear variation only for PeC-MFIE(*RWG,unxRWG*). However, PeC-EFIE(*RWG,RWG*) shows a similar behaviour. This must be attributed to the higher order R-dependence in the integrand of PeC-MFIE.

7.5.1 Higher-order expansion in PeC-EFIE(RWG,RWG) than in PeC-MFIE(RWG,unxRWG)

The previous results have shown that a relatively high density of physical edges imposes a higher-order expansion of the magnitudes -current and field-. One can easily understand this idea by analysing the opposite case. Over a wide conducting area -with the physical edges far away-, as it is well known from the physical optic theory and the Snell law, the induced current is directly proportional to the projection of the incident plane wave on the surface. This implies that the induced current must have a uniform vector distribution, which involves actually an expansion of very low order. Logically, by bringing the edges closer, the current and field distribution must become increasingly variable, whereby a higher-order expansion is accordingly required.

This high-order expansion has turned out to be better accomplished by PeC-EFIE since its behaviour is better for physical polyhedrons. For objects entirely curved, on the other hand, the PeC-MFIE appears more suitable because it takes less into consideration the effect of the physical edges due to the unavoidable planar discretization.

The author of this Dissertation Thesis has elaborated a reasoning that accounts for the *physical edge-sensitive* behaviour of PeC-EFIE(*RWG,RWG*), and the *curvature-sensitive* behaviour of PeC-MFIE(*RWG,unxRWG*). Strictly speaking, to undertake a complete expansion of the unknown-, one should resort to the sets of all the orders enclosed in the curl-conforming and divergence-conforming bases groups. In practice, one achieves a finite-order solution through the low-order sets *RWG* and *unxRWG* and with the help of the overdiscretization -when required, for example in electrically small objects, where the high-order influence of the physical edges is remarkable-.

The physical solution for a physical polyhedron presents total continuity across the edges. The solution obtained only ensures continuity of one component but, thanks to the high-order expansion, one can head for the continuity of the other component. Indeed, with an infinite-order expansion -that is; resorting to all the curl- or divergence-conforming sets- the total continuity would be ensured. However, being this of course unachievable, one can obtain a finite expansion of high enough order that yields an accurate expansion of the physical magnitude in practical terms -this is the case in Fig. 7.4, Fig. 7.9, Fig. 7.13 and Fig. 7.16-. I name this solution as the *complete solution.*

The boundary conditions over the interface surface for the PeC-MFIE and the PeC-EFIE stand for

$$\hat{n}\times\vec{H}=\vec{J} \tag{7.1}$$

$$\hat{n}\times\vec{E}=0 \tag{7.2}$$

The most accurate expansion of the physical magnitudes -the complete solution- is obtained whenever (7.1) -PeC-MFIE- and (7.2) -PeC-EFIE- are ensured over the edges for a high enough order of expansion. The reason why (7.2) -PeC-EFIE- is more easily achieved is that the right-hand side term of the equality is constant and independent of the discretization -coincident thus with the imposition in the continuous case-. It is hence reasonable that an increase on the degree of discretization heads faster towards the complete solution of the polyhedron. The PeC-MFIE boundary condition in (7.1), on the contrary, relates two differently expanded magnitudes $\vec{J}$ and $\vec{H}$. It makes thus sense that they need a higher degree of discretization to provide the complete solution of the polyhedron.

The presented PeC-MFIE approach assumes the solid angle value to be $\Omega_0=2\pi$, because it is applied on planar facets. A historical subject of discussion when building any PeC-MFIE operator has been the solid angle value choice. According to all the results shown, the slightly worse behaviour of PeC-MFIE(*RWG,unxRWG*) for electrically small objects with the important presence of physical edges does not come from a wrong choice of the solid angle value but from a low-order expansion of the magnitudes.

7.6 IMPROVEMENT OF THE BEHAVIOUR OF THE OPERATORS

In this section, another original contribution of this Dissertation Thesis, procedures to correct the misbehaviour of the operators are presented. In 7.6.1, a heuristic correction for PeC-MFIE(*unxRWG,RWG*) is supplied. In 7.6.2, it is provided a procedure to improve the performance of PeC-EFIE(*RWG,RWG*) for coarsely meshed spheres.

7.6.1 Solid angle correction for PeC-MFIE(unxRWG,RWG)

As it has been predicted theoretically in Chapter 6, it has been shown with examples in this Chapter the misbehaviour of PeC-MFIE(*unxRWG,RWG*). By trial and error, a modified PeC-MFIE(*unxRWG,RWG*) operator has been found that yields a more accurate RCS. In this modified PeC-MFIE(*unxRWG,RWG*) operator it is effectuated the testing of the Cauchy principal contributions with one point and it is imposed a new value for the solid angle on every triangle.

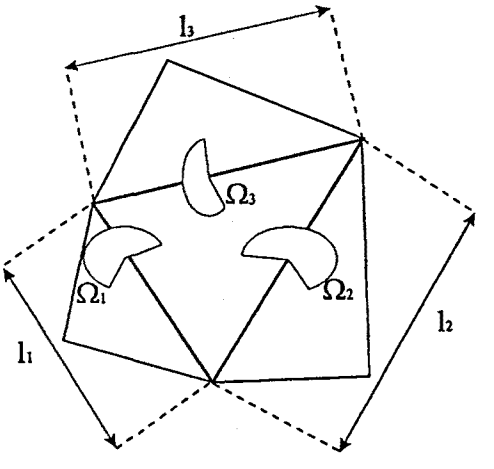

Fig. 7.29 Local estimate of the solid angle

The new equivalent solid angle value Ω_{eq} over any triangle has been defined as the weighted average of the local solid angles over each edge of the triangle -see Fig. 7.29-

$$\Omega_{eq} = \frac{(l_1\Omega_1 + l_2\Omega_2 + l_3\Omega_3)}{(l_1 + l_2 + l_3)} \tag{7.3}$$

Although the modified PeC-MFIE(*unxRWG,RWG*) improves the performance in any case, the improvement is especially noticeable in the cases where the discrepancy is most important[22]. Indeed, it is shown right away how the modified PeC-MFIE(*unxRWG,RWG*) approaches the PeC-EFIE(*RWG,RWG*) for the dimensionally small physical polyhedrons of 7.4 -see Fig. 7.30, Fig. 7.31 and Fig. 7.32- and the PeC-MFIE(*RWG,unxRWG*) for the coarsely meshed spheres in 7.5 -see Fig. 7.33 and Fig. 7.34-.

[22] An article about this issue has been submitted in August 2000 to *IEEE Transactions on Antennnas and Propagation*, with title "On the Testing of the Magnetic Field Integral Equation with RWG basis functions in Method of Moments".

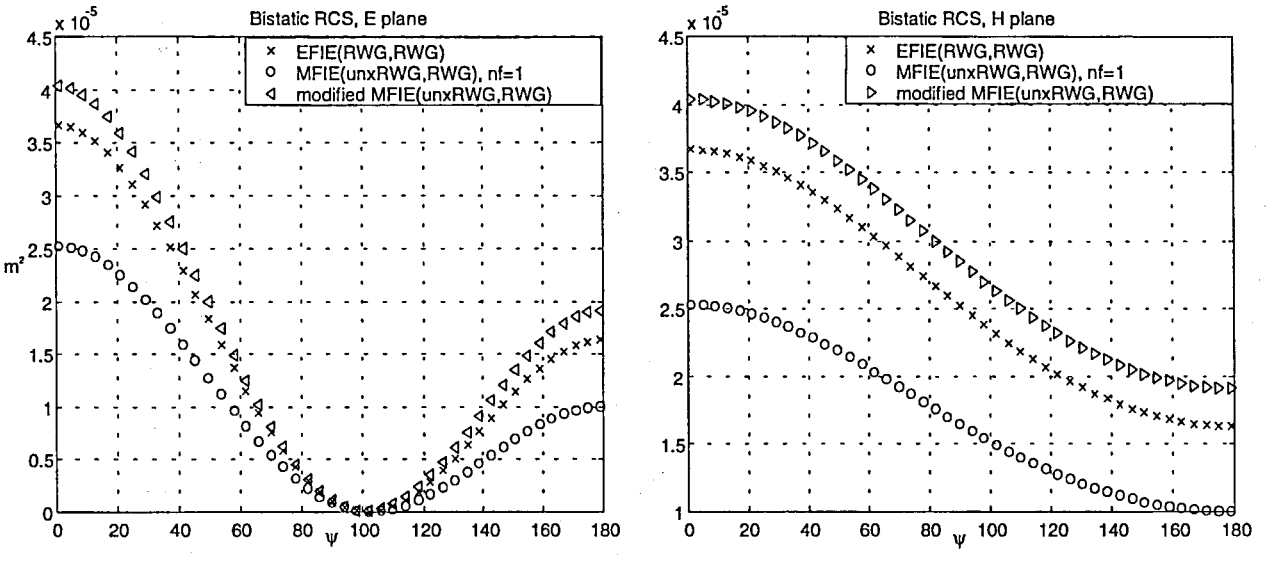

Fig. 7.30 RCS for the pyramid with 128 triangles

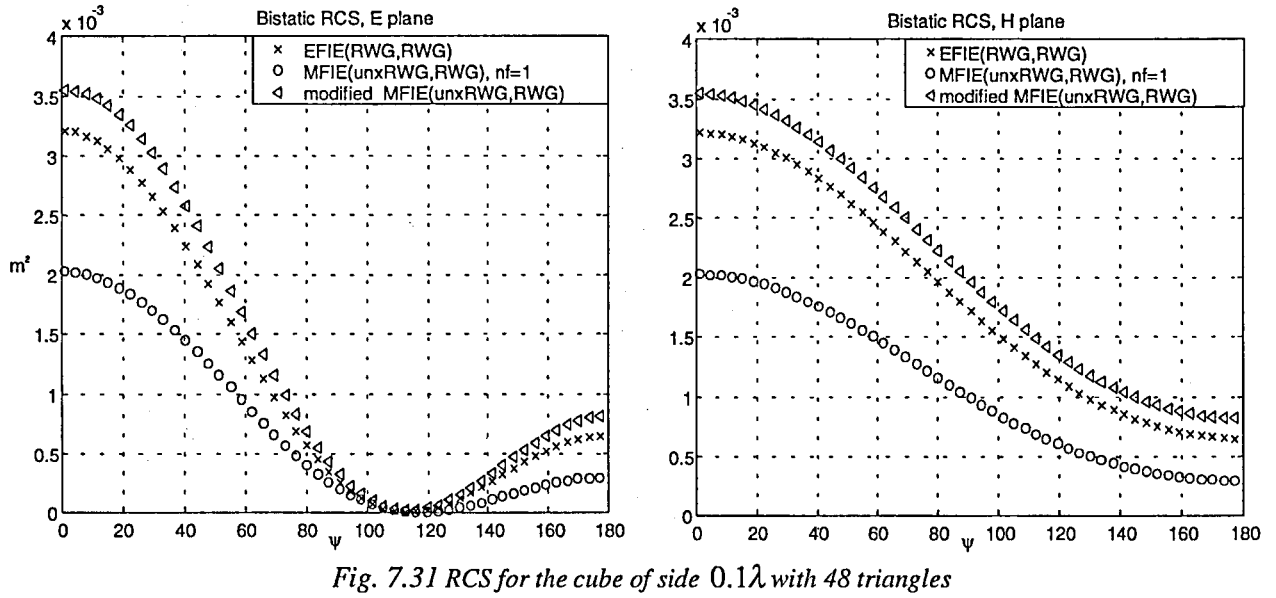

Fig. 7.31 RCS for the cube of side 0.1λ with 48 triangles

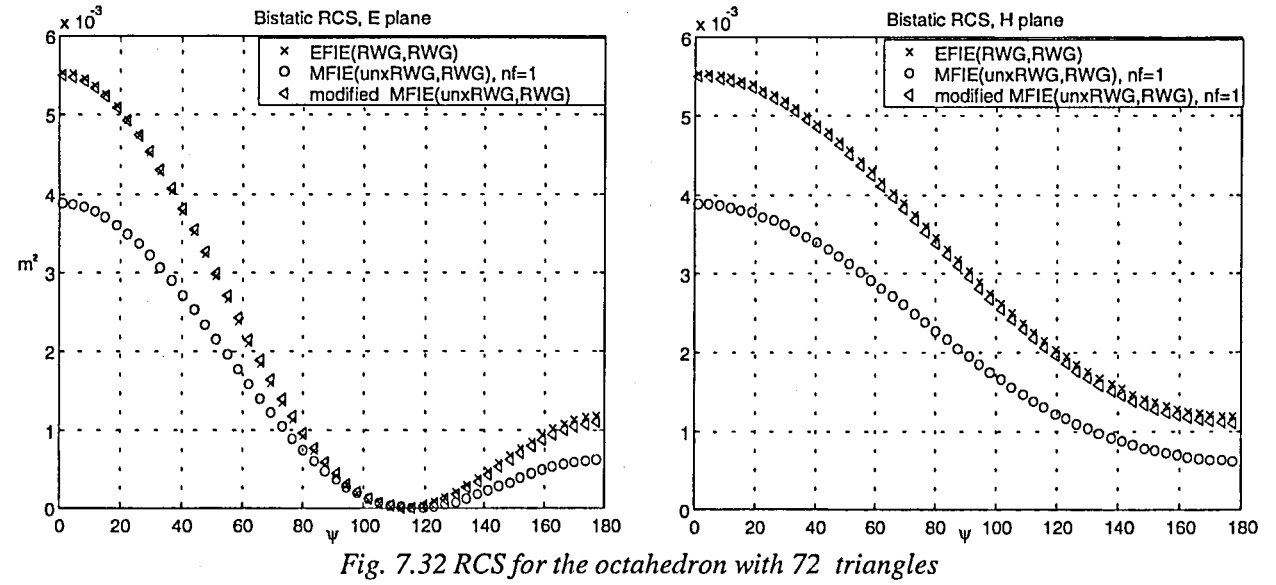

Fig. 7.32 RCS for the octahedron with 72 triangles

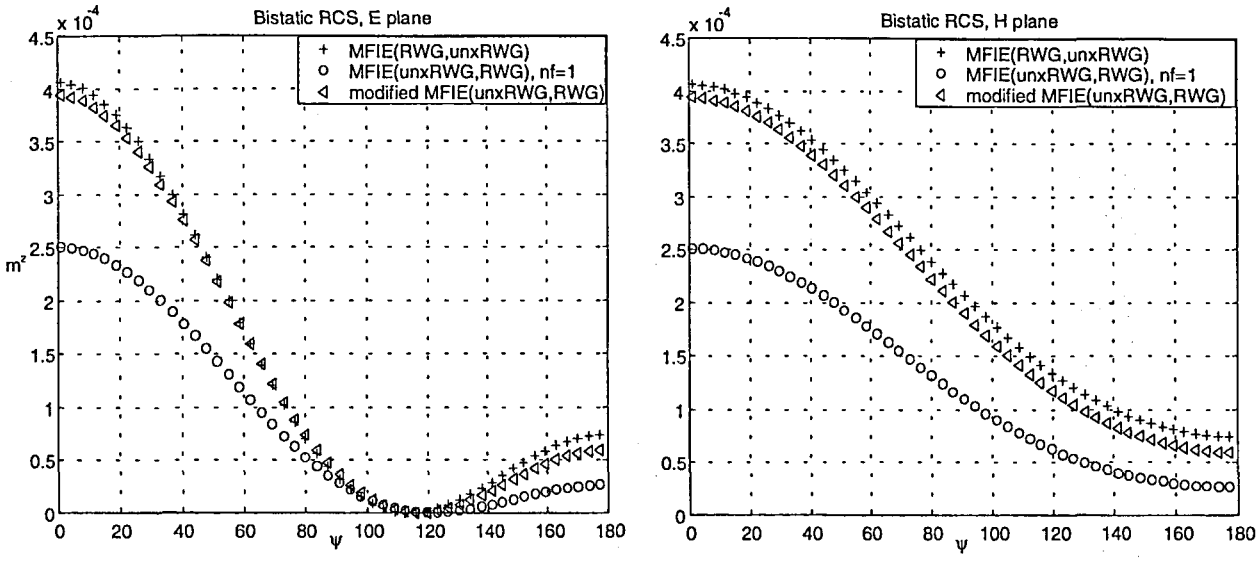

Fig. 7.33 RCS for the sphere of radius 0.05λ *with 32 triangles*

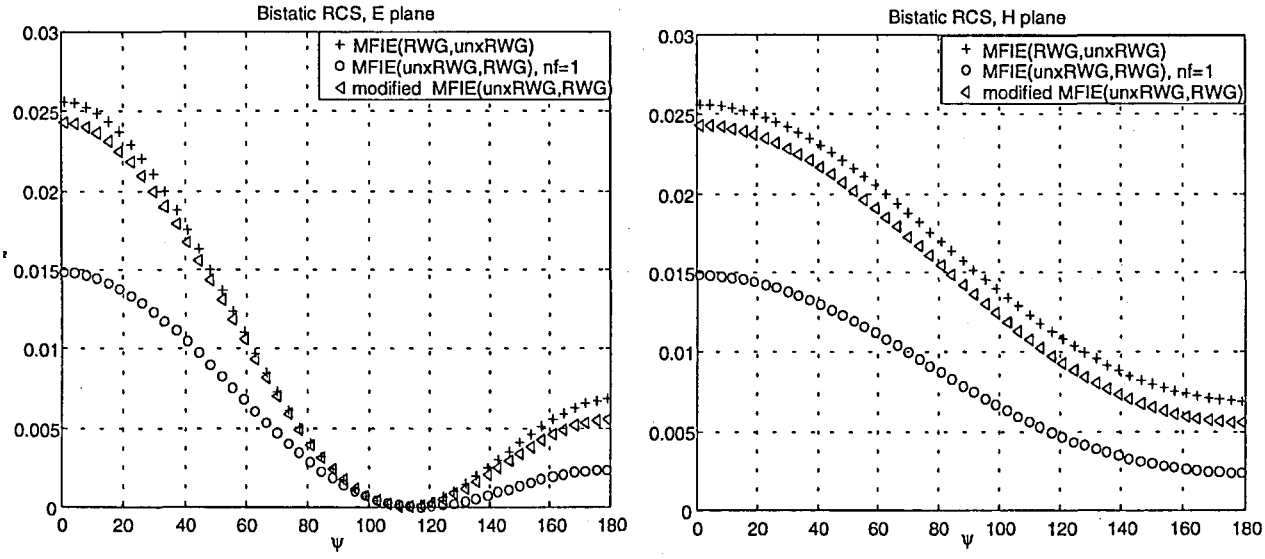

Fig. 7.34 RCS for the sphere of radius 0.1λ *with 32 triangles*

7.6.2 PeC-EFIE(RWG,RWG) post-correction for coarsely meshed spheres

It has been shown and discussed in detail in 7.5 the relative worse performance of PeC-EFIE(*RWG,RWG*) compared to PeC-MFIE(*RWG,unxRWG*) for entirely curved objects. This must happen because the PeC-EFIE yields a solution closer to the physical polyhedron adopted to model the curved surface.

Another original contribution of this dissertation Thesis is a correction for the specific case of a sphere on the value of the current obtained through PeC-EFIE(*RWG,RWG*) that approaches the PeC-MFIE(*RWG,unxRWG*) behaviour and thus the Mie solution. This procedure takes advantage of a specific discretization of the sphere to effectuate a parabolic current interpolation from the *RWG* current distribution obtained through the operator PeC-EFIE(*RWG,RWG*).

The discretization adopted for the sphere is such that, as the mesh becomes finer, the size of the triangles is maintained more or less uniform over the surface -see Fig. 7.17 -. The discretization is undertaken in an iterative way so that at every step the amount of triangles becomes multiplied by four -see Fig. 7.35-.

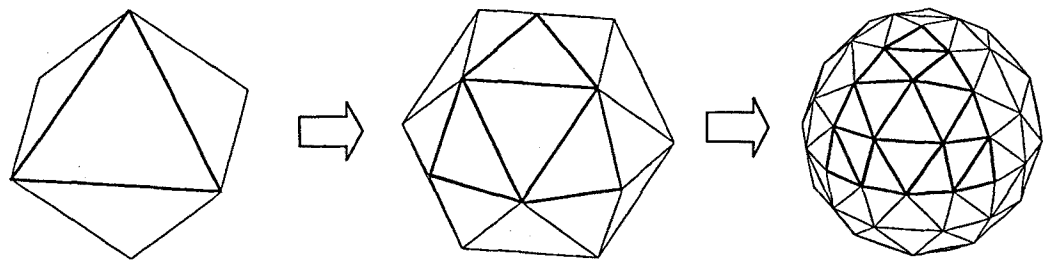

Fig. 7.35 Discretization of the sphere

In this particular discretization for any degree of iteration one finds a basic structure of four triangles; that is, six vertices. Note that this basic structure coincides with the disposition of the nodes of the basic element in a triangular parabolic nodal interpolation -see Fig. 2.12 in Chapter 2-.

In the procedure for improving the PeC-EFIE(*RWG,RWG*), one must obtain first the *RWG* current value over the vertices by weighting the contribution of all the triangles shaping in. After, it must be effectuated a parabolic nodal interpolation over the sphere up from the current distribution expanded by the *RWG* set on the vertices. This new expansion of the current allows for a parabolic curvature but assumes that the nodal values of the current are accurate enough. Indeed, PeC-EFIE(*RWG,RWG*) is the operator that can best fulfil this requirement since its current expansion resembles most the complete solution of the physical polyhedron.

The procedure behaves well as long as the sphere is coarsely meshed. When the dimensions of the sphere increase, the required discretization, derived from the imposition for the size of the patch of 0.1λ, reduces much the curvature error. Some results are provided below for the improved PeC-EFIE(*RWG,RWG*) compared to the original PeC-EFIE(*RWG,RWG*) and the PeC-MFIE(*RWG,unxRWG*) for the spheres in 7.5.

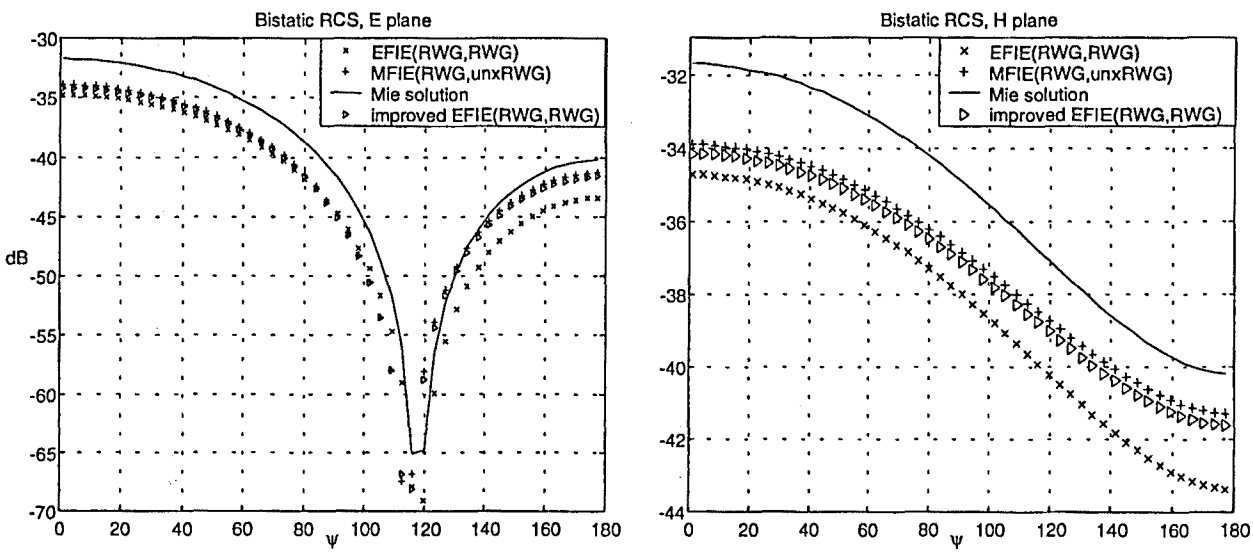

Fig. 7.36 RCS for the sphere of radius 0.05λ with 32 triangles

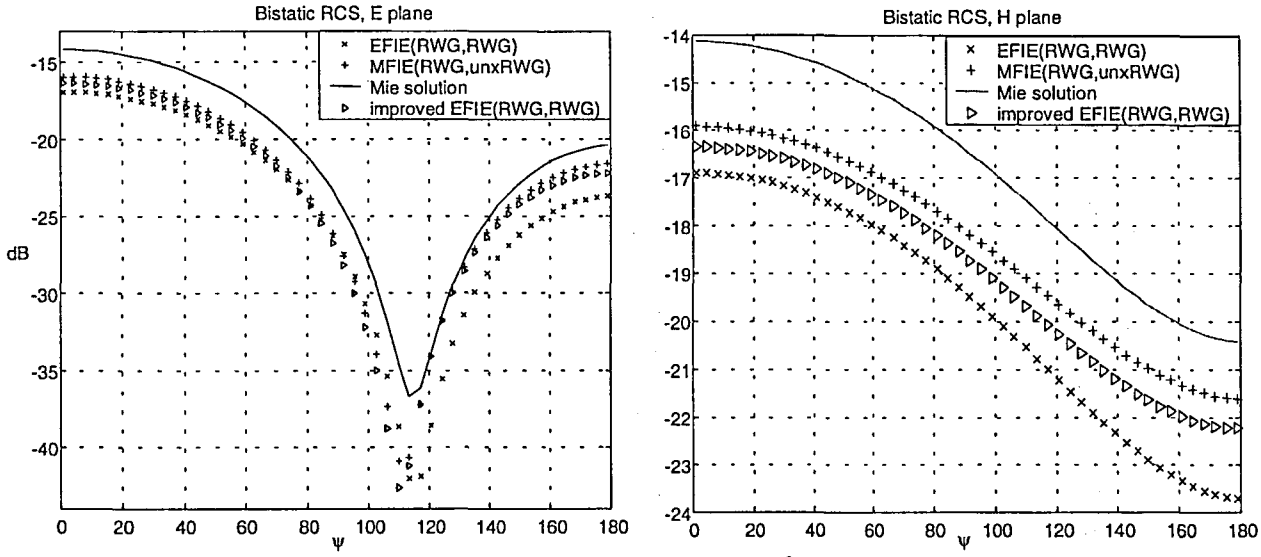

Fig. 7.37 RCS for the sphere of radius 0.1λ with 32 triangles

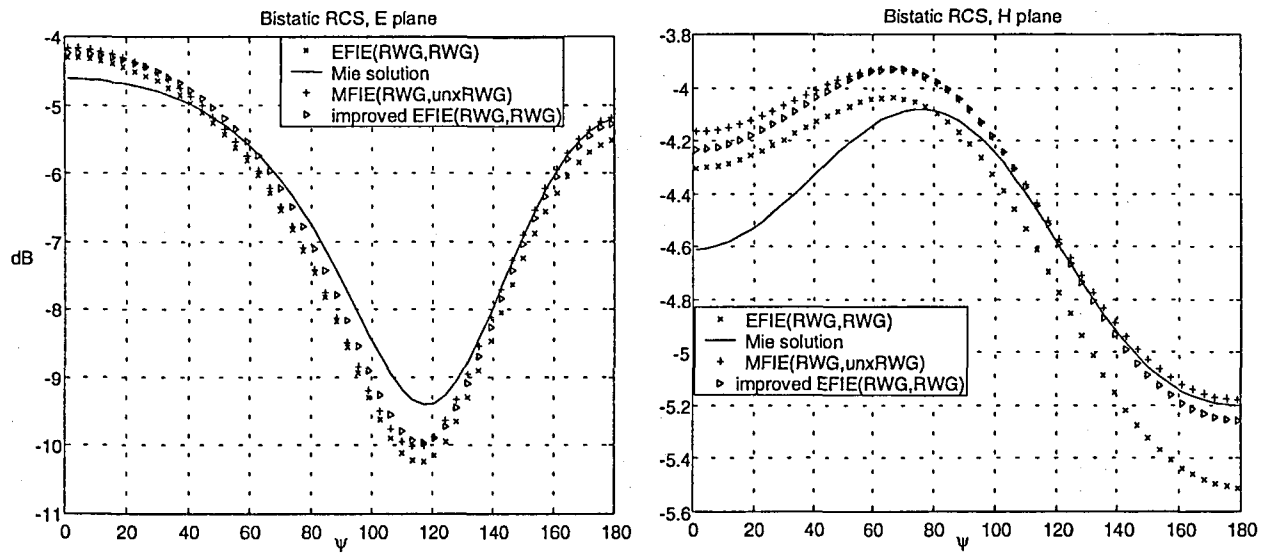

Fig. 7.38 RCS for the sphere of radius 0.2λ with 128 triangles

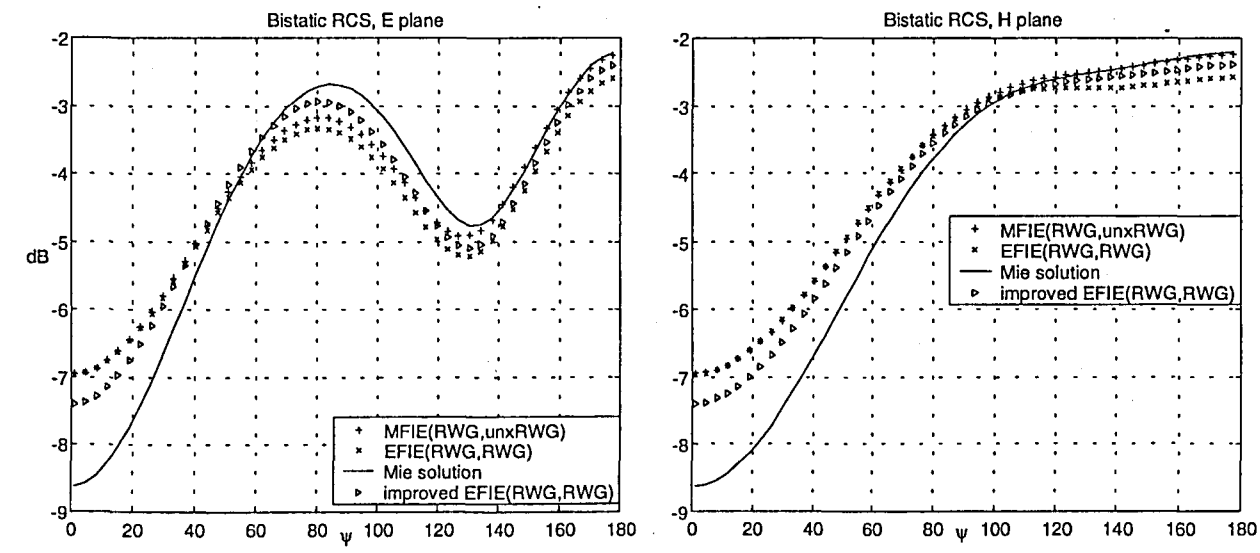

Fig. 7.39 RCS for the sphere of radius 0.25λ with 128 triangles

Chapter 8 RWG BASED METHOD OF MOMENTS FOR DIELECRIC 3D BODIES

Three dielectric operators appear in the dielectric case: EFIE, MFIE and PMCHW -see Chapter 2-. They respectively enforce the electric boundary condition, the magnetic boundary condition or both over the interface surface S. The integral expressions corresponding to the dielectric operators in terms of the basic PeC-operators stand for

EFIE:
$$\vec{E}^{S^{\pm}}\Big|_{\vec{r}\in S^{\mp}} = \left[\vec{E}^{S}_{PeC}\right]^{\pm}\left(\vec{J}^{\pm}\right)\Big|_{\vec{r}\in S^{\mp}} - \left[\vec{H}^{S}_{PeC}\right]^{\pm}\left(\vec{M}^{\pm}\right)\Big|_{\vec{r}\in S^{\mp}} \tag{8.1}$$

MFIE:
$$\vec{H}^{S^{\pm}}\Big|_{\vec{r}\in S^{\mp}} = \left[\vec{H}^{S}_{PeC}\right]^{\pm}\left(\vec{J}^{\pm}\right)\Big|_{\vec{r}\in S^{\mp}} - \frac{1}{\eta^{\pm 2}}\left[\vec{E}^{S}_{PeC}\right]^{\pm}\left(\vec{M}^{\pm}\right)\Big|_{\vec{r}\in S^{\mp}} \tag{8.2}$$

PMCHW:
$$\begin{aligned}\vec{E}^{S^{+}} - \vec{E}^{S^{-}} &= \left[\vec{E}^{S}_{PeC}\right]^{+}\left(\vec{J}^{+}\right) - \left[\vec{E}^{S}_{PeC}\right]^{-}\left(\vec{J}^{-}\right) \\ &\quad - \left[\vec{H}^{S}_{PeC}\right]^{+}\left(\vec{M}^{+}\right) + \left[\vec{H}^{S}_{PeC}\right]^{-}\left(\vec{M}^{-}\right) \\ \vec{H}^{S^{+}} - \vec{H}^{S^{-}} &= \left[\vec{H}^{S}_{PeC}\right]^{+}\left(\vec{J}^{+}\right) - \left[\vec{H}^{S}_{PeC}\right]^{-}\left(\vec{J}^{-}\right) \\ &\quad + \frac{1}{\eta^{+2}}\left[\vec{E}^{S}_{PeC}\right]^{+}\left(\vec{M}^{+}\right) - \frac{1}{\eta^{-2}}\left[\vec{E}^{S}_{PeC}\right]^{-}\left(\vec{M}^{-}\right)\end{aligned} \tag{8.3}$$

It is well known from the theorem of equivalence that the solution is unique all over S. Indeed, two field conditions are posed relying on two source magnitudes:

$$\vec{J}^{+} = -\vec{J}^{-} \qquad \vec{M}^{+} = -\vec{M}^{-} \tag{8.4}$$

8.1 DIELECTRIC POLYHEDRON

The study of the dielectric polyhedron -a singular contribution of this dissertation Thesis- is developed in the next subsections. In 8.1.1, the electric and magnetic charge conditions are provided. In 8.1.2, it is given a description of the field and current spaces of the EFIE and MFIE dielectric operators. It is shown again the fact that, after the discretization, the solution is not unique anymore, whereby the condition number of the matrix augments with the discretization. In section 8.1.3, the operators that come from a linear combination

of EFIE and MFIE are presented and it is discussed their validity; the most outstanding approaches are the PMCHW and the CFIE. Finally, in 8.1.4 it is provided a discussion about the effect of the adopted low-order expansion of the current -*RWG* and *unxRWG*- on the dielectric operators. It is shown how it becomes especially critical for the EFIE, MFIE operators.

8.1.1 Charge condition

Over the dielectric polyhedron one must consider the continuity conditions of the electric and magnetic currents. According to the development in 6.5.1 for the perfectly conducting polyhedron, one can analogously yield for this case

$$-\frac{1}{j\omega}\left(\vec{n}_{c,1}\cdot\vec{J}_1^{\pm}\Big|_{\vec{r}\in\partial_i}+\vec{n}_{c,2}\cdot\vec{J}_2^{\pm}\Big|_{\vec{r}\in\partial_i}\right)=\tau_e^{\pm}\Big|_{\vec{r}\in\partial_i} \tag{8.5}$$

$$-\frac{1}{j\omega}\left(\vec{n}_{c,1}\cdot\vec{M}_1^{\pm}\Big|_{\vec{r}\in\partial_i}+\vec{n}_{c,2}\cdot\vec{M}_2^{\pm}\Big|_{\vec{r}\in\partial_i}\right)=\tau_m^{\pm}\Big|_{\vec{r}\in\partial_i} \tag{8.6}$$

where $\tau_e^{\pm}$ and $\tau_m^{\pm}$ correspond respectively to the electric and magnetic linear charge densities over the two sides of an arbitrary edge $\partial_i^{\pm}$ of the polyhedron. Although four charge equations appear -two at each side of the surface-, they are really only two -one per side- because $\vec{J}^{+}=-\vec{J}^{-}$ and $\vec{M}^{+}=-\vec{M}^{-}$, which compels

$$\tau_e^{+}\Big|_{\vec{r}\in\partial_i}=-\tau_e^{-}\Big|_{\vec{r}\in\partial_i}\qquad \tau_m^{+}\Big|_{\vec{r}\in\partial_i}=-\tau_m^{-}\Big|_{\vec{r}\in\partial_i} \tag{8.7}$$

whereby four independent source magnitudes appear in the polyhedron: $\vec{M}^{\pm}$ and $\vec{J}^{\pm}$- associated to the theorem of equivalence- and $\tau_e^{\pm}$, $\tau_m^{\pm}$ -due to the discretization-.

The charge conditions must be kept always in mind when developing the dielectric operators. They have to be accomplished along with the field requirements across the edges for the three operators. Note that, being the magnetic charge non-null, the MFIE operator must rely on the charge condition as well. As it will be shown later, this fact makes that the dielectric MFIE cannot preserve anymore the advantageous properties with regard to the condition number of the PeC-MFIE. Indeed, in the dielectric case, the EFIE and the MFIE must allow for the same and dual requirements.

8.1.2 Electric and magnetic field boundary conditions: EFIE-MFIE

The study of the dielectric polyhedron represents the generalisation of the study of the perfectly conducting polyhedron carried out in Chapter 6. It is thus undertaken through the verification of the boundary conditions of the fields over the edges in the equivalent problems corresponding to the two regions.

The boundary conditions of the electric and magnetic flux densities are the ones that lead to the outstanding operators PeC-EFIE(*RWG*,*RWG*) and PeC-MFIE(*RWG*,*unxRWG*). Since the other boundary conditions are either not possible -PeC-EFIE- or show some inherent error -PeC-MFIE-, they are dismissed to develop the dielectric operators. Therefore, the boundary conditions that must be accomplished in the dielectric case become

$$\vec{n}\cdot\left(\vec{D}_1^{\pm}-\vec{D}_2^{\pm}\right)\Big|_{\vec{r}\in\partial_i}=\tau_e^{\pm}\Big|_{\vec{r}\in\partial_i} \tag{8.8}$$

$$\vec{n}\cdot\left(\vec{B}_1^{\pm}-\vec{B}_2^{\pm}\right)\Big|_{\vec{r}\in\partial_i}=\tau_m^{\pm}\Big|_{\vec{r}\in\partial_i} \tag{8.9}$$

In the dielectric polyhedron, the EFIE and the MFIE become dual approaches that are influenced by the same factors. Therefore, now one cannot expect anymore the advantages of the PeC-MFIE in front of the PeC-EFIE described in Chapter 6. The dielectric EFIE and MFIE must behave then in a similar way.

According to (8.8), the ruling boundary conditions at both sides of an arbitrary edge ∂_i for the operator EFIE must be

$$\vec{n}\cdot\left(\vec{E}_1^{\pm}-\vec{E}_2^{\pm}\right)\Big|_{\vec{r}\in\partial_i}=\frac{\tau_e^{\pm}}{\varepsilon^{\pm}}\Big|_{\vec{r}\in\partial_i} \tag{8.10}$$

which, according to the parameters in Fig. 6.8, is readily expressed as

$$\vec{n}_{c,1}{}^{\pm}\cdot\vec{E}_1^{\pm}\Big|_{\vec{r}\in\partial_i}+\vec{n}_{c,2}{}^{\pm}\cdot\vec{E}_2^{\pm}\Big|_{\vec{r}\in\partial_i}=\frac{\tau_e^{\pm}}{\varepsilon^{\pm}}\Big|_{\vec{r}\in\partial_i} \tag{8.11}$$

The integration of $\nabla_s\cdot\vec{E}$ over a portion of surface -$\Delta S\to 0$- around a point on the edge -$\vec{r}\in\partial_i$- with the length of the transversal side tending to zero -$\Delta t\to 0$-see Fig. 6.9-, as shown in 6.5.2.2 for the PeC-EFIE, leads to

$$\vec{n}_{c,1}{}^{\pm}\cdot\vec{E}_1^{\pm}\Big|_{\vec{r}\in\partial_i}+\vec{n}_{c,2}{}^{\pm}\cdot\vec{E}_2^{\pm}\Big|_{\vec{r}\in\partial_i}=\frac{1}{-j\omega\varepsilon^{\pm}}\left(\vec{n}_{c,1}{}^{\pm}\cdot\vec{J}_1^{\pm}+\vec{n}_{c,2}{}^{\pm}\cdot\vec{J}_2^{\pm}\right)\Big|_{\vec{r}\in\partial_i} \tag{8.12}$$

Evidently, to merge (8.10) and (8.12) in one condition, it must be accomplished

$$\frac{1}{-j\omega}\left(\vec{n}_{c,1}{}^{\pm}\cdot\vec{J}_1^{\pm}+\vec{n}_{c,2}{}^{\pm}\cdot\vec{J}_2^{\pm}\right)\Big|_{\vec{r}\in\partial_i}=\tau_e^{\pm}\Big|_{\vec{r}\in\partial_i} \tag{8.13}$$

which is the condition for the electric current to yield the electric field boundary condition over the edge. Note that it is coincident with the electric charge condition. This is very important because the two conditions regarding the electric current -the charge condition and the electric field condition- are the same.

On the other hand, from the theorem of equivalence, it is well-known that

$$\vec{M}_{\{112\}}^{\pm}\Big|_{\vec{r}\in\partial_i}=-\hat{n}_{\{112\}}^{\pm}\times\vec{E}_{\{112\}}^{\pm}\Big|_{\vec{r}\in\partial_i} \tag{8.14}$$

which readily yields

$$\vec{E}_{\{112\}}^{\pm}\Big|_{\vec{r}\in\partial_i}=\hat{n}_{\{112\}}^{\pm}\times\vec{M}_{\{112\}}^{\pm}\Big|_{\vec{r}\in\partial_i} \tag{8.15}$$

When introduced in (8.11), one obtains a condition for $\vec{M}$ at both sides of the surface

$$\vec{n}_{c,1}^{\pm}\cdot\left(\hat{n}_1^{\pm}\times\vec{M}_1^{\pm}\Big|_{\vec{r}\in\partial_i}\right)+\vec{n}_{c,2}^{\pm}\cdot\left(\hat{n}_2^{\pm}\times\vec{M}_2^{\pm}\Big|_{\vec{r}\in\partial_i}\right)=\frac{\tau_e^{\pm}}{\varepsilon^{\pm}}\Bigg|_{\vec{r}\in\partial_i} \tag{8.16}$$

In the expressions (8.13) and (8.16), there have been presented the conditions that must be accomplished by the source magnitudes $\vec{J}^{\pm}$, $\vec{M}^{\pm}$ and $\tau_e^{\pm}$ to fulfil the electric field condition on an arbitrary edge ∂_i. There are, hence, two field-conditions -corresponding to the two dielectric regions- relying on three independent source magnitudes: $\vec{J}^{\pm}$, $\vec{M}^{\pm}$, $\tau_e^{\pm}$. This corresponds to an ambiguous or undetermined problem with one degree of freedom per edge -as in the PeC-EFIE(*RWG*,*RWG*)-. In any case, the degree of ambiguity in the dielectric EFIE must be bigger than in the PeC-EFIE because it is less consistent to have ambiguously defined two magnitudes per edge than one.

Following the reasoning developed for PeC-EFIE(*RWG*,*RWG*), $\tau_e^{\pm}$ represents a source of ambiguity in the EFIE approach that is not present in the original problem -before the discretization-. In the same terms expounded for the PeC-EFIE(*RWG*,*RWG*), it has to be imposed *no electric charge accumulation* -$\tau_e^{\pm}=0$- to find a solution, which can be satisfied in objects with a density of edges not very high.

So, according to the required imposition $\tau_e^{\pm}=0$, the ruling boundary conditions for the electric field over an arbitrary edge ∂_i at both sides of a polyhedron become

$$\vec{n}_{c,1}^{\pm}\cdot\vec{E}_1^{\pm}\Big|_{\vec{r}\in\partial_i}+\vec{n}_{c,2}^{\pm}\cdot\vec{E}_2^{\pm}\Big|_{\vec{r}\in\partial_i}=0 \tag{8.17}$$

which is accomplished by means of the updated electric current condition of (8.13)

$$\left(\vec{n}_{c,1}^{\pm}\cdot\vec{J}_1^{\pm}+\vec{n}_{c,2}^{\pm}\cdot\vec{J}_2^{\pm}\right)\Big|_{\vec{r}\in\partial_i}=0 \tag{8.18}$$

and the corresponding magnetic current condition of (8.16)

$$\vec{n}_{c,1}^{\pm}\cdot\left(\hat{n}_1^{\pm}\times\vec{M}_1^{\pm}\Big|_{\vec{r}\in\partial_i}\right)+\vec{n}_{c,2}^{\pm}\cdot\left(\hat{n}_2^{\pm}\times\vec{M}_2^{\pm}\Big|_{\vec{r}\in\partial_i}\right)=0 \tag{8.19}$$

which can be easily rewritten as

$$\vec{M}_1^{\pm}\Big|_{\vec{r}\in\partial_i}\cdot\hat{l}^{\pm}=\vec{M}_2^{\pm}\Big|_{\vec{r}\in\partial_i}\cdot\hat{l}^{\pm} \tag{8.20}$$

The expressions (8.17) and (8.18) involve continuity of the normal component of respectively $\vec{E}^{\pm}$ and $\vec{J}^{\pm}$ across an arbitrary edge ∂_i, whereby a suitable set of basis functions for both magnitudes is *RWG* -in general, a divergence-conforming set-. The expression (8.20), on the other hand, demands continuity of the tangential component of $\vec{M}^{\pm}$ over the edges; it is then fit to choose *unxRWG* - in general, a curl-conforming set- as basis function. Both *RWG* and *unxRWG* effectuate a low-order expansion.

For the MFIE operator, which corresponds to the dual problem of the EFIE operator, in view of (8.9), the expressions to be accomplished are

$$\vec{n}\cdot\left(\vec{H}_1^{\pm}-\vec{H}_2^{\pm}\right)\Big|_{\vec{r}\in\partial_i}=\frac{\tau_m^{\pm}}{\mu^{\pm}}\Big|_{\vec{r}\in\partial_i} \tag{8.21}$$

Again an ambiguity associated to $\tau_m^{\pm}$ appears in the MFIE in the same terms as in the EFIE. It is thus required the imposition $\tau_m^{\pm}=0$, which yields for each side of an arbitrary edge of the polyhedron

$$\vec{n}_{c,1}^{\pm}\cdot\vec{H}_1^{\pm}\Big|_{\vec{r}\in\partial_i}+\vec{n}_{c,2}^{\pm}\cdot\vec{H}_2^{\pm}\Big|_{\vec{r}\in\partial_i}=0 \tag{8.22}$$

By means of the duality properties, the development of the MFIE operator is straightforward. In accordance with the magnetic charge condition and resorting to the well-known expression

$$\vec{J}_{\{12\}}^{\pm}\Big|_{\vec{r}\in\partial_i}=\hat{n}_{\{12\}}^{\pm}\times\vec{H}_{\{12\}}^{\pm}\Big|_{\vec{r}\in\partial_i} \tag{8.23}$$

the ruling conditions across the edges for $\vec{J}^{\pm}$ and $\vec{M}^{\pm}$ accordingly become

$$\vec{J}_1^{\pm}\Big|_{\vec{r}\in\partial_i}\cdot\hat{l}^{\pm}=\vec{J}_2^{\pm}\Big|_{\vec{r}\in\partial_i}\cdot\hat{l}^{\pm} \tag{8.24}$$

$$\vec{n}_{c,1}^{\pm}\cdot\vec{M}_1^{\pm}\Big|_{\vec{r}\in\partial_i}+\vec{n}_{c,2}^{\pm}\cdot\vec{M}_2^{\pm}\Big|_{\vec{r}\in\partial_i}=0 \tag{8.25}$$

whereby it is suitable to use *RWG* - or any divergence-conforming set- as weighting set and expanding set of $\vec{M}^{\pm}$, and *unxRWG* -or any curl-conforming set- as expanding set of $\vec{J}^{\pm}$.

According to the definitions in (8.1) and (8.2), the dielectric EFIE and MFIE operators must result from the combination of the well behaving operators PeC-EFIE(*RWG*,*RWG*) and PeC-MFIE(*RWG*,*unxRWG*). One can equivalently reach this conclusion through the superposition of the compatible PeC-spaces described in Chapter 6 that ensure normal continuity of the basic $\vec{E}_{PeC}^{S}$ and $\vec{H}_{PeC}^{S}$. Indeed, these PeC-operators are best defined and yield the same results when analysing physical polyhedrons -see the results on Chapter 7-. It is also important to remark that $\vec{J}^{\pm}$ and $\vec{M}^{\pm}$ are expanded in orthogonal sets, *RWG* and *unxRWG*, for both EFIE and MFIE, which agrees with the physical notion of electromagnetic coupling.

The presented EFIE formulation is already present in literature [15][30] for PeC-dielectric composite geometries. The MFIE is a contribution of this dissertation Thesis. The EFIE is normally more advantageous than the MFIE because it allows the analysis of structures with conducting open surfaces, such as, for example, the microstrip antennas; that is why it is more often chosen.

8.1.3 Linear combination of the electric and the magnetic field conditions: CFIE, PMCHW

In the continuous case -in the step previous to the discretization-, some linear combination of the EFIE and MFIE conditions at both sides of the interface surfaces are valid as well. The PMCHW results from the subtraction of the inner and outer EFIE and MFIE conditions. The CFIE comes from the addition of the inner EFIE and MFIE and the outer EFIE and MFIE.

So as to let the field and current spaces perfectly defined, in all these approaches one has to provide at the same time the electric and the magnetic field boundary conditions over the edges, (8.17) and (8.22). According to the analysis carried out for the EFIE, $\vec{J}^{\pm}$ and $\vec{M}^{\pm}$ must accomplish

$$\vec{M}_1^{\pm}\big|_{\vec{r}\in\partial_i}\cdot\hat{l}^{\pm}=\vec{M}_2^{\pm}\big|_{\vec{r}\in\partial_i}\cdot\hat{l}^{\pm}\qquad\qquad \vec{n}_{c,1}^{\pm}\cdot\vec{J}_1^{\pm}\big|_{\vec{r}\in\partial_i^{\pm}}+\vec{n}_{c,2}^{\pm}\cdot\vec{J}_2^{\pm}\big|_{\vec{r}\in\partial_i^{\pm}}=0 \tag{8.26}$$

and the analysis for the MFIE accordingly yields

$$\vec{n}_{c,1}^{\pm}\cdot\vec{M}_1^{\pm}\big|_{\vec{r}\in\partial_i^{\pm}}+\vec{n}_{c,2}^{\pm}\cdot\vec{M}_2^{\pm}\big|_{\vec{r}\in\partial_i^{\pm}}=0\qquad\qquad \vec{J}_1^{\pm}\big|_{\vec{r}\in\partial_i^{\pm}}\cdot\hat{l}^{\pm}=\vec{J}_2^{\pm}\big|_{\vec{r}\in\partial_i^{\pm}}\cdot\hat{l}^{\pm} \tag{8.27}$$

where of course it is imposed the necessary restriction of *no electric and magnetic charge accumulation*. In consequence, (8.26) and (8.27) enforce the continuity of both components of $\vec{J}^{\pm}$ and $\vec{M}^{\pm}$. This problem in general has no solution since through two field conditions one cannot enforce four different source conditions over the edges. Indeed, one can understand this when compared with EFIE and MFIE -section 8.1.2-, where two field conditions are automatically well satisfied with two source conditions. Indeed, a linear combination of EFIE and MFIE cannot be developed in general since the required expanding functions for $\vec{J}^{\pm}$ and $\vec{M}^{\pm}$ are different in both cases.

Despite everything, some formulations for the CFIE - X. Sheng *et al.* [44]- and for the PMCHW - K. Umashankar *et al.* [25]- have been carried out using the *RWG* set. These formulations are advantageous because they yield a solution free of the interior resonance corruption; indeed, it is widely known that the EFIE and MFIE approaches cannot supply an accurate solution in this case. In the development of these formulations, though, the field and the magnetic conditions at the edges can not be accomplished completely. This involves that their use may be restricted to particular and simple cases where the performance of these operators can be acceptable. Indeed, this can be the case of a single penetrable sphere -without interior resonances-.

It is shown in the following sections -8.1.3.1 and 8.1.3.2- a thorough study for the PMCHW operator, which was presented by Umashankar and Taflove [25] for the case of homogeneous lossy dielectric objects. In 8.1.3.1, it is shown the field condition enforced over the edges, which makes the field and current requirements compatible. In 8.1.3.2, it is analysed the capacity of this field constraint on the edges to approach the electromagnetic requirements on the polyhedron. It is reasoned the range of problems with satisfactory behaviour for the PMCHW, which, on the other hand, embraces a significant variety of problems, but of course not all.

8.1.3.1 Field conditions on the edges to yield a compatible problem in PMCHW

According to the structure of the operator shown in (8.3), the field conditions enforced across the edges can be the subtraction of the magnetic and electric field conditions at both sides of the edges -see (8.10) and (8.21)-; that is,

$$\vec{n}\cdot\left(\vec{E}_1^{+}-\vec{E}_2^{+}\right)\Big|_{\vec{r}\in\partial_i}-\vec{n}\cdot\left(\vec{E}_1^{-}-\vec{E}_2^{-}\right)\Big|_{\vec{r}\in\partial_i}=\frac{\tau_e^{+}}{\varepsilon^{+}}\Big|_{\vec{r}\in\partial_i}-\frac{\tau_e^{-}}{\varepsilon^{-}}\Big|_{\vec{r}\in\partial_i} \tag{8.28}$$

$$\vec{n}\cdot\left(\vec{H}_1^{+}-\vec{H}_2^{+}\right)\Big|_{\vec{r}\in\partial_i}-\vec{n}\cdot\left(\vec{H}_1^{-}-\vec{H}_2^{-}\right)\Big|_{\vec{r}\in\partial_i}=\frac{\tau_m^{+}}{\mu^{+}}\Big|_{\vec{r}\in\partial_i}-\frac{\tau_m^{-}}{\mu^{-}}\Big|_{\vec{r}\in\partial_i} \tag{8.29}$$

In view of (8.7), the previous expressions become

$$\vec{n}\cdot\left(\vec{E}_1^{+}-\vec{E}_2^{+}\right)\Big|_{\vec{r}\in\partial_i}-\vec{n}\cdot\left(\vec{E}_1^{-}-\vec{E}_2^{-}\right)\Big|_{\vec{r}\in\partial_i}=\left(\frac{1}{\varepsilon^{+}}+\frac{1}{\varepsilon^{-}}\right)\tau_e^{+}\Big|_{\vec{r}\in\partial_i} \tag{8.30}$$

$$\vec{n}\cdot\left(\vec{H}_1^{+}-\vec{H}_2^{+}\right)\Big|_{\vec{r}\in\partial_i}-\vec{n}\cdot\left(\vec{H}_1^{-}-\vec{H}_2^{-}\right)\Big|_{\vec{r}\in\partial_i}=\left(\frac{1}{\mu^{+}}+\frac{1}{\mu^{-}}\right)\tau_m^{+}\Big|_{\vec{r}\in\partial_i} \tag{8.31}$$

In an analogous way as in PeC-EFIE, and the dielectric EFIE and MFIE, the field expressions show a dependence on the linear charge densities on $\vec{r}\in\partial_i$, which yields an ambiguity. In this case, there are two independent sources of ambiguity, $\tau_e^{\pm}$ and $\tau_m^{\pm}$. Since there are two field conditions, (8.30) and (8.31), and four independent source magnitudes - $\vec{J}^{\pm}$, $\vec{M}^{\pm}$, $\tau_e^{\pm}$ and $\tau_m^{\pm}$- there are two degrees of freedom per edge, which involves that the PMCHW is more undetermined than the EFIE and MFIE. Therefore its condition number must be accordingly higher. Similarly, the rate of growth of the condition number as the discretization becomes finer must also be steeper.

It is thus required the imposition $\tau_e^{\pm}=0$ and $\tau_m^{\pm}=0$ to find a solution, which is as robust as low the condition number is. The ruling field conditions over the edges then become

$$\vec{n}\cdot\left(\vec{E}_1^{+}-\vec{E}_2^{+}\right)\Big|_{\vec{r}\in\partial_i}-\vec{n}\cdot\left(\vec{E}_1^{-}-\vec{E}_2^{-}\right)\Big|_{\vec{r}\in\partial_i}=0 \tag{8.32}$$

$$\vec{n}\cdot\left(\vec{H}_1^{+}-\vec{H}_2^{+}\right)\Big|_{\vec{r}\in\partial_i}-\vec{n}\cdot\left(\vec{H}_1^{-}-\vec{H}_2^{-}\right)\Big|_{\vec{r}\in\partial_i}=0 \tag{8.33}$$

Furthermore, in view of (8.12) and its corresponding dual condition, the left-hand side terms of (8.32) and (8.33) become

$$\begin{aligned}&\vec{n}_{c,1}{}^{+}\cdot\vec{E}_1^{+}\Big|_{\vec{r}\in\partial_i}+\vec{n}_{c,2}{}^{+}\cdot\vec{E}_2^{+}\Big|_{\vec{r}\in\partial_i}-\vec{n}_{c,1}{}^{-}\cdot\vec{E}_1^{-}\Big|_{\vec{r}\in\partial_i}-\vec{n}_{c,2}{}^{-}\cdot\vec{E}_2^{-}\Big|_{\vec{r}\in\partial_i}\\&=\frac{1}{-j\omega\varepsilon^{+}}\left(\vec{n}_{c,1}{}^{+}\cdot\vec{J}_1^{+}+\vec{n}_{c,2}{}^{+}\cdot\vec{J}_2^{+}\right)\Big|_{\vec{r}\in\partial_i}-\frac{1}{-j\omega\varepsilon^{-}}\left(\vec{n}_{c,1}{}^{-}\cdot\vec{J}_1^{-}+\vec{n}_{c,2}{}^{-}\cdot\vec{J}_2^{-}\right)\Big|_{\vec{r}\in\partial_i}\end{aligned} \tag{8.34}$$

$$\begin{aligned}&\vec{n}_{c,1}^{\,+}\cdot\vec{H}_1^{+}\Big|_{\vec{r}\in\partial_i}+\vec{n}_{c,2}^{\,+}\cdot\vec{H}_2^{+}\Big|_{\vec{r}\in\partial_i}-\vec{n}_{c,1}^{\,-}\cdot\vec{H}_1^{-}\Big|_{\vec{r}\in\partial_i}-\vec{n}_{c,2}^{\,-}\cdot\vec{H}_2^{-}\Big|_{\vec{r}\in\partial_i}\\&=\frac{1}{-j\omega\mu^{+}}\left(\vec{n}_{c,1}^{\,+}\cdot\vec{M}_1^{+}+\vec{n}_{c,2}^{\,+}\cdot\vec{M}_2^{+}\right)\Big|_{\vec{r}\in\partial_i}-\frac{1}{-j\omega\mu^{-}}\left(\vec{n}_{c,1}^{\,-}\cdot\vec{M}_1^{-}+\vec{n}_{c,2}^{\,-}\cdot\vec{M}_2^{-}\right)\Big|_{\vec{r}\in\partial_i}\end{aligned}\tag{8.35}$$

which, resorting to (8.4), become

$$\begin{aligned}&\vec{n}_{c,1}^{\,+}\cdot\vec{E}_1^{+}\Big|_{\vec{r}\in\partial_i}+\vec{n}_{c,2}^{\,+}\cdot\vec{E}_2^{+}\Big|_{\vec{r}\in\partial_i}-\vec{n}_{c,1}^{\,-}\cdot\vec{E}_1^{-}\Big|_{\vec{r}\in\partial_i}-\vec{n}_{c,2}^{\,-}\cdot\vec{E}_2^{-}\Big|_{\vec{r}\in\partial_i}\\&=-\frac{1}{j\omega}\left(\frac{1}{\varepsilon^{+}}+\frac{1}{\varepsilon^{-}}\right)\left(\vec{n}_{c,1}^{\,+}\cdot\vec{J}_1^{+}+\vec{n}_{c,2}^{\,+}\cdot\vec{J}_2^{+}\right)\Big|_{\vec{r}\in\partial_i}\end{aligned}\tag{8.36}$$

$$\begin{aligned}&\vec{n}_{c,1}^{\,+}\cdot\vec{H}_1^{+}\Big|_{\vec{r}\in\partial_i}+\vec{n}_{c,2}^{\,+}\cdot\vec{H}_2^{+}\Big|_{\vec{r}\in\partial_i}-\vec{n}_{c,1}^{\,-}\cdot\vec{H}_1^{-}\Big|_{\vec{r}\in\partial_i}-\vec{n}_{c,2}^{\,-}\cdot\vec{H}_2^{-}\Big|_{\vec{r}\in\partial_i}\\&=-\frac{1}{j\omega}\left(\frac{1}{\mu^{+}}+\frac{1}{\mu^{-}}\right)\left(\vec{n}_{c,1}^{\,+}\cdot\vec{M}_1^{+}+\vec{n}_{c,2}^{\,+}\cdot\vec{M}_2^{+}\right)\Big|_{\vec{r}\in\partial_i}\end{aligned}\tag{8.37}$$

Evidently, to merge (8.32) and (8.36) in one condition regarding the source magnitudes, it must be accomplished

$$\left(\vec{n}_{c,1}^{\,\pm}\cdot\vec{J}_1^{\pm}+\vec{n}_{c,2}^{\,\pm}\cdot\vec{J}_2^{\pm}\right)\Big|_{\vec{r}\in\partial_i}=0\tag{8.38}$$

and, analogously, for (8.33) and (8.37),

$$\left(\vec{n}_{c,1}^{\,\pm}\cdot\vec{M}_1^{\pm}+\vec{n}_{c,2}^{\,\pm}\cdot\vec{M}_2^{\pm}\right)\Big|_{\vec{r}\in\partial_i}=0\tag{8.39}$$

which are the conditions for the electric and the magnetic current to yield the electric and magnetic field boundary conditions (8.36) and (8.37) over an arbitrary edge. Note that they are coincident with the electric and magnetic charge conditions with the assumed required imposition $\tau_e^{\pm}=\tau_m^{\pm}=0$.

Furthermore, from the theorem of equivalence and the well-known expressions

$$\vec{E}_{\{12\}}^{\pm}\Big|_{\vec{r}\in\partial_i}=\hat{n}_{\{12\}}^{\pm}\times\vec{M}_{\{12\}}^{\pm}\Big|_{\vec{r}\in\partial_i}\qquad\vec{H}_{\{12\}}^{\pm}\Big|_{\vec{r}\in\partial_i}=-\hat{n}_{\{12\}}^{\pm}\times\vec{J}_{\{12\}}^{\pm}\Big|_{\vec{r}\in\partial_i}\tag{8.40}$$

introduced in the left-hand side terms of the field conditions (8.32) and (8.33), one can write

$$\vec{n}_{c,1}^{\,+}\cdot\left(\hat{n}_1^{+}\times\vec{M}_1^{+}\right)\Big|_{\vec{r}\in\partial_i}+\vec{n}_{c,2}^{\,+}\cdot\left(\hat{n}_2^{+}\times\vec{M}_2^{+}\right)\Big|_{\vec{r}\in\partial_i}-\vec{n}_{c,1}^{\,-}\cdot\left(\hat{n}_1^{-}\times\vec{M}_1^{-}\right)\Big|_{\vec{r}\in\partial_i}-\vec{n}_{c,2}^{\,-}\cdot\left(\hat{n}_2^{-}\times\vec{M}_2^{-}\right)\Big|_{\vec{r}\in\partial_i}\tag{8.41}$$

$$\vec{n}_{c,1}^{\,+}\cdot\left(\hat{n}_1^{+}\times\vec{J}_1^{+}\right)\Big|_{\vec{r}\in\partial_i}+\vec{n}_{c,2}^{\,+}\cdot\left(\hat{n}_2^{+}\times\vec{J}_2^{+}\right)\Big|_{\vec{r}\in\partial_i}-\vec{n}_{c,1}^{\,-}\cdot\left(\hat{n}_1^{-}\times\vec{J}_1^{-}\right)\Big|_{\vec{r}\in\partial_i}-\vec{n}_{c,2}^{\,-}\cdot\left(\hat{n}_2^{-}\times\vec{J}_2^{-}\right)\Big|_{\vec{r}\in\partial_i}\tag{8.42}$$

If it is taken into account that $\hat{n}^{+}=-\hat{n}^{+}$, $\hat{n}_c^{+}=\hat{n}_c^{-}$ and (8.4), (8.41) and (8.42) yield zero, as imposed in (8.32) and in (8.33), irrespective of the values of the current. This means that the only two necessary source conditions to fulfil the field conditions (8.32) and (8.33) are

the electric and magnetic charge conditions (8.38) and (8.39). This is advantageous because, being the two new field requirements over the edges accomplished through two source conditions, the problem becomes well posed. That is, there is a solution for $\vec{J}^{\pm}$ and $\vec{M}^{\pm}$ capable to fulfil the field boundary conditions on the edges (8.32) and (8.33).

However, the field boundary conditions (8.32) and (8.33) do not correspond to the required field boundary conditions to settle the dielectric polyhedron solution according to the Maxwell equations. That is, as it also happened when describing the PeC-MFIE(*unxRWG,RWG*), the enforced field boundary conditions do not correspond exactly to the electromagnetic boundary conditions derived from the Maxwell equations, although they approach. Indeed, PMCHW ensures the subtraction of the electric and magnetic field boundary conditions at the two sides of an arbitrary edge. On the other hand, the field boundary conditions deducted from the Maxwell equations demand the separate accomplishment of the electric and magnetic field boundary conditions at each side of the edge. Of course, if the conditions are ensured at both sides, so is the subtraction; but one cannot say so if one enforces only the subtraction. Therefore, the PMCHW operator must only give an appropriate solution whenever the adopted and less stringent field boundary conditions accomplish the required continuity separately at both sides.

The proof of the fact that the field conditions (8.32) and (8.33) do not enforce the electromagnetic solution of the polyhedron can be shown falling back on (8.30) and (8.31). If one applies again the expressions in (8.40) relating fields and currents, one obtains

$$\begin{aligned}&\vec{n}_{c,1}{}^{+}\cdot\left(\hat{n}_1^{+}\times\vec{M}_1^{+}\right)\Big|_{\vec{r}\in\partial_i}+\vec{n}_{c,2}{}^{+}\cdot\left(\hat{n}_2^{+}\times\vec{M}_2^{+}\right)\Big|_{\vec{r}\in\partial_i}\\&-\vec{n}_{c,1}{}^{-}\cdot\left(\hat{n}_1^{-}\times\vec{M}_1^{-}\right)\Big|_{\vec{r}\in\partial_i}-\vec{n}_{c,2}{}^{-}\cdot\left(\hat{n}_2^{-}\times\vec{M}_2^{-}\right)\Big|_{\vec{r}\in\partial_i}=\left(\frac{\tau_e^{+}}{\varepsilon^{+}}-\frac{\tau_e^{-}}{\varepsilon^{-}}\right)\Big|_{\vec{r}\in\partial_i}\end{aligned}\tag{8.43}$$

$$\begin{aligned}&\vec{n}_{c,1}{}^{+}\cdot\left(\hat{n}_1^{+}\times\vec{J}_1^{+}\right)\Big|_{\vec{r}\in\partial_i}+\vec{n}_{c,2}{}^{+}\cdot\left(\hat{n}_2^{+}\times\vec{J}_2^{+}\right)\Big|_{\vec{r}\in\partial_i}\\&-\vec{n}_{c,1}{}^{-}\cdot\left(\hat{n}_1^{-}\times\vec{J}_1^{-}\right)\Big|_{\vec{r}\in\partial_i}-\vec{n}_{c,2}{}^{-}\cdot\left(\hat{n}_2^{-}\times\vec{J}_2^{-}\right)\Big|_{\vec{r}\in\partial_i}=\left(\frac{\tau_m^{+}}{\mu^{+}}-\frac{\tau_m^{-}}{\mu^{-}}\right)\Big|_{\vec{r}\in\partial_i}\end{aligned}\tag{8.44}$$

If one applies on the left-hand side terms the relation of the expressions at both sides - $\hat{n}^{+}=-\hat{n}^{-}$, $\hat{n}_c^{+}=\hat{n}_c^{-}$ and (8.4)-, it is obtained a zero on the left side, which compels

$$\left(\frac{\tau_e^{+}}{\varepsilon^{+}}-\frac{\tau_e^{-}}{\varepsilon^{-}}\right)\Big|_{\vec{r}\in\partial_i}=0\quad\left(\frac{\tau_m^{+}}{\mu^{+}}-\frac{\tau_m^{-}}{\mu^{-}}\right)\Big|_{\vec{r}\in\partial_i}=0\tag{8.45}$$

This is absurd because it disagrees with the electromagnetic expressions in (8.3), which, in turn, derive from the application of the theorem of equivalence on the dielectric polyhedron and thus assume that $\vec{M}^{+}=-\vec{M}^{-}$ and $\vec{J}^{+}=-\vec{J}^{-}$. Note that this is another proof that the PMCHW cannot be well set because of the discretization; indeed, $\tau_e^{\pm}$ and $\tau_m^{\pm}$ only appear in the polyhedron.

The previous analysis for the PMCHW confirms the formulation presented by Umashankar and Taflove [25]. Indeed, since the required conditions for the electric and magnetic current over the edges -(8.38) and (8.39)- demand continuity of the normal component,

RWG is a low-order suitable set to expand $\vec{M}^{\pm}$ and $\vec{J}^{\pm}$. Similarly, since the adopted field boundary conditions on the edges demand normal continuity across the edges for the magnitudes $\left(\vec{E}^{+}-\vec{E}^{-}\right)$ and $\left(\vec{H}^{+}-\vec{H}^{-}\right)$, it is also justified the use of *RWG* as weighting set.

8.1.3.2 Discussion about the resemblance of the solution given by PMCHW with the Maxwell-consistent solution of the polyhedron

The electric and magnetic field conditions ensured by the PMCHW are less stringent than the Maxwell requirements. It is assessed in this section the range of validity of the PMCHW approach, which relies on the capacity to fulfil the complete electromagnetic requirement.

One can equivalently understand the dielectric operators through the revision of each of the valid PeC operators shown in Chapter 6. In view of the expression of PMCHW in terms of the PeC-operators -see (8.3)-, the Umashankar and Taflove choice enforces the use of the basic PeC-operators PeC-EFIE(*RWG*,*RWG*) and PeC-MFIE(*RWG*,*RWG*). According to Chapter 6, the part of the PMCHW operator relying on PeC-EFIE(*RWG*,*RWG*) is well defined, which makes sense because the chosen conditions correspond to the electric and magnetic charge conditions. However, the PeC-MFIE(*RWG*,*RWG*) is not at all well defined because the magnetic field due to *RWG* on the perfectly conducting polyhedron presents continuity of the tangential component, which disagrees with the space spanned by *RWG* as weighting set, with continuity of the normal component. Therefore, PeC-MFIE(*RWG*,*RWG*) must account for the presumable misbehaviour of PMCHW. It is very important to assess hence in which terms this part of the operator is relevant for the solution.

As the PMCHW operator results from the subtraction of the magnetic and electric fields at both sides, the operators that must be actually taken into account are the subtraction of PeC-EFIE and PeC-MFIE updated with the corresponding dielectric constants at both sides -see (8.3)-. That is, $\vec{E}^{S\,+}_{PeC}\big|_{\vec{r}\in S^-} - \vec{E}^{S\,-}_{PeC}\big|_{\vec{r}\in S^+}$, $\vec{H}^{S\,+}_{PeC}\big|_{\vec{r}\in S^-} - \vec{H}^{S\,-}_{PeC}\big|_{\vec{r}\in S^+}$. Allowing for (8.4), they result in

$$\vec{E}^{S\,+}_{PeC}\left(\vec{J}^{+}\right)\Big|_{\vec{r}\in S^-} - \vec{E}^{S\,-}_{PeC}\left(\vec{J}^{-}\right)\Big|_{\vec{r}\in S^+} = \left[\vec{E}^{S\,+}_{PeC}\Big|_{\vec{r}\in S^-} + \vec{E}^{S\,-}_{PeC}\Big|_{\vec{r}\in S^+}\right]\left(\vec{J}^{+}\right) \tag{8.46}$$

$$\vec{H}^{S\,+}_{PeC}\left(\vec{J}^{+}\right)\Big|_{\vec{r}\in S^-} - \vec{H}^{S\,-}_{PeC}\left(\vec{J}^{-}\right)\Big|_{\vec{r}\in S^+} = \left[\vec{H}^{S\,+}_{PeC}\Big|_{\vec{r}\in S^-} + \vec{H}^{S\,-}_{PeC}\Big|_{\vec{r}\in S^+}\right]\left(\vec{J}^{+}\right) \tag{8.47}$$

According to the general integral expressions presented in Chapter 2, both integral operators rely on two terms: the Cauchy principal value contribution and the integration of the singularity. The Cauchy principal values are computed by means of the discretization of the space and depend on the dielectric parameters, $\eta^{\pm}$ and $k^{\pm}$. That is why in general they do not sum to zero. Moreover, even with the same dielectric characteristics at both sides, they add in phase.

The integration of the singularity is only non-null for PeC-MFIE and is carried out analytically through the solid angle value $\Omega_0^{\pm}$ and the unitary normal vectors $\hat{n}^{+}=-\hat{n}^{-}$. In

accordance with the planar characteristic inside the facets of the polyhedron, $\Omega_0^{\pm} = 2\pi$ must be taken. Falling back on the analytical expression for this term presented in Chapter 2, one sees that the sum is identically null. Indeed,

$$\left[\vec{H}_{PeC}^{S}{}^{+}\Big|_{\text{sing},\vec{r}\in S^-} + \vec{H}_{PeC}^{S}{}^{-}\Big|_{\text{sing},\vec{r}\in S^+}\right]\left(\vec{J}^+\right) = \frac{1}{2}\left(\vec{J}^+(\vec{r})\times\hat{n}^- + \vec{J}^+(\vec{r})\times\hat{n}^+\right) = 0 \qquad (8.48)$$

This fact implies that through the subtraction in (8.3), a very important part of the rank of the original PeC-MFIE can be ignored.

Therefore, the development of PMCHW, which imposes the use of PeC-MFIE(*RWG,RWG*), has to allow only for the Cauchy principal value contribution. This term is ill-defined since its rank ensures the tangential component of the field to be continuous but the space spanned by the weighting functions space presents continuity of the normal component. This does not necessarily imply that the inner-product between both spaces is null. Indeed, in general, the corresponding impedance terms are non-null. Logically, according to the MoM theory, the solution will present a minimum norm-error with the weighting space. Note that the cancellation of the terms due to the integration of the singularity is very advantageous since, as shown in (8.48), their analytical expression does not only ensure continuity of the tangential component -as corresponds to PeC-MFIE(*RWG*)- but it is orthogonal to the Weighting space, whereby not even a minimum norm-error solution could ever be attained.

An inherent error in the PMCHW has to be assumed in any case. However, the importance of this error relies on the relevance of the contribution of PeC-MFIE in the particular dielectric problem. Note that the presence of this error is equivalent to the impossibility for the PMCHW operator to accomplish the normal continuity of the field components at both sides Indeed, as the PeC-MFIE(*RWG,RWG*) terms become more important, the normal field components across the edges at both sides become more discontinuous and therefore the electromagnetic requirements are less well satisfied. So, this PMCHW operator must provide good results as long as the PeC-MFIE contribution in the operator for that specific problem is insignificant in comparison to the PeC-EFIE contribution.

In Chapter 6, the formal structure of the PeC-MFIE(*RWG*) operator is presented. It is remarkable the fact that the influences between nearly coplanar facets tend to zero. Indeed, when $\vec{r}' \to \vec{r}$, $\nabla G(\vec{r}-\vec{r}') \propto (\vec{r}-\vec{r}')$ is nearly coplanar with $\vec{\rho}_q'^{\pm}$, whereby the core of the PeC-MFIE operator $\left[\nabla G(\vec{r}-\vec{r}')\times\vec{\rho}_q'^{\pm}\right]$ tends to be normal to the surface and thus perpendicular to the weighting vector. Therefore, when involving near facets, which are those that present the most important contribution, the PeC-MFIE contribution must be comparatively much less important than the PeC-EFIE one. It must be pointed out that the PeC-MFIE operator relies in this case much on the integration of the singularity. However, as above-mentioned, this contribution is irrelevant for the PMCHW operator. Hence, in bodies where the most important influences coming from the PeC-MFIE operator involve facets that are coplanar or nearly coplanar, the inherent error associated to PMCHW must be least remarkable. This is the case, for instance, of single bodies.

In other problems, though, there appear important influences between facets that are not on the same surface. It is outstanding in this case the PeC-MFIE influence between near triangles facing each other in parallel planes. Indeed, as shown in Fig. 8.1, being

$\nabla G(\vec{r}-\vec{r}') \propto (\vec{r}-\vec{r}')$ perpendicular to both the source and field vectors, $\vec{\rho}'^{\pm}_{q}$ and $\vec{\rho}^{\pm}_{s}$, $\left[\nabla G(\vec{r}-\vec{r}')\times\vec{\rho}'^{\pm}_{q}\right]$ lies in the weighting domain of $\vec{\rho}^{\pm}_{s}$. Hence, the PeC-MFIE influence is now most enhanced in comparison with the PeC-EFIE one.

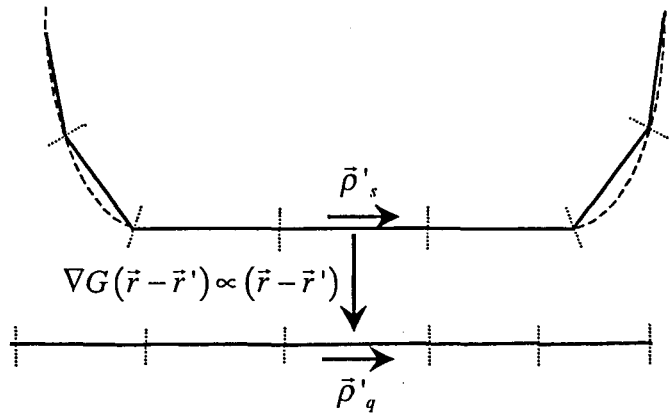

Fig. 8.1 The PeC-MFIE influence is relevant on facets facing each other

This error must become especially critical for structures with a conducting and a penetrable region facing each other with a small gap between. The physical solution for the magnetic current on the penetrable side must tend to zero because it is indeed null on the conducting side. Therefore, the fields on the penetrable side must rely essentially on the electric current contribution. This implies that the magnetic field definition on the penetrable side cannot be well satisfied because it depends mostly on the PeC-MFIE term.

8.1.4 Influence of the low-order expansion of the current on the performance of EFIE-MFIE

With the imposition of *no charge accumulation*, the solution for $\vec{J}^{\pm}$ and $\vec{M}^{\pm}$ is fixed. That is, among all the possible solutions associated to the inherent ambiguity of the problem, it is chosen a solution with $\tau_e^{\pm}$ and $\tau_m^{\pm}$ identically null. Of course, as long as the condition number is low enough -the system is little undetermined-, there is very little difference among the different solutions and the fixed solution can be taken in practice as the unique solution of the physical polyhedron. This is the case for the conducting bodies shown in Chapter 7. The previous sections 8.1.1, 8.1.2 and 8.1.3 have to assume a well-determined solution for $\vec{J}^{\pm}$ and $\vec{M}^{\pm}$ to build the current and field edge requirements.

In the PeC-polyhedron, the edge requirements are to be ensured for only one field magnitude, either the electric or the magnetic field. Indeed, since for the perfectly conducting case the surface component of the total electric field is zero, the magnetic current must be zero. Therefore, one has to enforce the boundary condition for one field magnitude -either the electric or the magnetic field- and for one source magnitude -the electric current-.

In the dielectric case, though, one has to ensure the correct definition of both the electric and magnetic fields since one disposes of two independent source magnitudes, $\vec{M}^{\pm}$ and $\vec{J}^{\pm}$. Moreover, as shown in the previous sections, PMCHW, EFIE and MFIE ensure the normal continuity across the edges respectively of the pairs of magnitudes $\left(\vec{E}^{+}-\vec{E}^{-}\right)|\left(\vec{H}^{+}-\vec{H}^{-}\right)$, $\vec{E}^{+}|\vec{E}^{-}$ and $\vec{H}^{+}|\vec{H}^{-}$. It is surprising the fact that the EFIE and MFIE approaches do not demand any continuity requirement respectively for the magnetic and the electric field if they both implicitly depend on the good definition of these magnitudes. Indeed, the integral expressions of the scattered fields $\vec{E}^{s\pm}$ and $\vec{H}^{s\pm}$ depend on $\vec{J}^{\pm}$ and $\vec{M}^{\pm}$, which in turn are univocally related with $\vec{H}^{\pm}$ and $\vec{E}^{\pm}$ through (8.15) and (8.23).

The theoretical reasoning in 8.1.2 assumes a complete expansion of the current, which leads to the -in practice- unique solution for $\vec{J}^{\pm}$ and $\vec{M}^{\pm}$. This implies that, as long as the source magnitudes are completely expanded, the ignored field requirements in the EFIE and in the MFIE, respectively the magnetic and the electric field, become automatically incorporated. This accounts for the apparent contradiction in the paragraph above because with the complete expansion one achieves the continuous expression of $\vec{J}^{\pm}$ and $\vec{M}^{\pm}$, whereby the dual field edge requirements are not needed anymore and can be thus indeed ignored.

The sets of any order belonging to the curl-conforming and the divergence-conforming functions groups ensure the continuity of one component. So as to achieve a complete expansion of a magnitude, the continuity of the other component must be enforced as well. This can only be effectuated through an infinite series grouping together the terms of all the orders belonging to the same fundamental group of expanding functions -curl- or divergence-conforming-. Evidently, the total continuity for the expanded magnitude will only be ensured in the limit when embracing all the contributions, which is of course in practice unachievable. One has to make do with a high enough expansion that, in any case, performs often satisfactorily.

For the PeC-operators and the dielectric PMCHW, the currents and the fields correspond to a low-order expansion of the physical fields and currents. For the dielectric EFIE and MFIE, though, the situation is particularly different. The theoretical study in 8.1.2 shows that the field requirements can rely only on one field magnitude as long as the expansion of the source magnitudes $\vec{J}^{\pm}$ and $\vec{M}^{\pm}$ is accurate enough. Therefore, the relevance of the error relies on the capacity of the chosen expansion to expand precisely the physical current. If a too low-order expansion for the current is assumed, the dual field requirements cannot in general be ignored, and thus the problem may be badly posed. The importance of this error in the performance of EFIE-MFIE depends on the characteristics of the physical currents for a given problem. One can intuitively asses that it must be especially critical in bodies with small electrical dimensions because in that case the influence of the physical edges becomes very important. It is reasonable that for electrically larger bodies a low-order expansion through patches of size $0.1\lambda_d$ can be satisfactory. Increasing the order of the expansion of the current can diminish this error. For example, in physical polyhedrons, this can be done through the overdiscretization of the planar faces.

Similarly, this misbehaviour of EFIE-MFIE must be most important in any structure with only penetrable regions -preferably with regions of small electrical dimensions-. For problems with some conducting region, though, the effect of this error must be lessened

since over the conducting surface, only one field condition is required -the dual condition is indeed ignored-. Therefore, the EFIE and MFIE become robust throughout the interface surface with the conducting region. Indeed, the evident improvement relies on the good definition of the PeC-EFIE and the PeC-MFIE.

8.1.5 Conclusions

1. An increasingly fine discretization applied in a dielectric polyhedron produces an increasing condition number for any operator. In an analogous way as shown for the PeC-EFIE, one has to impose the constraint of *no electric and magnetic charge accumulation* to define the current - $\vec{J}^{\pm}$, $\vec{M}^{\pm}$ - and field spaces. Of course, the problem will always carry an inherent ambiguity, which can be satisfied as long as the discretization is not very fine. In order to obtain the definition of the rank and domain spaces it has been assumed $\tau_e^{\pm}=0$ for EFIE, $\tau_m^{\pm}=0$ for MFIE and $\tau_e^{\pm}=\tau_m^{\pm}=0$ for PMCHW.

2. For all the dielectric operators -EFIE, MFIE and PMCHW-, the system is inherently ambiguously defined. The EFIE and MFIE dielectric operators must behave in a similar way in regard to the value of the condition number -the same accuracy and degree of discretization-. The PMCHW operator must present worse condition number as the discretization becomes finer because it disposes of two degrees of freedom to accomplish the edge flux density continuity conditions. On the other hand, EFIE-MFIE dispose of one degree of freedom, which represents a lower degree of ambiguity. At last, PeC-EFIE, with only one degree of freedom and one source magnitude ambiguously defined per edge must yield a lower condition number for the same number of edges.

3. To develop the different dielectric operators for an arbitrary dielectric polyhedron, different boundary conditions over the edges must be enforced. EFIE and MFIE must respectively ensure the continuity of the normal component of the electric and the magnetic flux density across the edges. It is impossible to find a solution for PMCHW enforcing at the same time the edge requirements of EFIE and MFIE, which are antagonistic. However, it is possible to build consistently the PMCHW operator by enforcing the continuity of the normal component of the subtraction of the electric and magnetic fields at both sides of the interface surface.

4. The PMCHW operator in general does not accomplish the electromagnetic requirements. This is due to the bad definition of the PeC-MFIE(*RWG,RWG*), which enforces continuity of the tangential component of the fields. However, this inherent error associated to the PMCHW operator must be less important whenever the PeC-MFIE contribution is very little compared to the PeC-EFIE one. This happens in isolated penetrable bodies, where the uppermost PeC-MFIE influences are due to coplanar or nearly coplanar facets. In more complex structures, such as multilayered bodies or groups of disjoint bodies in proximity, this error is more important because there can be facets facing each other in parallel surfaces, where the PeC-MFIE contribution becomes important. In case there is a conducting and penetrable region facing closely each other, this error must become much more relevant. Indeed, since the magnetic current is close to zero along the side of the penetrable region, the magnetic field is most influenced by the badly posed PeC-MFIE contribution.

5. All the requirements to define $\vec{J}^{\pm}$ and $\vec{M}^{\pm}$ properly demand *no charge accumulation.* The EFIE and the MFIE demand respectively no electric and no magnetic charge accumulation, meanwhile the PMCHW demands both. That is why the use of patch-based functions, which focus on the patches and ignore the edges, is suitable. In consequence, the use of approaches based on node-based finite elements to undertake the dielectric operators must turn out in general less accurate. Indeed, they cannot provide the necessary imposition of *no charge accumulation.*

6. In an analogous way as in the PeC case, this study has focused on the necessary conditions for the field and the current across the edges. The chosen *RWG* and *unxRWG* sets represent low-order expanding bases over the triangle subdomain. The higher-order bases enclosed in the wide families of the divergence-conforming and curl-conforming bases -where *RWG* and *unxRWG* respectively belong- stand for suitable bases as well. One has to assume thus in the results of this work the error due to the low-order expansion of the current, which must be different for each operator. Note that the expansion of the source magnitudes, $\vec{J}^{\pm}$ and $\vec{M}^{\pm}$, is effectuated by means of different sets for each operator. Indeed, the electric current is expanded by *RWG* in EFIE and PMCHW and by *unxRWG* in MFIE. Similarly, the magnetic current is expanded by *RWG* in MFIE and PMCHW and by *unxRWG* in EFIE.

7. The error due to the low-order expansion of the current is particularly critical for the EFIE and MFIE operators. The EFIE and MFIE approaches enforce either the magnetic or the electric field requirements and ignore the dual ones. All their theoretical behaviour and therefore their properties rely on an accurate enough expansion of the current because only in this case the ignorance of the dual field requirements is justified. The relevance of this error depends on the capacity of the chosen expansion to resemble the physical solution; in electrically small objects -with an important density of edges-, this error must be more evident. For electrically larger bodies, one expects that the usual choice for the subdomain size of $0.1\lambda_d$ can be sufficient. The effect of the low-order expansion for the EFIE and MFIE operators can be lessened by overdiscretizing the facets on the physical polyhedrons, which implies actually increasing the order of the discretization. In objects with conducting regions, the importance of this error must decrease since over the conducting interfaces only one field condition is required and thus the dual field requirement is implicitly ignored.

8.2 RESULTS FOR BODIES WITH TWO REGIONS SHAPING THE INTERFACE SURFACE

The implications of the theoretical study for the dielectric polyhedron are shown in the following subsections. It is shown first in 8.2.1 the values of the condition number for EFIE, MFIE and PMCHW. Secondly, in 8.2.2, the performance of the dielectric operators in electrically small structures with only penetrable regions is shown. It is assessed the relevance of the MFIE and EFIE error for electrically small physical polyhedrons. It is also presented in detail the improvement of the behaviour when undertaking the overdiscretization of the polyhedron, which corresponds effectively to a higher order expansion. In 8.2.3, some reference results are presented for electrically bigger bodies with penetrable regions, where it can be well assessed the fact that for regions of bigger electrical dimensions the EFIE-MFIE misbehaviour practically disappears. Finally, in 8.2.4, the performance of the dielectric operators in structures with the presence of a

conducting region is shown. In this case the error due to the less stringent field requirements in PMCHW becomes more noticeable and the EFIE and MFIE error declines since the operators are well defined on the conducting surface.

The particularisation of the PMCHW operator to this case can only yield the E-PMCHW operator -see Chapter 2-. This means that the EFIE is applied on the conductor. Note that, in accordance with the field requirements, which demand the use of *RWG* as weighting and expanding set, only the PeC-EFIE(*RWG,RWG*) can be used. Therefore, the theoretical alternative H-PMCHW must be dismissed since PeC-MFIE(*RWG,RWG*) is very ill-defined.

The dielectric EFIE and MFIE operators have been undertaken through the precise computation of the basic PeC-EFIE(*RWG,RWG*) and PeC-MFIE(*RWG,unxRWG*) in the terms mentioned in Chapter 7. The PMCHW operator relies also on the accurate development of PeC-EFIE(*RWG,RWG*) and PeC-MFIE(*RWG,RWG*). That is, the terms of higher-order are analytically integrated and a four-point Gaussian quadrature rule is employed for the low-order terms. The self-terms have been computed very precisely through the application of a four-point quadrature rule in the outer integral.

The PeC-MFIE(*RWG,RWG*) operator has been dismissed in Chapter 6 because it yields a null integration of the singularity. Therefore, one needs to concentrate only on the computation of the Cauchy principal contributions, which is straightforward because the source-integration is the same as the one shown in Chapter 6 for PeC-MFIE(*unxRWG,RWG*).

8.2.1 Conditioning of the matrices

In Table 8.1 the condition numbers of the impedance matrices associated to the dielectric operators EFIE, MFIE and PMCHW are shown for a homogeneous dielectric cube with side $0.05\lambda_0 = 0.1\lambda_d$ -$\varepsilon_r = 4$-.

N. of triangles	Cond. Number - EFIE	Cond. Number - MFIE	Cond. Number - PMCHW
48	506	351	633
192	1879	1340	4317
300	2641	1847	19515
432	3796	2657	31828

Table 8.1 Condition number of a cube with side of 0.1λ *and* $\varepsilon_r = 4$

In view of this table, the MFIE and EFIE values turn out to be of the same order of magnitude. The PMCHW values, though, show a steeper increase, as predicted; there is indeed an order of magnitude of difference from the 300 triangles on. It is also indicative the comparison of these values with the condition numbers of the PeC-EFIE for a cube of the same electrical dimensions in Table 7.1. Indeed, EFIE and MFIE show a faster progression than the PeC-EFIE, which confirms the inherent bigger ambiguity reasoned before.

In Chapter 2 it is presented the definition of the condition number as a ratio between the source and the field magnitudes. In the PeC case, the source magnitudes and the field magnitudes are the same for each operator. All the dielectric operators, though, present two

different source magnitudes: $\vec{J}$ and $\vec{M}$; furthermore, the PMCHW presents even two different field magnitudes: $\vec{H}$ and $\vec{E}$. Therefore, in order to compare the condition numbers of the different dielectric approaches, it is indispensable to normalise the field and source magnitudes so as to make them dimensionally compatible. Otherwise, the values of the condition number are enhanced according to the dimensional incompatibility. As shown in the duality properties in Chapter 2, one can pass from the magnetic dimensions to the electric ones -current and field- by means of a product by η_0, the wave-impedance in the vacuum. The condition numbers shown in Table 8.1 correspond to matrices that take this change into account.

8.2.2 Electrically small bodies with only penetrable regions

In 8.2.2.1 it is verified explicitly the existence of the EFIE and MFIE error due the low-order expansion of the current -explained in detail in 8.1.4-. It is also valued the relative smaller importance of the error in PMCHW. In 8.2.2.2 it is shown the reduction of the error of EFIE and MFIE on electrically small physical polyhedrons by carrying out a higher-order expansion of the current, which is fulfilled through the overdiscretization of the planar faces. It is accordingly confirmed that the PMCHW operator shows a much better performance. This implies that the error due to the less stringent field requirements in PMCHW is unimportant compared to the EFIE and MFIE low-order error for bodies with penetrable regions. In 8.2.2.3 some results for electrically small spheres are shown, where the effect of the physical edges becomes important with a coarse discretization.

8.2.2.1 Relevance of the EFIE-MFIE low-order error

It is effectuated the comparison of the results for two problems -with pretty small electrical dimensions- that theoretically provide the same solution for each of the three general approaches: EFIE, MFIE and PMCHW. It is thus proved the existence of the errors in the dielectric operators and their different relevance in the solution is compared. Indeed, the RCS for a single dielectric body and the RCS of a structure of two bodies, where one is the same as the first dielectric body and the other has $\varepsilon_r = 1$ -the constant of the free-space-, must be theoretically the same. By checking the performance for each of the dielectric operators, one can verify the importance of the inherent errors of the operators.

The bistatic RCS with an axial impinging plane wave are presented for two different pairs of disjoint objects -two cubes and a cone and a cylinder-.

- **Two cubes**

  The evolution of the bistatic RCS for the pair of disjoint cubes in Fig. 8.2 for the values of $d = 1e-5\lambda_0$ and $d = 0.05\lambda_0$ is presented for the three possible operators EFIE, MFIE and PMCHW -Fig. 8.3, Fig. 8.4 and Fig. 8.5-.

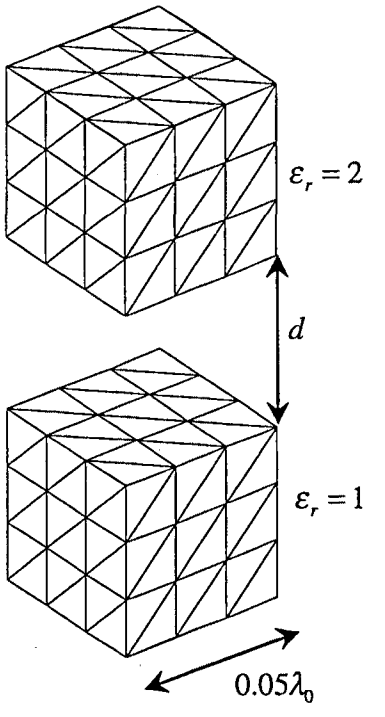

Fig. 8.2 Pair of cubes with 108 triangles each

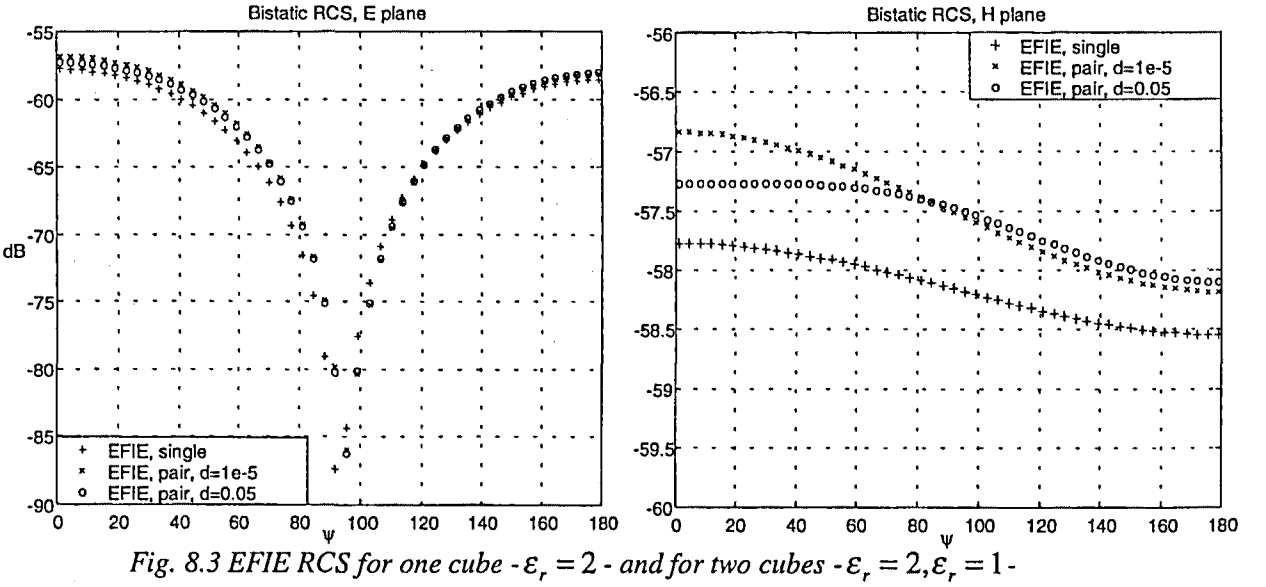

Fig. 8.3 EFIE RCS for one cube - $\varepsilon_r = 2$ - and for two cubes - $\varepsilon_r = 2, \varepsilon_r = 1$ -

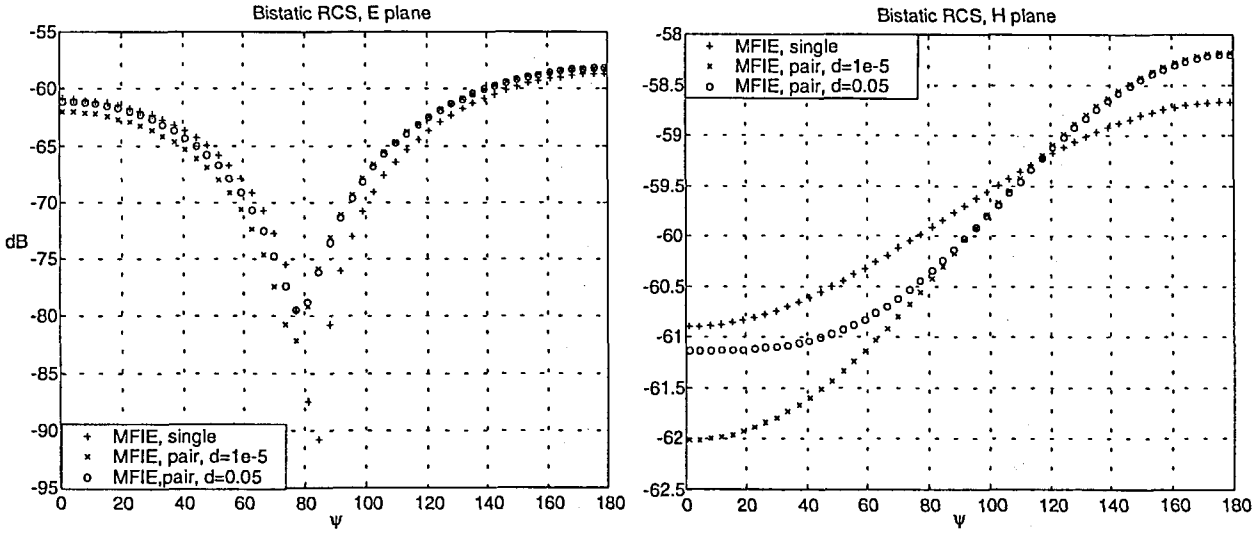

Fig. 8.4 MFIE RCS for one cube - $\varepsilon_r = 2$ - and for two cubes - $\varepsilon_r = 2$, $\varepsilon_r = 1$ -

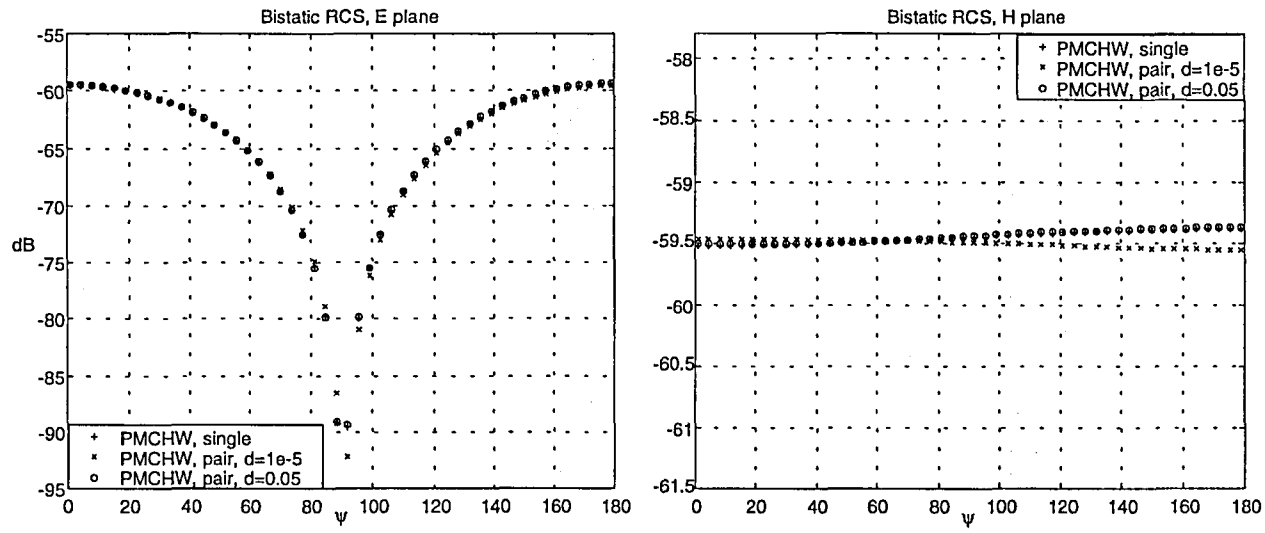

Fig. 8.5 PMCHW RCS for one cube - $\varepsilon_r = 2$ - and for two cubes - $\varepsilon_r = 2, \varepsilon_r = 1$ -

- **A cone and a cylinder**

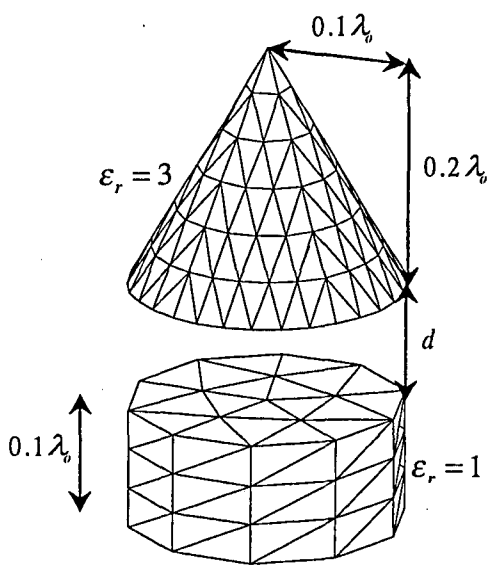

Fig. 8.6 Cone with 360 triangles and cylinder with 100 triangles

The evolution of the bistatic RCS for the cone and the cylinder in Fig. 8.6 for the values of $d = 1e-5\lambda_o$ and $d = 0.1\lambda_0$ is presented for the three possible operators EFIE, MFIE and PMCHW -Fig. 8.7, Fig. 8.8 and Fig. 8.9 -.

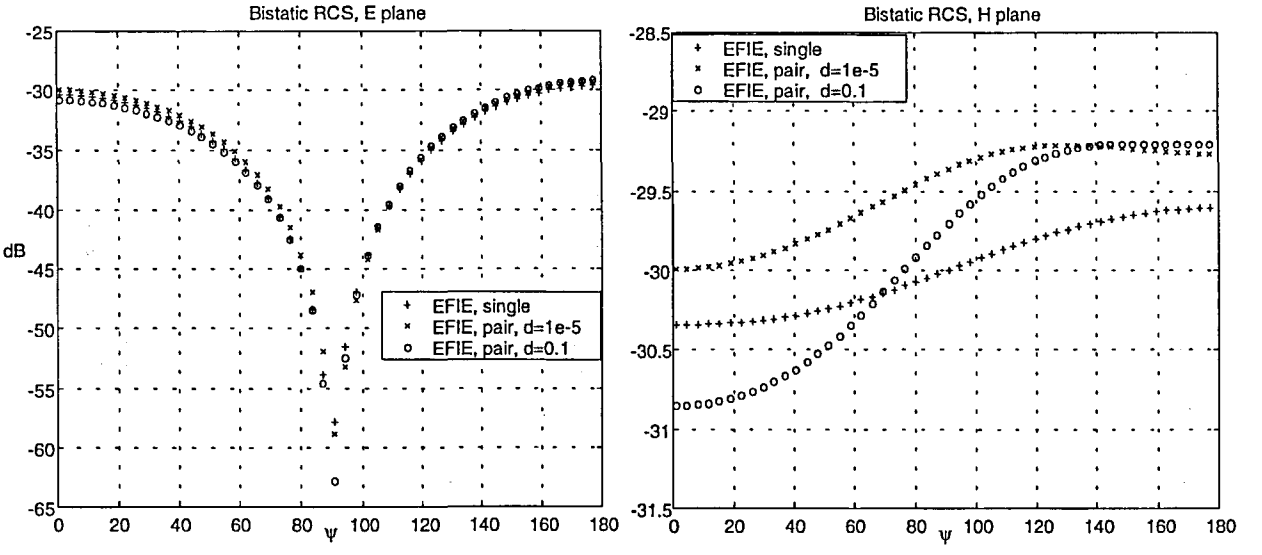

Fig. 8.7 EFIE RCS for one cone - $\varepsilon_r = 3$ *- and one cone-cylinder pair -* $\varepsilon_r = 3, \varepsilon_r = 1$ *-*

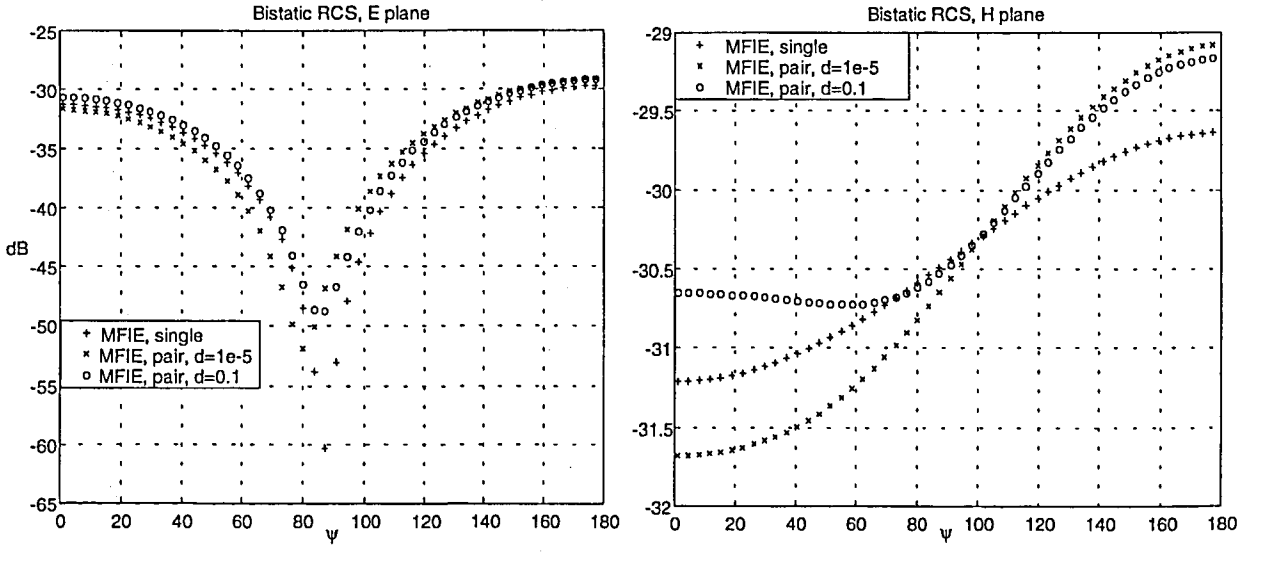

Fig. 8.8 MFIE RCS for one cone - $\varepsilon_r = 3$ *- and one cone-cylinder pair -* $\varepsilon_r = 3, \varepsilon_r = 1$ *-*

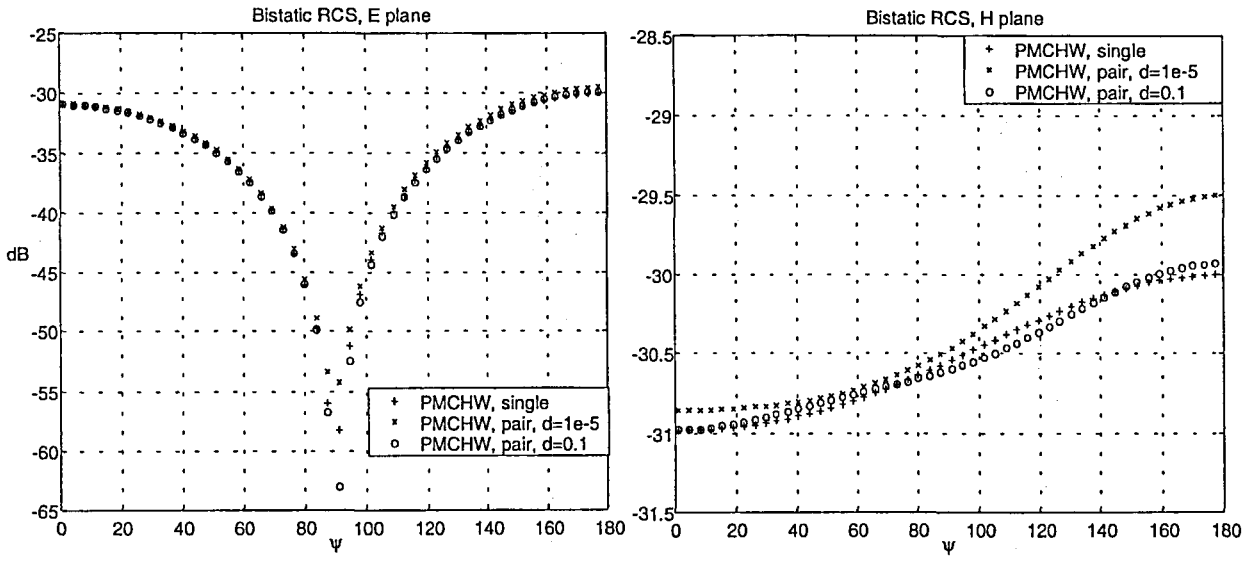

Fig. 8.9 PMCHW RCS for one cone - $\varepsilon_r = 3$ *- and one cone-cylinder pair -* $\varepsilon_r = 3, \varepsilon_r = 1$ *-*

The two dielectric structures demonstrate an analogous behaviour. The EFIE and MFIE results with the two bodies show a much more evident dissimilarity in comparison to the corresponding results of the single body; this fact has to be attributed to the expected error in the dielectric EFIE and MFIE described in 8.1.4.

According to the results, the error associated to PMCHW tuns out much less important than the error in EFIE-MFIE. Moreover, the reasoning presented in 8.1.3.2 is confirmed by the PMCHW results in the two cases. For the cubes, the PeC-MFIE(*RWG*) impedance contributions are relatively less important because there are many influences between coplanar functions, which yield a null PeC-MFIE contribution. For curved objects, on the other hand, there is always some PeC-MFIE influence between an element an its neighbouring elements. That is why the dissimilarity between the results with the single reference for the bigger value of d is more important for the cone and cylinder- Fig. 8.9- than for the cubes -Fig. 8.5-. When setting the value of $d = 1e-5\lambda_0$ for the cubes, the PMCHW error becomes more important because there are many near elements in parallel planes facing each other -in this case the PeC-MFIE contribution becomes more important- . The cone and the cylinder allow also for this contribution and so the $d = 1e-5\lambda_0$ results turn out even worse than those due to $d = 0.1\lambda_0$.

It has just been presented a relative analysis because the results are compared with reference results that are biased by the same sources of error. In any case, the conclusions can be extended to the robustness of the results for the single bodies. According to the bigger robustness of PMCHW in front of the EFIE and MFIE in all the results, one can infer that the PMCHW approach is more reliable in the analysis of these electrically small structures with only penetrable regions. Furthermore, one can also conclude that the PMCHW behaviour is especially good for cubes -and therefore for regular polyhedrons-.

8.2.2.2 Physical polyhedrons

The previous section has shown the importance of the error in the EFIE and MFIE approaches that the author of this dissertation Thesis attributes to the unsatisfactory expansion of the current. This misbehaviour must accordingly decrease as the order of the expansion $\vec{J}^{\pm}$ and $\vec{M}^{\pm}$ increases. For physical polyhedrons, the order of the expansion can be augmented without changing the modelling of the surface by overdiscretizing the planar facets with low-order expanding functions -as effectuated in the PeC-results of Chapter 7-. Furthermore, the previous section has shown the robustness of the PMCHW approach in the analysis of regular penetrable polyhedrons. The bistatic RCS for fine discretizations for the three dielectric operators on the electrically small physical polyhedrons of Chapter 7 are presented.

- **Pyramid:**

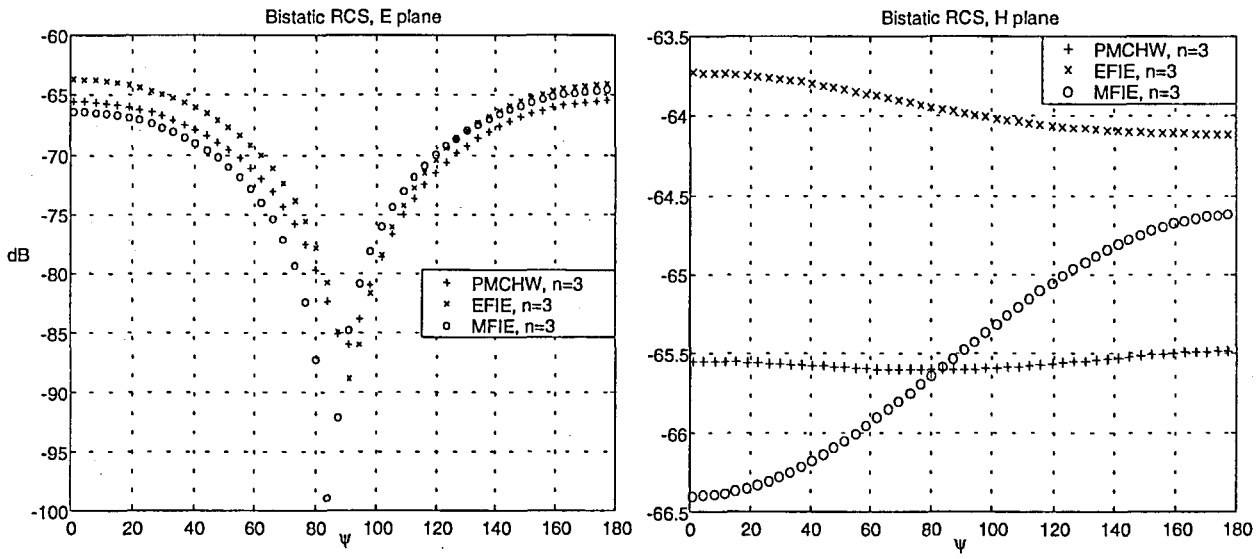

Fig. 8.10 RCS for the pyramid - $\varepsilon_r = 3$ - with 72 triangles

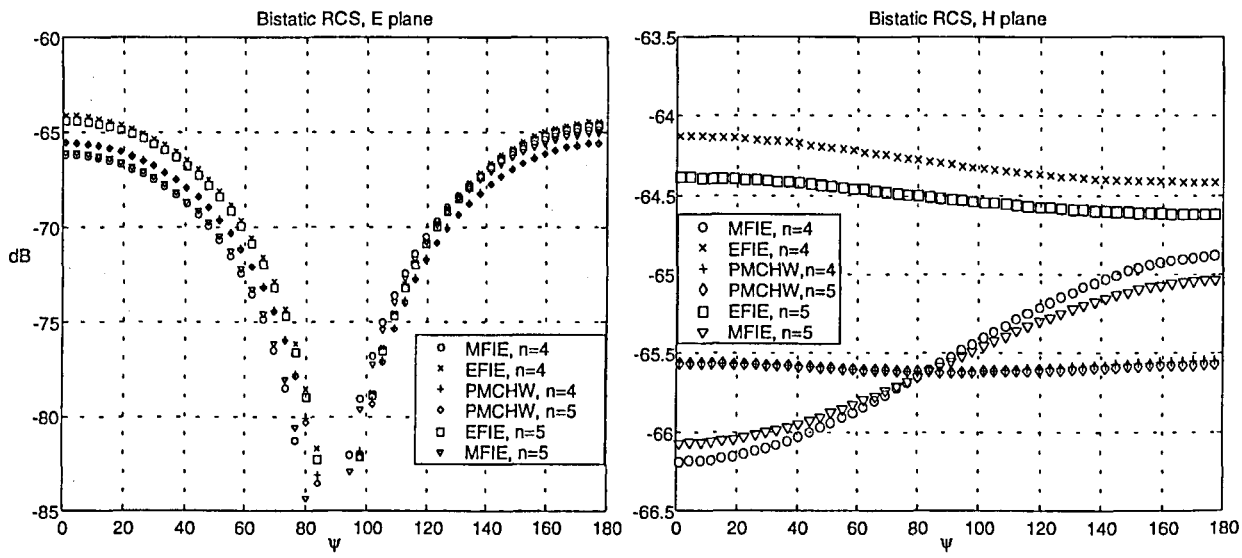

Fig. 8.11 RCS for the pyramid - $\varepsilon_r = 3$ - with 128 and 200 triangles

A pyramid -see Fig. 7.1- with height $0.03\lambda_0$, basis side $0.04\lambda_0$ and $\varepsilon_r = 3$ is analysed with five different discretizations -3, 4, 5, 6 and 7 segments per edge-, which correspond respectively to 72, 128, 200, 288 and 392 triangles. The RCS results are presented in Fig. 8.10, Fig. 8.11 and Fig. 8.12.

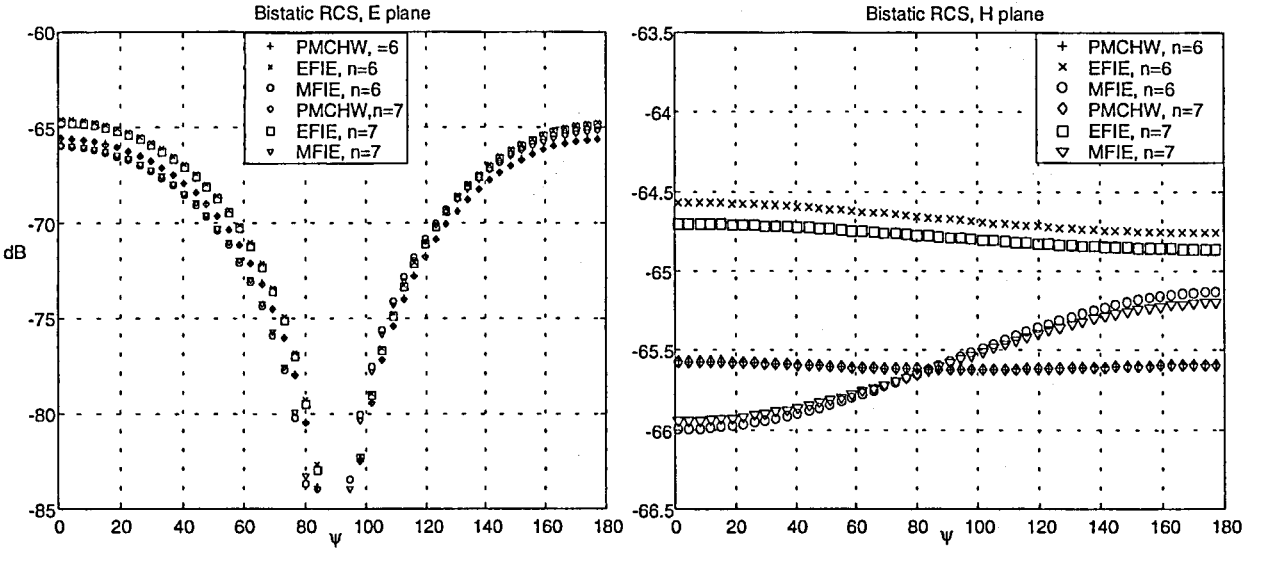

Fig. 8.12 RCS for the pyramid - $\varepsilon_r = 3$ - with 288 and 392 triangles

- **Cube:**

A cube -see Fig. 7.5- with side $0.05\lambda_0$ and $\varepsilon_r = 4$ is analysed with three different discretizations -2, 4 and 5 segments per edge-, which correspond respectively to 48, 192 and 300 triangles. The RCS results are presented in Fig. 8.13, Fig. 8.14 and Fig. 8.15 .

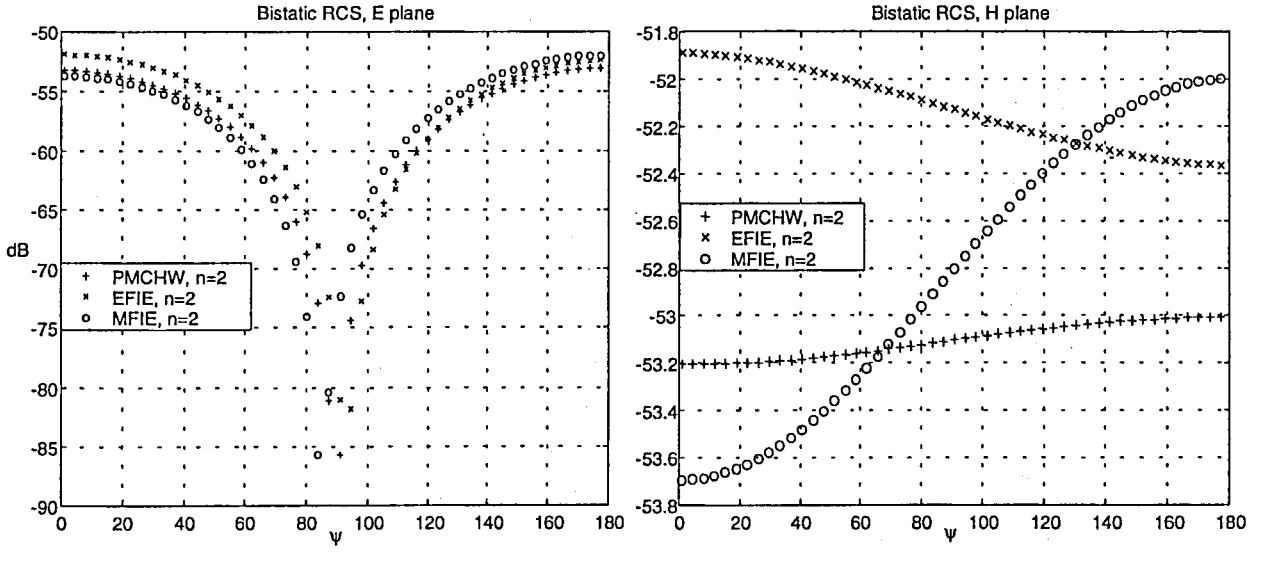

Fig. 8.13 RCS for the cube - $\varepsilon_r = 4$ - with 48 triangles

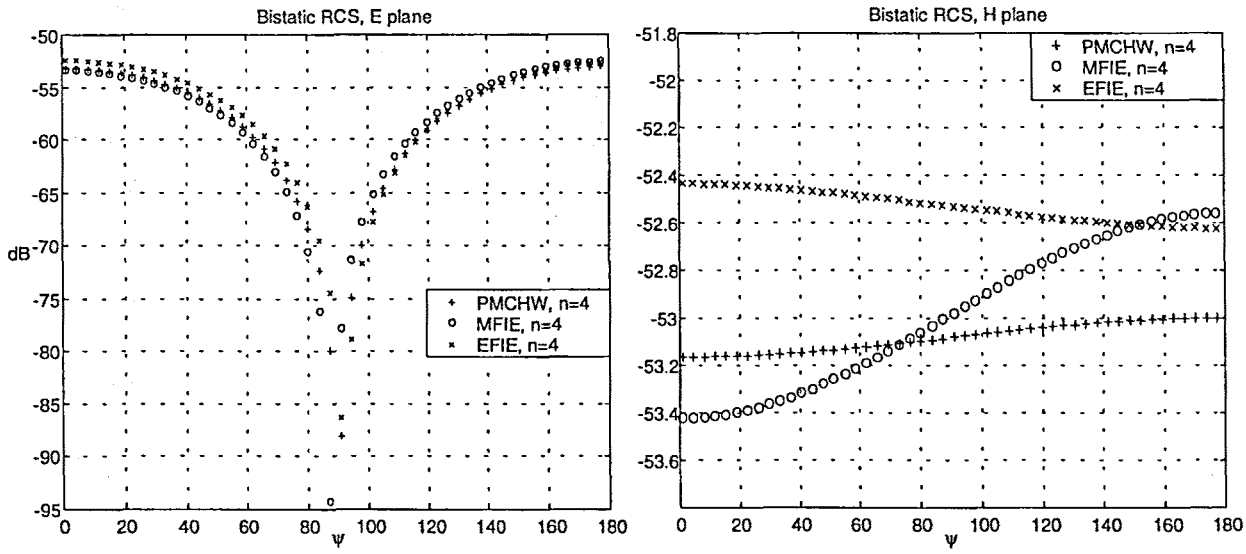

Fig. 8.14 RCS for the cube - $\varepsilon_r = 4$ - with 192 triangles

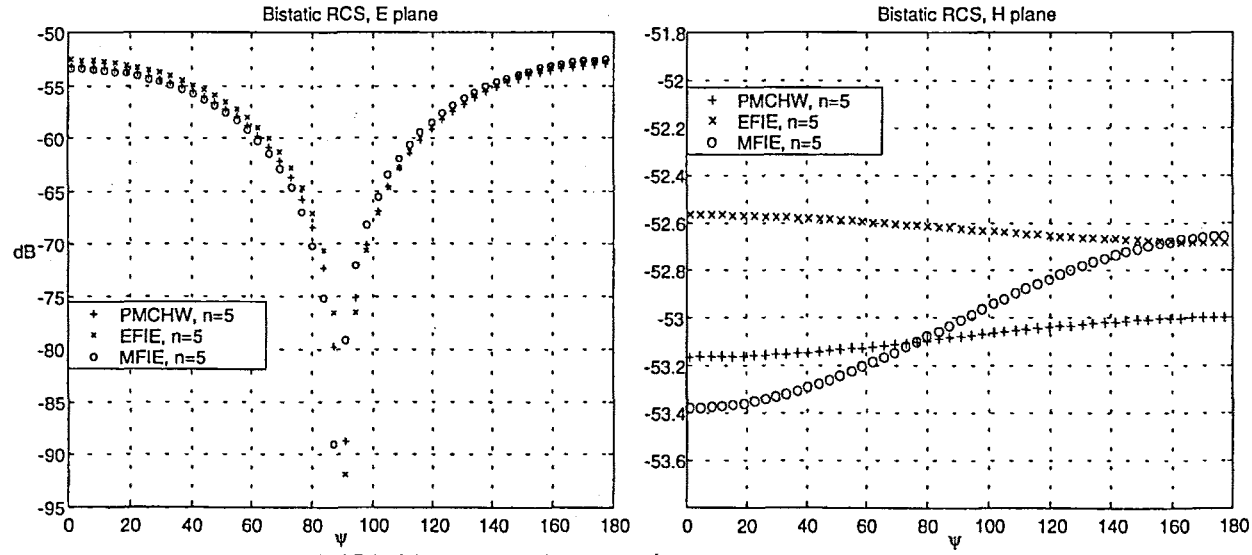

Fig. 8.15 RCS for the cube - $\varepsilon_r = 4$ - with 300 triangles

- **Octahedron:**

A regular octahedron -see Fig. 7.14- with height of $0.07\lambda_0$ and $\varepsilon_r = 2$ is analysed with three different discretizations -3, 5, 6 and 7 segments per edge-, which correspond respectively to 72, 200, 288 and 392 triangles. The RCS results are presented in Fig. 8.16 and Fig. 8.17.

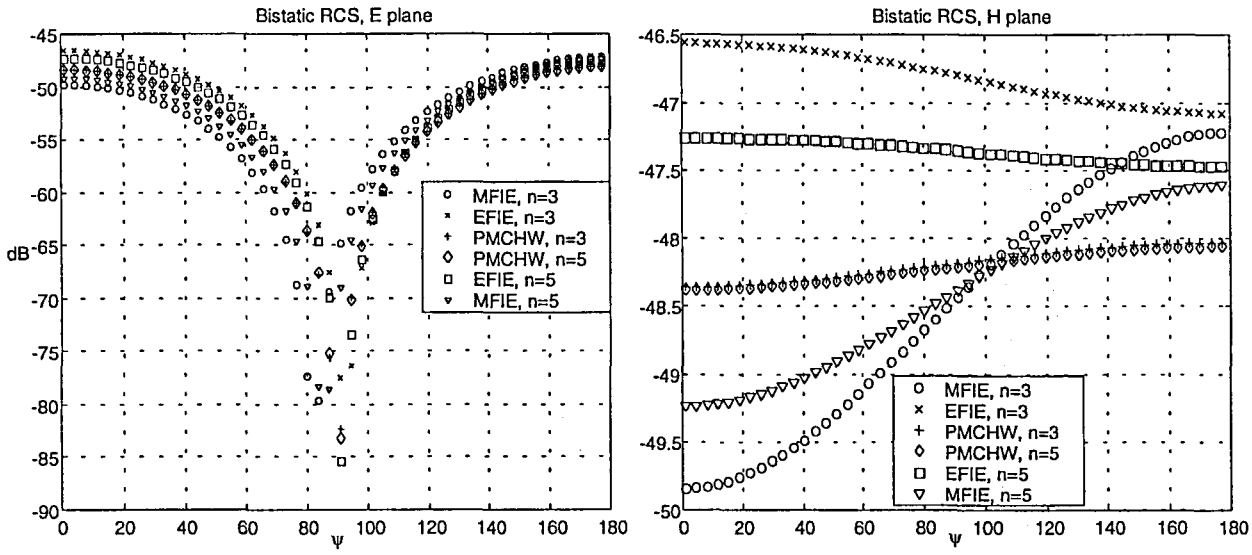

Fig. 8.16 RCS for the octahedron - $\varepsilon_r = 2$ - with 72 and 200 triangles

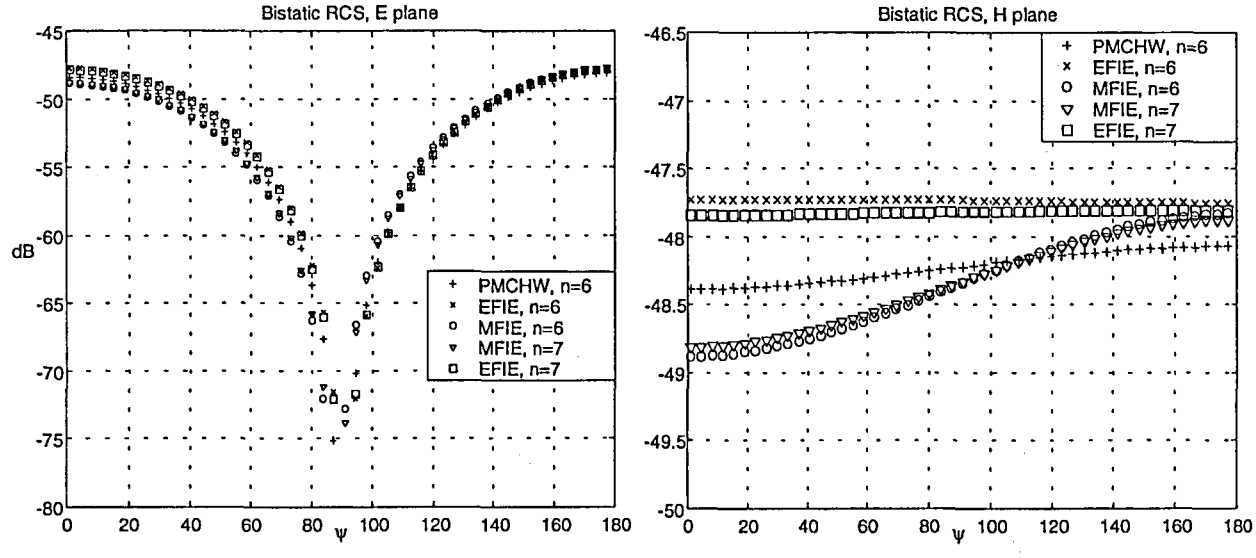

Fig. 8.17 RCS for the octahedron - $\varepsilon_r = 2$ - with 288 and 392 triangles

In view of the results for the pyramid, the cube and the octahedron, one can confirm that the EFIE and the MFIE operators require overdiscretization to improve their behaviour. Indeed, for all the polyhedrons, the EFIE and the MFIE results approach each other as the discretization becomes finer. According to the theoretical reasoning presented in 8.1.4, both MFIE and EFIE must merge for a high enough order of expansion.

The PMCHW operator, on the other hand, is extremely robust and does not need any finer discretization to improve its performance. Indeed, the results are nearly the same from the coarsest to the finest mesh in all the polyhedrons. PMCHW excels as a stable result, to which EFIE and MFIE seem to tend when yielding the mesh finer. Note that the inherent error of PMCHW is not even noticed because it is inside the range comprised in the evolution of the results of EFIE and MFIE. This is again a proof of the much smaller relevance of the PMCHW error compared with the EFIE-MFIE one in penetrable bodies - for these objects of electrically small dimensions-.

Note that these results are in agreement with the behaviour in the conducting physical polyhedrons. In that case, when overdiscretizing the facets, PeC-EFIE(*RWG,RWG*) yields more stable results than PeC-MFIE(*RWG,unxRWG*). It is thus reasonable that the operators that depend on PeC-MFIE(*RWG,unxRWG*) in the dielectric case -EFIE and MFIE- provide a less stable performance for finely meshed physical polyhedrons than PMCHW.

8.2.2.3 Curved objects

PMCHW excels as the operator that yields the most stable and accurate behaviour in regard with the electrically small physical polyhedrons. For the curved objects, which are analysed through a planar modelling, the PMCHW must yield the most accurate description of the corresponding polyhedron -compared to EFIE and MFIE-. In consequence, an appreciable error must appear for coarsely meshed spheres, in an analogous way as it happens for the PeC-EFIE(*RWG,RWG*) for conducting spheres -see Chapter 7-.

EFIE and MFIE have shown a low-order misbehaviour too evident for the electrically small polyhedrons. They cannot hence make up for the curvature effect so well as PeC-MFIE(*RWG,unxRWG*) can do for the entirely curved conducting bodies -see Chapter 7-. In consequence, EFIE and MFIE cannot improve the PMCHW performance appreciably, although they partially do succeed.

Bistatic RCS results for a sphere with radius $0.05\lambda_0$ $\varepsilon_r = 2$ and $\varepsilon_r = 4$ under an axially incident plane wave are presented -Fig. 8.18 and Fig. 8.19- for the three operators. As the discretization becomes fine, logically the curvature error must decline -Fig. 8.19-.

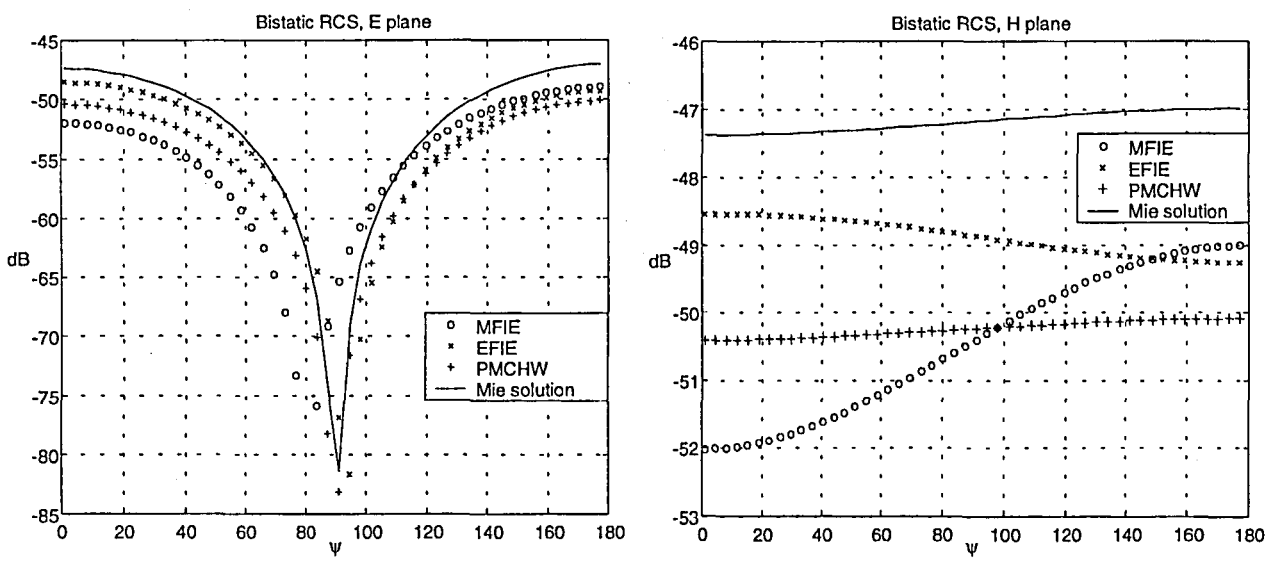

Fig. 8.18 RCS for the sphere - $\varepsilon_r = 2$ *- with radius* $0.05\lambda_0$ *and 32 triangles*

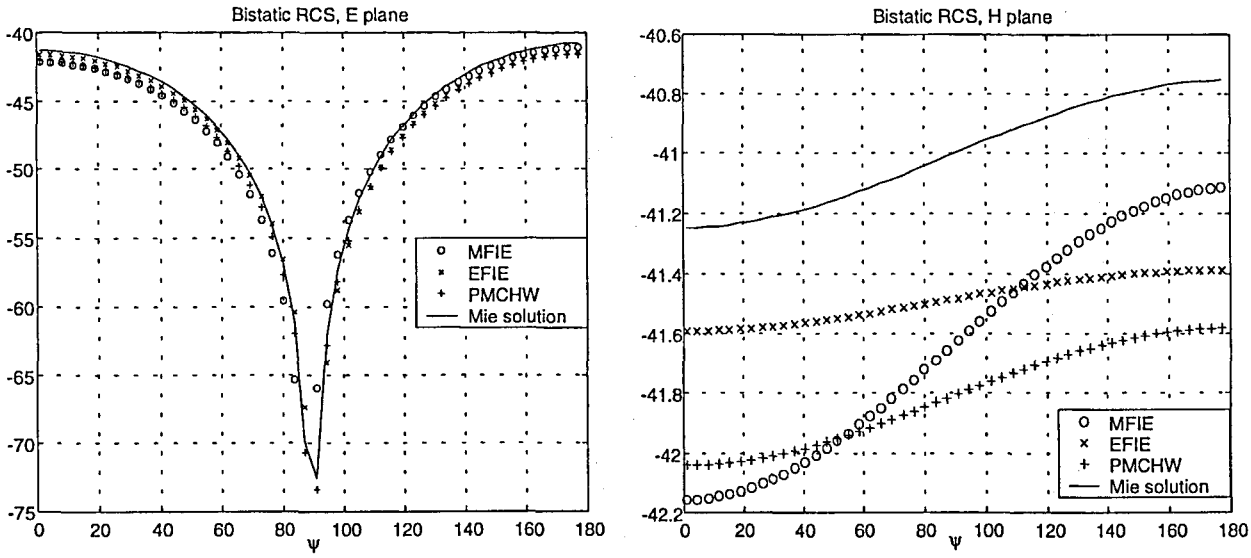

Fig. 8.19 RCS for the sphere -$\varepsilon_r = 4$- with radius $0.05\lambda_0$ and 128 triangles

8.2.3 Electrically bigger bodies with only penetrable regions

Since all the examples presented in the previous sections are electrically pretty small -the cube provides the longest physical edge with $0.1\lambda_d$ -, the influence of the physical edges must be remarkable, which implies a pretty important high-order presence in the physical solution -see 7.5.1-. One can see how those physical polyhedrons with a higher density of physical edges -pyramid and octahedron- or the sphere more coarsely meshed show more dissimilarity between the PMCHW and the EFIE-MFIE behaviour. One expects that for bodies with bigger electrical dimensions the influence of the EFIE-MFIE error -directly dependent on the relative presence of physical edges- will be decreasingly important and the contribution incorporated in a patch size choice of $0.1\lambda_d$ can be enough. Some examples in this section confirm this.

The bistatic RCS results under an impinging axial wave for some electrically bigger penetrable bodies are presented for EFIE, MFIE and PMCHW. The behaviour for a sphere considerably bigger than Fig. 8.18 and Fig. 8.19 is compared with the Mie solution. The behaviour for some cubes is compared with a solution obtained using the volumetric equivalence theorem [16]. The solution for a half-sphere is compared with the null-field approach of S. Ström and W. Xheng [21]. Finally, results are shown for a cylinder and a group of a cone and a cylinder.

- **Sphere:**

Bistatic RCS for a sphere with radius $0.2\lambda_0$ and $\varepsilon_r = 4$ with 512 triangles.

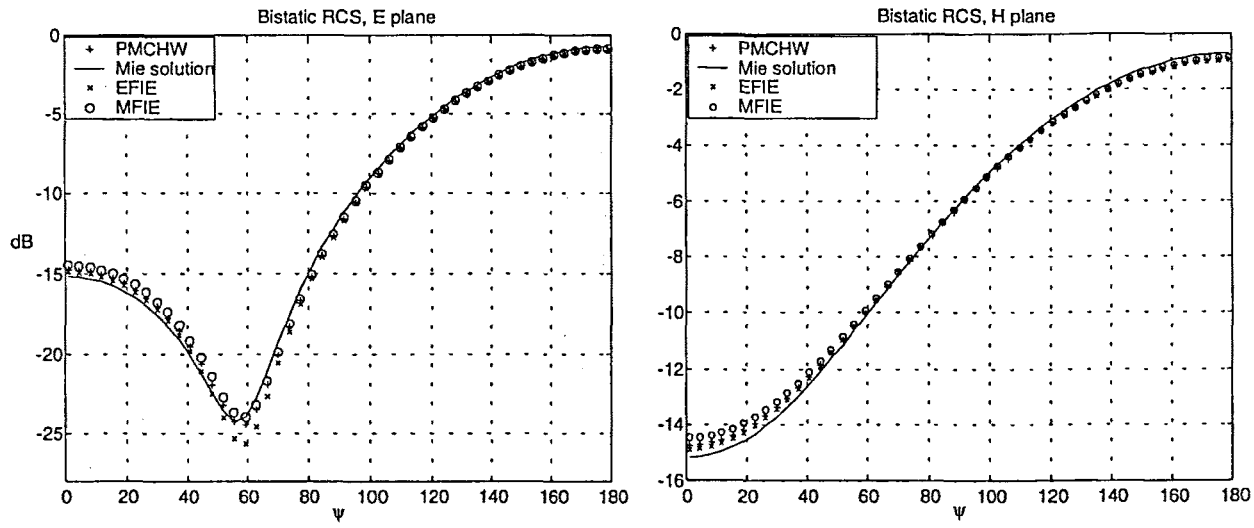

Fig. 8.20 RCS for the sphere -$\varepsilon_r = 4$ - with radius $0.2\lambda_0$ and 512 triangles

- **Cubes:**

Bistatic RCS for two cubes with side $0.2\lambda_0$ and respectively $\varepsilon_r = 4$ -see Fig. 8.21- and $\varepsilon_r = 9$ -see Fig. 8.22-.

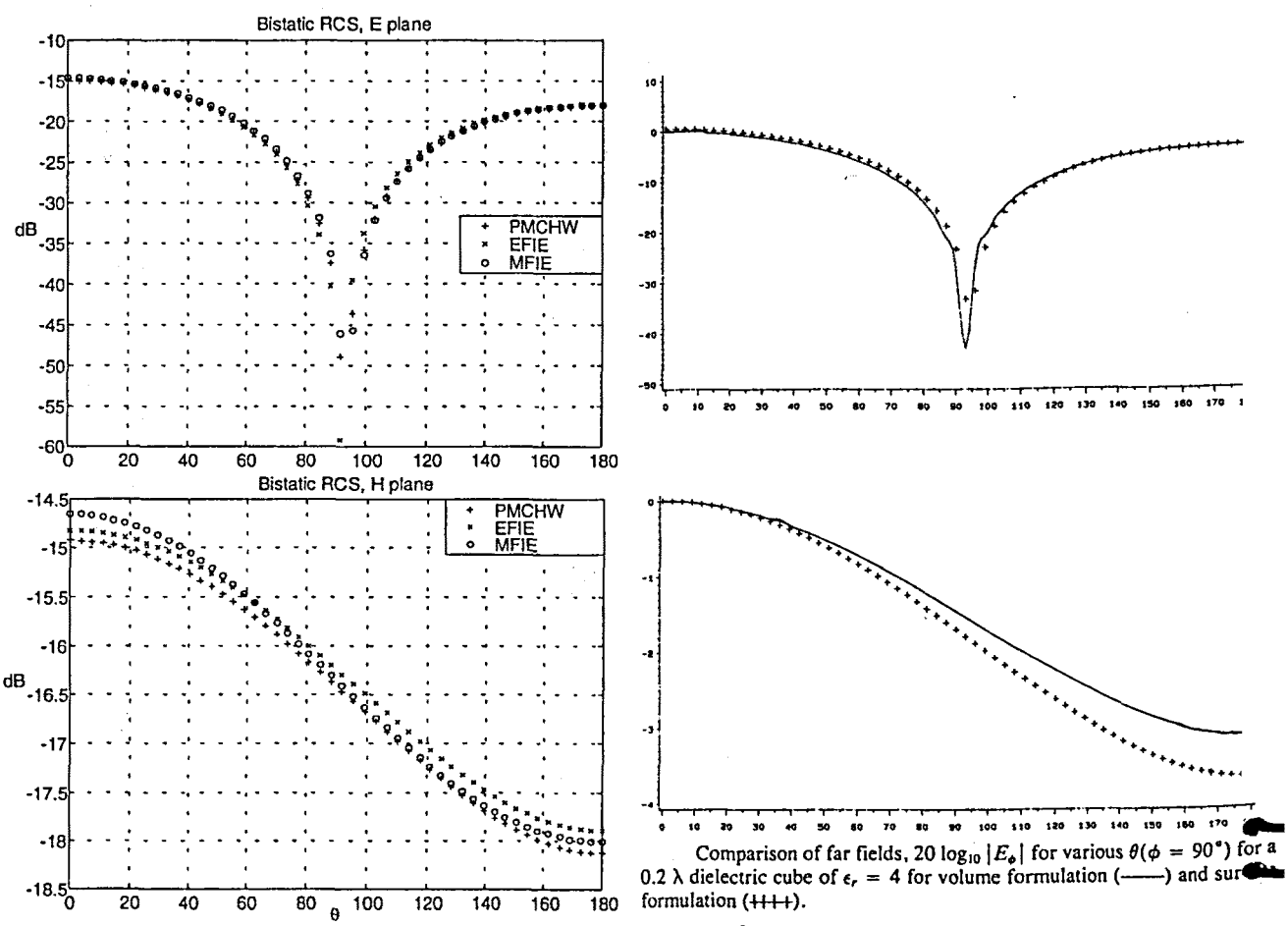

Comparison of far fields, 20 $\log_{10} |E_\phi|$ for various $\theta(\phi = 90°)$ for a 0.2 λ dielectric cube of $\epsilon_r = 4$ for volume formulation (——) and sur formulation (++++).

Fig. 8.21 RCS for the cube -$\varepsilon_r = 4$ - with side $0.2\lambda_0$ and 192 triangles

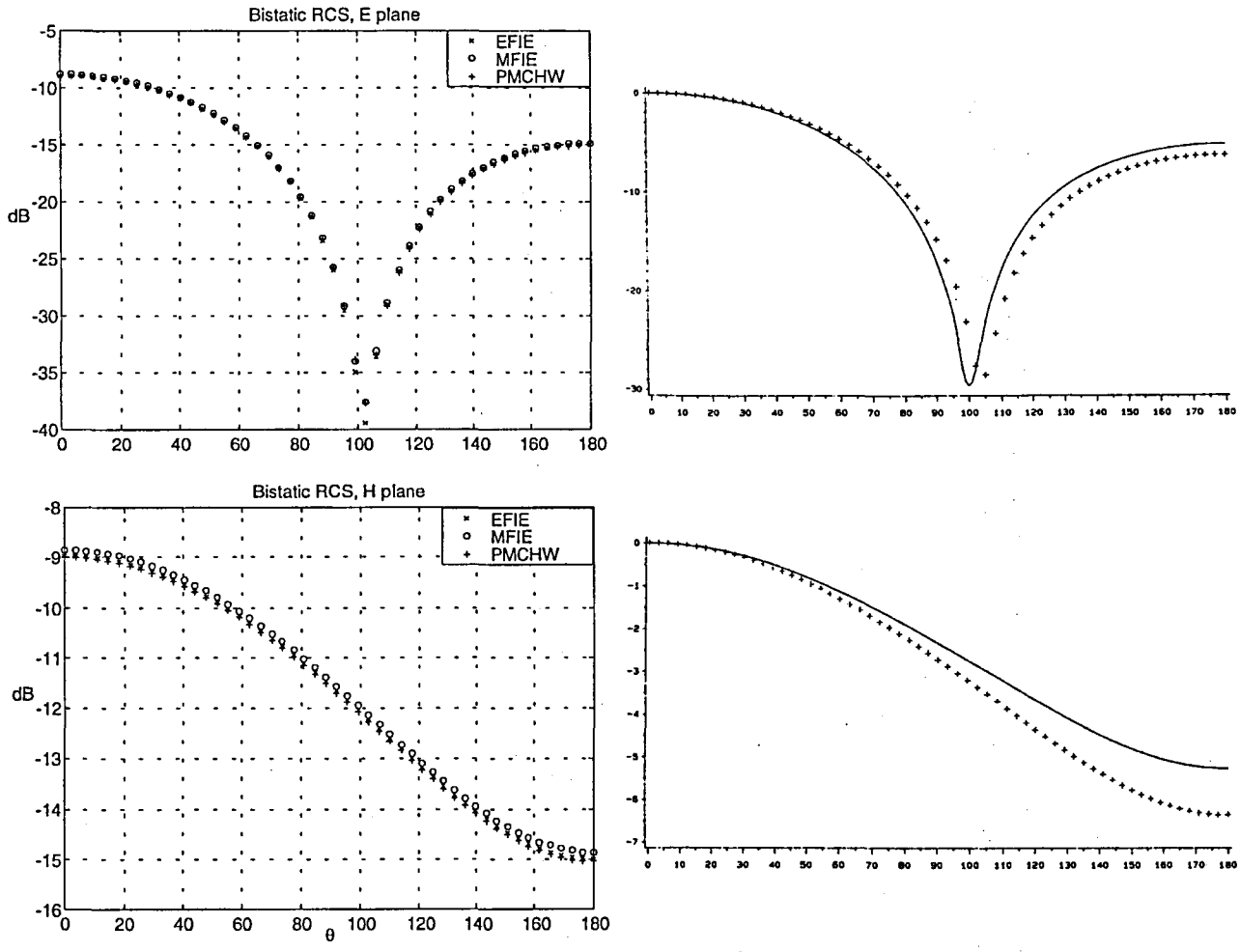

Fig. 8.22 RCS for the cube - $\varepsilon_r = 9$ - with radius $0.2\lambda_0$ and 768 triangles

- **Half-sphere**

Bistatic RCS for a half-sphere with radius $0.477\lambda_0$ and $\varepsilon_r = 4$ with 512 triangles - see Fig. 8.23-

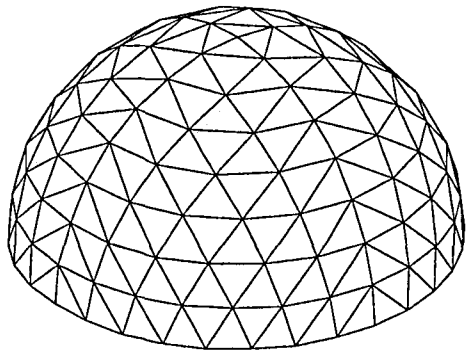

Fig. 8.23 Half- sphere with 512 triangles

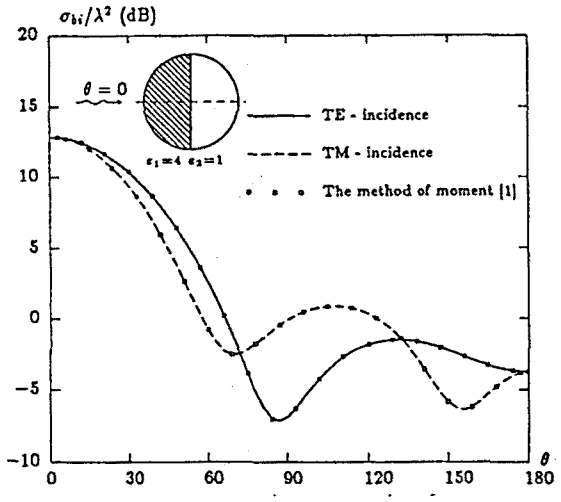

Fig. 8.24 Bistatic RCS for the half-sphere according to the null-field method and the MoM-BoR

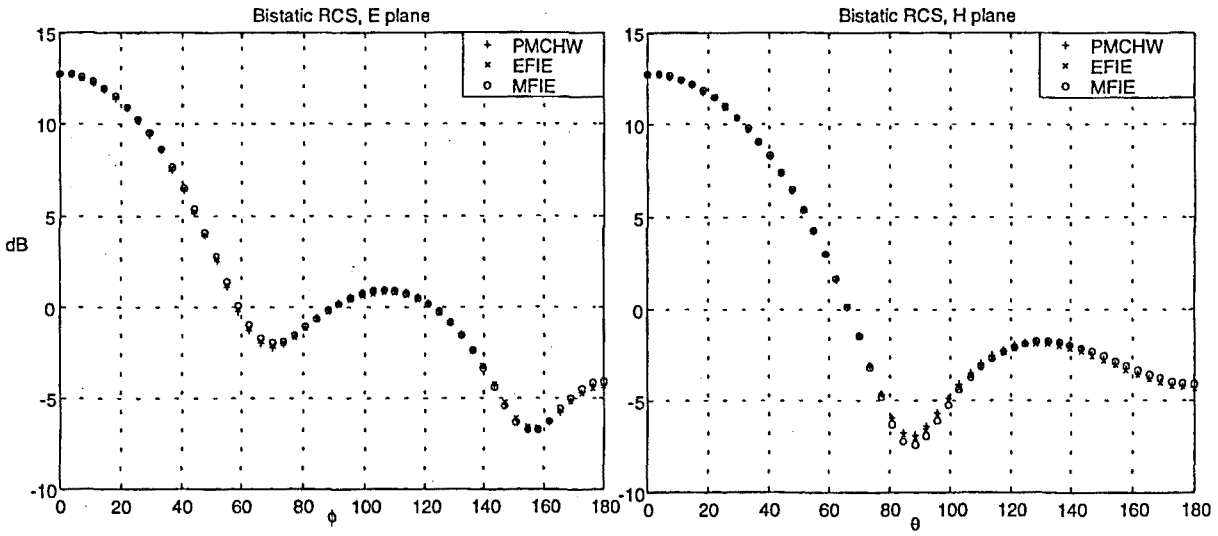

Fig. 8.25 Bistatic RCS for the half-sphere - $\varepsilon_r = 4$ - with radius $0.477\lambda_0$ and 512 triangles

- **Cylinder:**

The RCS results for the cylinder in Fig. 8.26 with radius $0.1\lambda_0$, height $0.2\lambda_0$ and $\varepsilon_r = 2$ under an axially incident plane wave are shown in Fig. 8.27 .

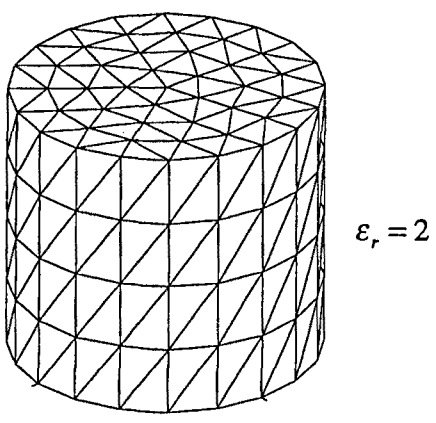

Fig. 8.26 Cylinder discretized with 320 triangles

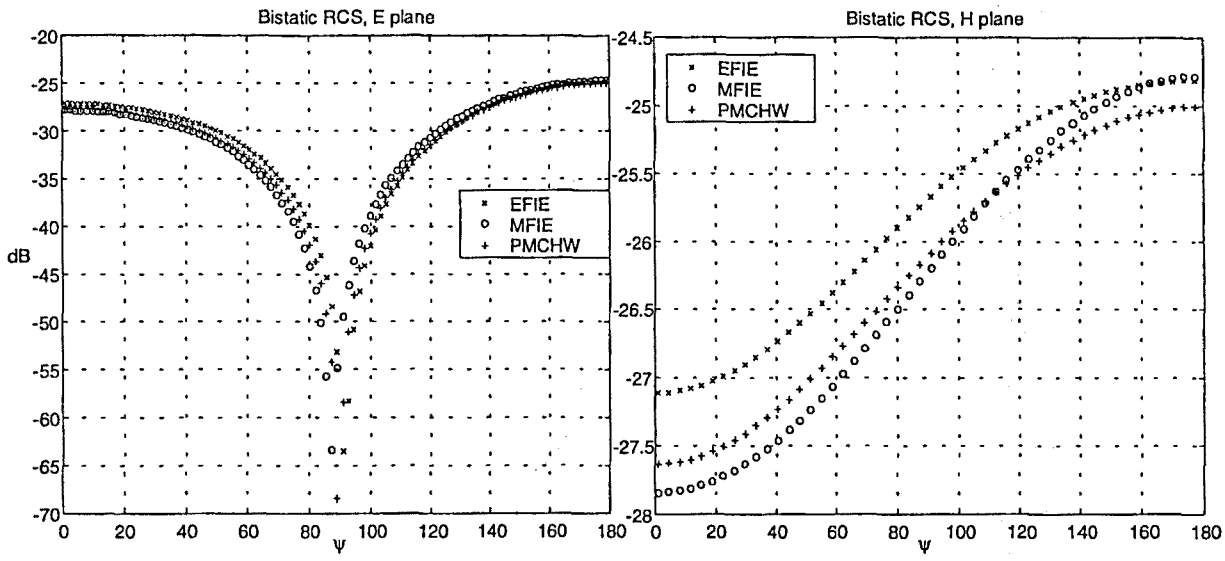

Fig. 8.27 RCS for the cylinder - $\varepsilon_r = 2$ - of radius $0.1\lambda_0$ and height $0.2\lambda_0$ with 320 triangles

- **Cone and cylinder**

The cone with $\varepsilon_r = 3$ of Fig. 8.6 and the cylinder with $\varepsilon_r = 2$ of Fig. 8.26 are juxtaposed as shown in the structure of Fig. 8.6 with $d = 0.02\lambda_0$.

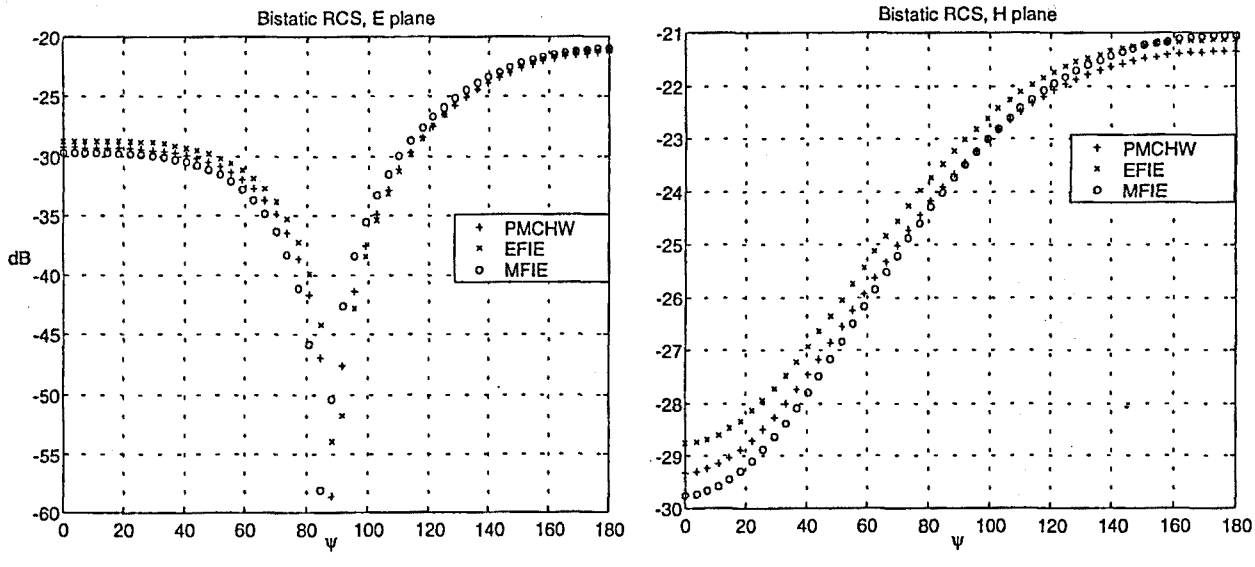

Fig. 8.28 RCS for the cone-cylinder - $\varepsilon_r = 3, \varepsilon_r = 2$ - structure with 360 and 320 triangles

All these results confirm that, as the electromagnetic dimensions increase, the EFIE and MFIE behaviour follow more closely the PMCHW result, which, in accordance with the behaviour for smaller objects, is maintained as reference. Indeed, the results for the half-sphere, with perimeter of $5\lambda_d$, -see Fig. 8.23-, for the cube of $\varepsilon_r = 9$, with perimeter $2.5\lambda_d$, - see Fig. 8.22 -, and for the sphere of $\varepsilon_r = 4$, with perimeter $2.5\lambda_d$ -see Fig. 8.20-, resemble best. This behaviour is in agreement with the theory expounded in 8.1.4 for the influence of the physical edges -associated to either the physical polyhedron or to the

modelling of the curved surface- declines. Therefore, a lower-order expansion of the current through a patch size of about $0.08\lambda_d$ is satisfactory to expand the physical solution.

It must be noted that in the results of the cylinder -see Fig. 8.27- the disagreement is still noticeable because the electric dimensions are comparatively rather low, with perimeter $1.1\lambda_d$ -. This makes sense because the decrease of the low-order error associated to EFIE and MFIE must be gradual. In any case, it can be verified in Fig. 8.27 that the error at this point is rather small, mainly compared with the small physical polyhedrons in 8.2.2.2.

Finally, the results for the structure in Fig. 8.28 show again that the less stringent field requirements in PMCHW are not noticeable in front of the low-order EFIE and MFIE misbehaviour, which in any case at this point is small. This fact is interesting because even for a structure with such a small gap between $-d = 0.02\lambda_0$- the PeC-MFIE influences between elements facing each other turn out comparatively unimportant.

8.2.4 Bodies with perfectly conducting and dielectric regions

The misbehaviour of PMCHW -explained in detail in 8.1.3.2- due to the fact that the imposed magnetic and electric field requirements are less stringent than the necessary electromagnetic field requirements must be important in structures with important conducting regions facing closely dielectric interfaces. Indeed, since the magnetic current value is close to zero over the conducting interfaces, the badly defined PeC-MFIE(*RWG,RWG*) contributions become really important to define the magnetic field. Furthermore, in this case, the EFIE and MFIE operators improve remarkably their low-order misbehaviour for electrically small objects thanks to the application of the robust PeC-EFIE(*RWG,RWG*) and PeC-MFIE(*RWG,unxRWG*) over the conducting interfaces.

8.2.4.1 Relevance of the PMCHW error due to the less stringent electromagnetic requirements

Some RCS results for an axially incident plane wave are presented for pairs of disjoint objects -conductor and dielectric- with a small gap d between.

- **Two cubes:**

  It is shown for EFIE, MFIE and PMCHW the bistatic RCS for two cubes with side $0.2\lambda_0$ -PeC and $\varepsilon_r = 4$ -, both discretized with 192 triangles, for the values $d = 1e-5\lambda_0$ and $d = 0.01\lambda_0$ -see Fig. 8.29 and Fig. 8.30- .

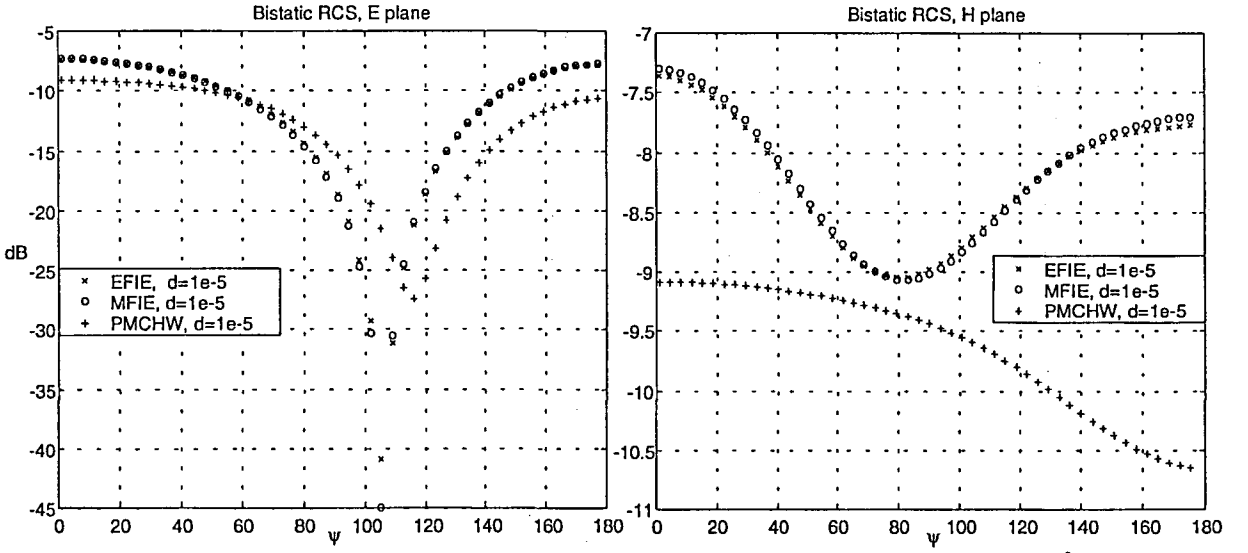

Fig. 8.29 RCS for the two cubes - $\varepsilon_r = 4$, PeC- both with 192 triangles and $d = 1e-5\lambda_0$

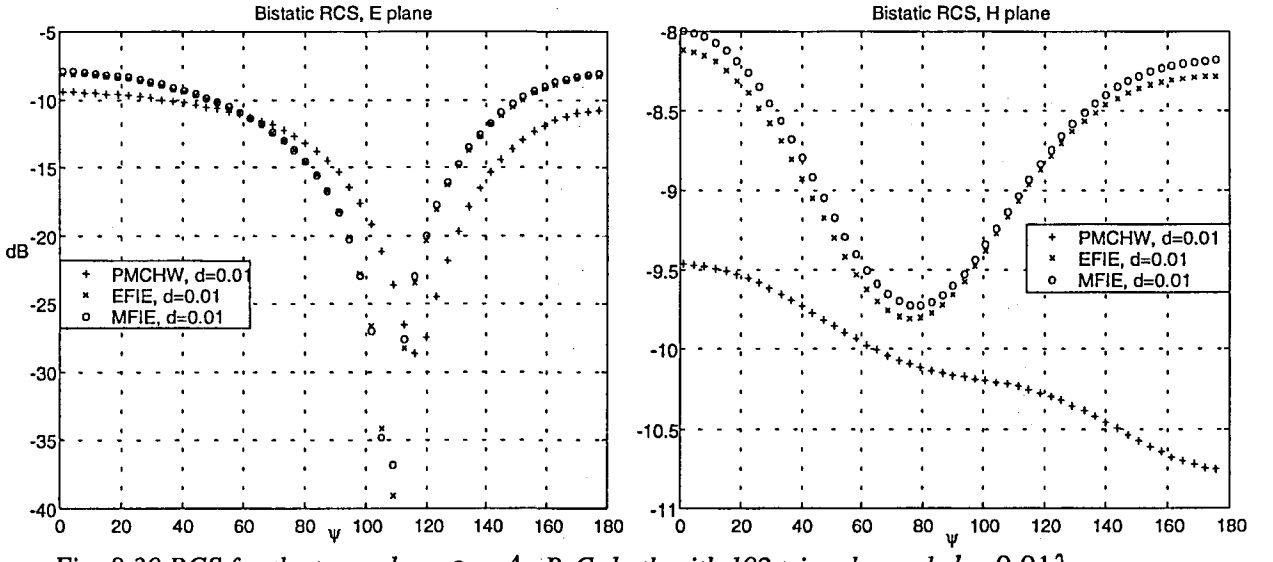

Fig. 8.30 RCS for the two cubes - $\varepsilon_r = 4$, PeC- both with 192 triangles and $d = 0.01\lambda_0$

- **A cone and a cylinder:**

A cone-cylinder group with $d = 1e-5\lambda_0$ is presented. The cone -radius $0.3\lambda_0$, height $0.6\lambda_0$ and $\varepsilon_r = 2$ - over a PeC-cylinder -radius $0.3\lambda_0$ and height $0.6\lambda_0$- respectively discretized with 250 and 500 triangles -see Fig. 8.31-. It is compared with a MoM-BoR reference in [30].

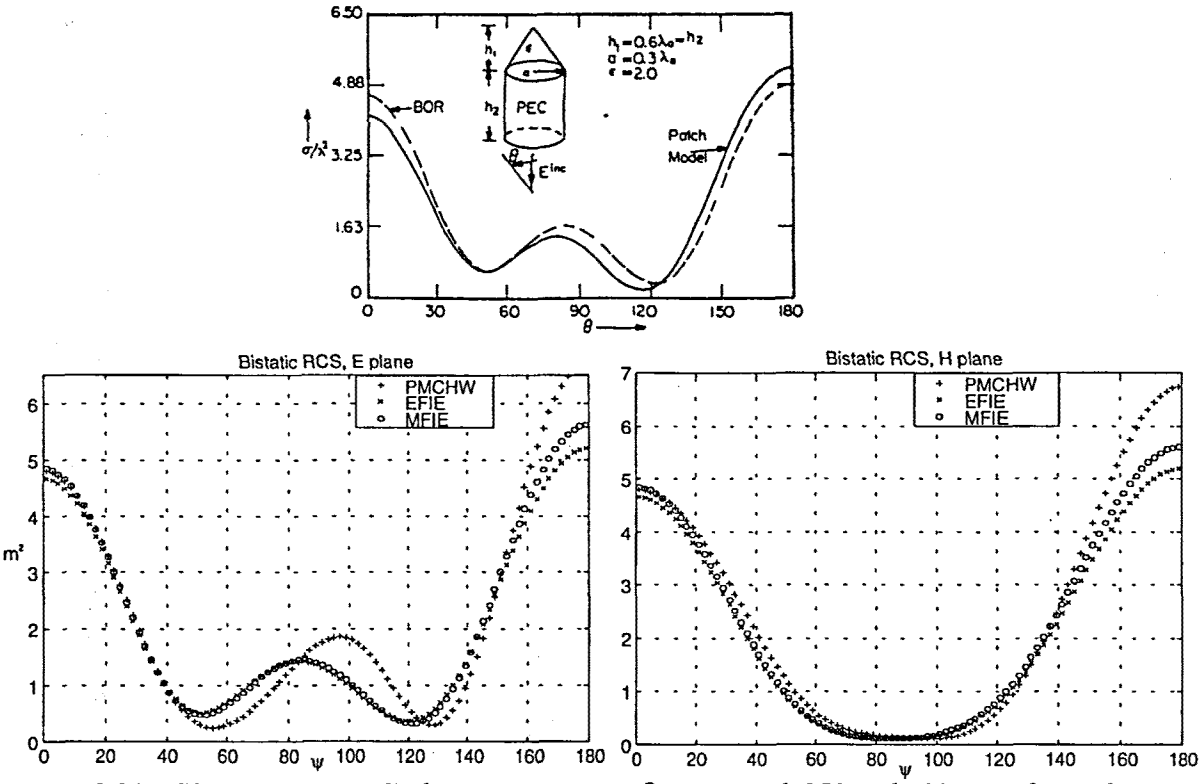

Fig. 8.31 RCS for the cone-cylinder structure - $\varepsilon_r = 2$, PeC- with 250 and 500 triangles and $d = 1e-5\lambda_0$

8.2.4.2 Reference results

In the previous section, the PMCHW operator has been set aside for tiny values of d, which dismisses its use on the analysis of composite conducting and penetrable bodies -see section 8.3-. However, PMCHW can be used, along with EFIE and MFIE, for the case of disjoint objects as long as d is not very small -see the examples below-

- **Two cubes:**

The two cubes presented in Fig. 8.29 and Fig. 8.30 for tiny values of d are shown now for $d = 0.3\lambda_0$

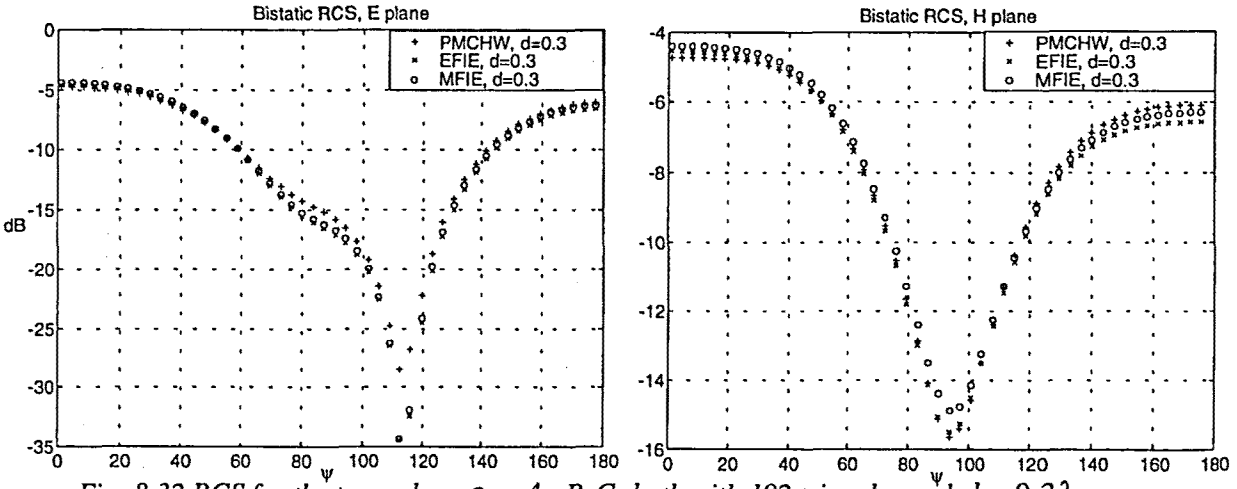

Fig. 8.32 RCS for the two cubes - $\varepsilon_r = 4$, PeC- both with 192 triangles and $d = 0.3\lambda_0$

- **Concentric spheres:**

The bistatic RCS of two concentric spheres in Fig. 8.33 with axial incidence is shown in Fig. 8.35 and it is compared with a Kishk and Shafai reference [6] - Fig. 8.34-

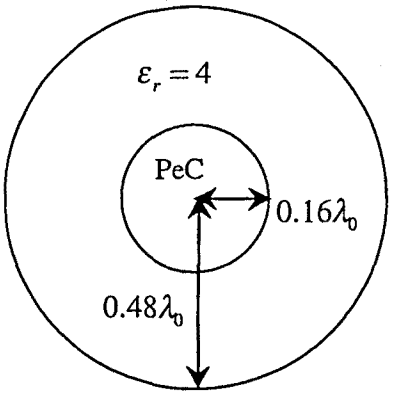

Fig. 8.33 Concentric spheres discretized with 128 and 512 triangles

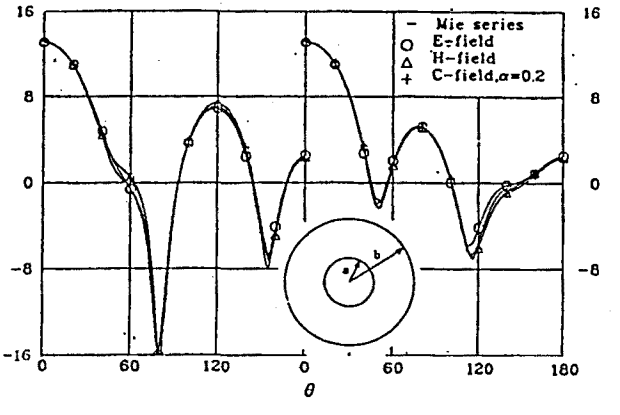

Fig. 8.34 RCS for the concentric spheres obtained by Kishk and Shafai [6]

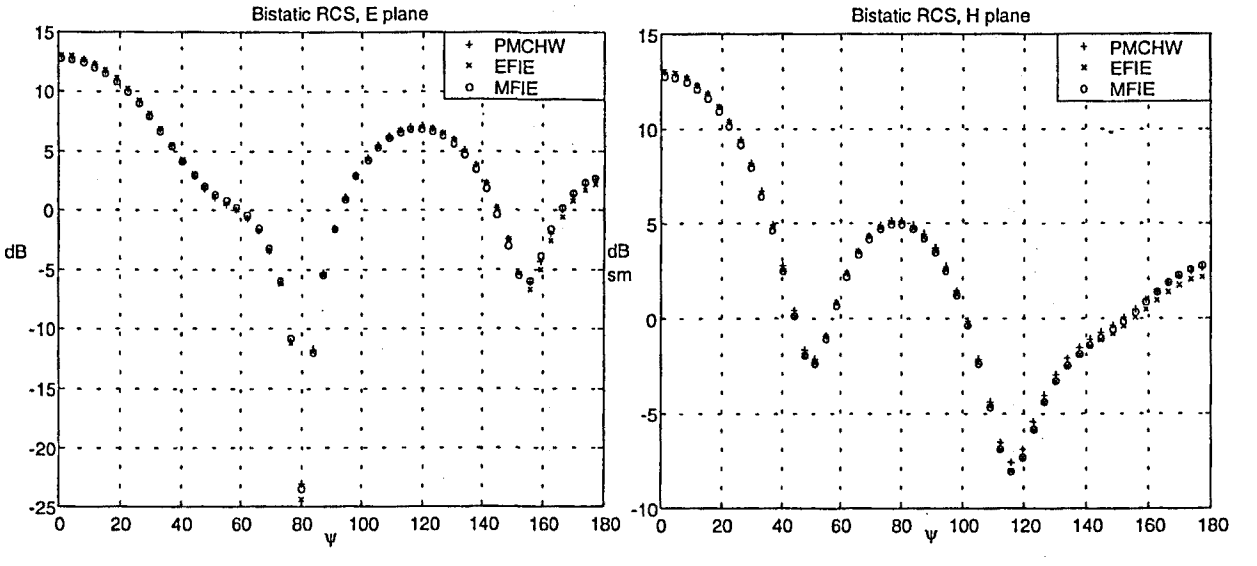

Fig. 8.35 RCS for the concentric spheres with 128 and 512 triangles

8.3 GENERALISATION TO BODIES WITH MORE THAN TWO REGIONS SHAPING THE INTERFACE SURFACES

In the previous section all the possible problems with one region shaping the interface surfaces have been presented -single bodies, layered bodies or groups of disjoint objects- For the sake of generality, the problems with more than two regions shaping the interface surfaces have to be considered as well.

A composite structure -with dielectric and conducting regions attached- belongs to this group. Note that it is pretty important since it embraces important types of antennas, such as the microstrip antennas, with a conducting ground plane and a dielectric slab put together.

The author of this dissertation Thesis considers the composite bodies as a group of disjoint bodies with $d=0$. In the previous section, several problems with groups of disjoint bodies separated by minuscule distances - $d=1e-5\lambda_0$ - have been presented -see Fig. 8.3, Fig. 8.4, Fig. 8.5, Fig. 8.7, Fig. 8.8, Fig. 8.9, Fig. 8.29, Fig. 8.31- and confirmed with reference results.

Since the physical magnitudes are indeed continuous, it is reasonable that the physical solution for these problems but with an identically null distance -composite bodies- must be the same as the solution assuming $d=1e-5$. Moreover, since the dielectric operators result from the combination of the PeC-operators, one has to assess if the basic PeC-operators can accomplish the physical continuity of the fields when $d\rightarrow 0$ according to the particular choice of expanding and weighting functions. This aspect is analysed in detail for each of the dielectric operators right away.

- **EFIE-MFIE:**

  These operators rely on the basic PeC-EFIE(*RWG*,*RWG*) and PeC-MFIE(*RWG*,*unxRWG*). It has been proved analytically in Chapter 6 that *RWG* as weighting functions expand the rank space of PeC-EFIE(*RWG*) and of PeC-MFIE(*unxRWG*). Therefore, the continuity of the expanded magnitudes when $d\rightarrow 0$ is maintained, which allows EFIE and MFIE to obtain the same results for minuscule values of d as for $d=0$ in any case -approaching either dielectric or PeC-dielectric regions-.

- **PMCHW:**

  This operator relies on PeC-EFIE(*RWG*,*RWG*) -continuous as reasoned above when $d\rightarrow 0$- and on PeC-MFIE(*RWG*,*RWG*). It has been repeatedly mentioned that PeC-MFIE depends on the contribution of two terms: the integration of the singularity and the Cauchy principal value. Note that when $d\neq 0$ the principal value is in general non null but when d is identically null it becomes zero. Since the term due to the integration of the singularity is only then non-null, the continuity can be maintained. However, PeC-MFIE(*RWG*,*RWG*) ignores the contribution of the integration of the singularity because *RWG* is orthogonal to this part of the rank space, whereby PMCHW cannot yield accurate results for $d=0$ in any case. The PMCHW operator must then rely only on the Cauchy principal contribution of PeC-MFIE when d is tiny enough but non zero.

Note that this fact does not necessarily imply that the results are precise because it still remains the inherent bad definition of PeC-MFIE(*RWG,RWG*) linked to the enforcement. of the continuity of the tangential component. As long as the associated error due to this is unimportant, the PMCHW can be taken into account. This is the case for penetrable bodies facing each other closely because the PeC-EFIE(*RWG,RWG*) contributions are much more relevant -see Fig. 8.5, Fig. 8.8 and Fig. 8.28-. Unfortunately, this cannot be satisfied for pairs of close enough conducting and dielectric regions -see Fig. 8.29, Fig. 8.30 and Fig. 8.31-.

In continuation, it is shown the degradation of the PMCHW performance and the robustness of EFIE and MFIE with $d=0$ compared to minuscule values of d. A pair of dielectric cubes -$\varepsilon_r=2$, $\varepsilon_r=4$- with side $0.05\lambda_0$ are chosen. Note that since they are electrically pretty small, the EFIE-MFIE low-order error must be evident -each cube is discretized with 108 triangles-.

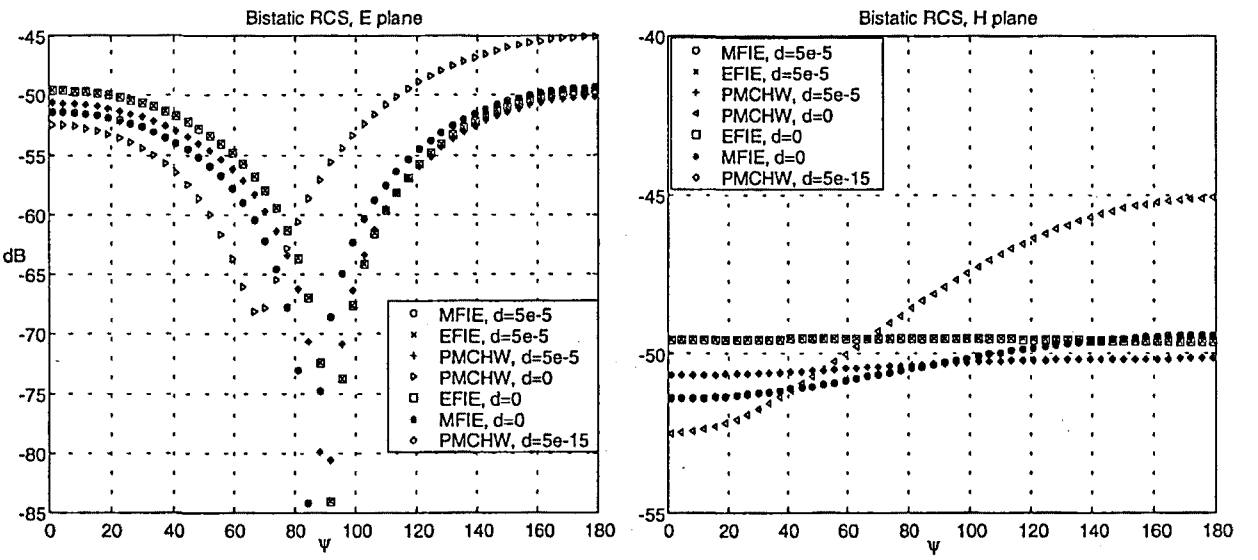

Fig. 8.36 RCS for the two cubes -$\varepsilon_r=2, \varepsilon_r=4$- with 108 triangles each

Obviously, the computer assumes a zero whenever d overpasses the accuracy of the machine. That's why the PMCHW performance is still acceptable for $d=5e-15$, which is slightly over 2.2e-16, the precision of MATLAB.

Finally, the bistatic RCS under +z directed axial incidence for the case of a composite body that consists of a dielectric cone -height $0.6\lambda_0$, radius $0.3\lambda_0$ and $\varepsilon_r=2$- lying over a conducting disk -radius $0.3\lambda_0$- is presented -see Fig. 8.37-. Since the disk stands for an open surface, the MFIE operator cannot be used. Only the EFIE and E-PMCHW approaches are then employed. Again, the E-PMCHW results in Fig. 8.38 are unacceptable when compared with the BoR-reference [30], which agrees with the theory in 8.1.3.2.

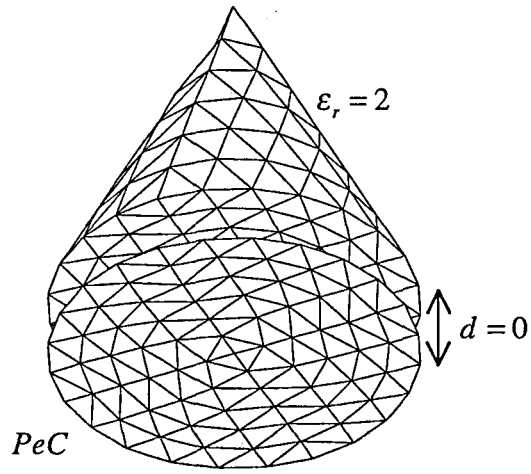

Fig. 8.37 Cone-disk structure-$\varepsilon_r = 2$,PeC- with respectively 288 and 144 triangles

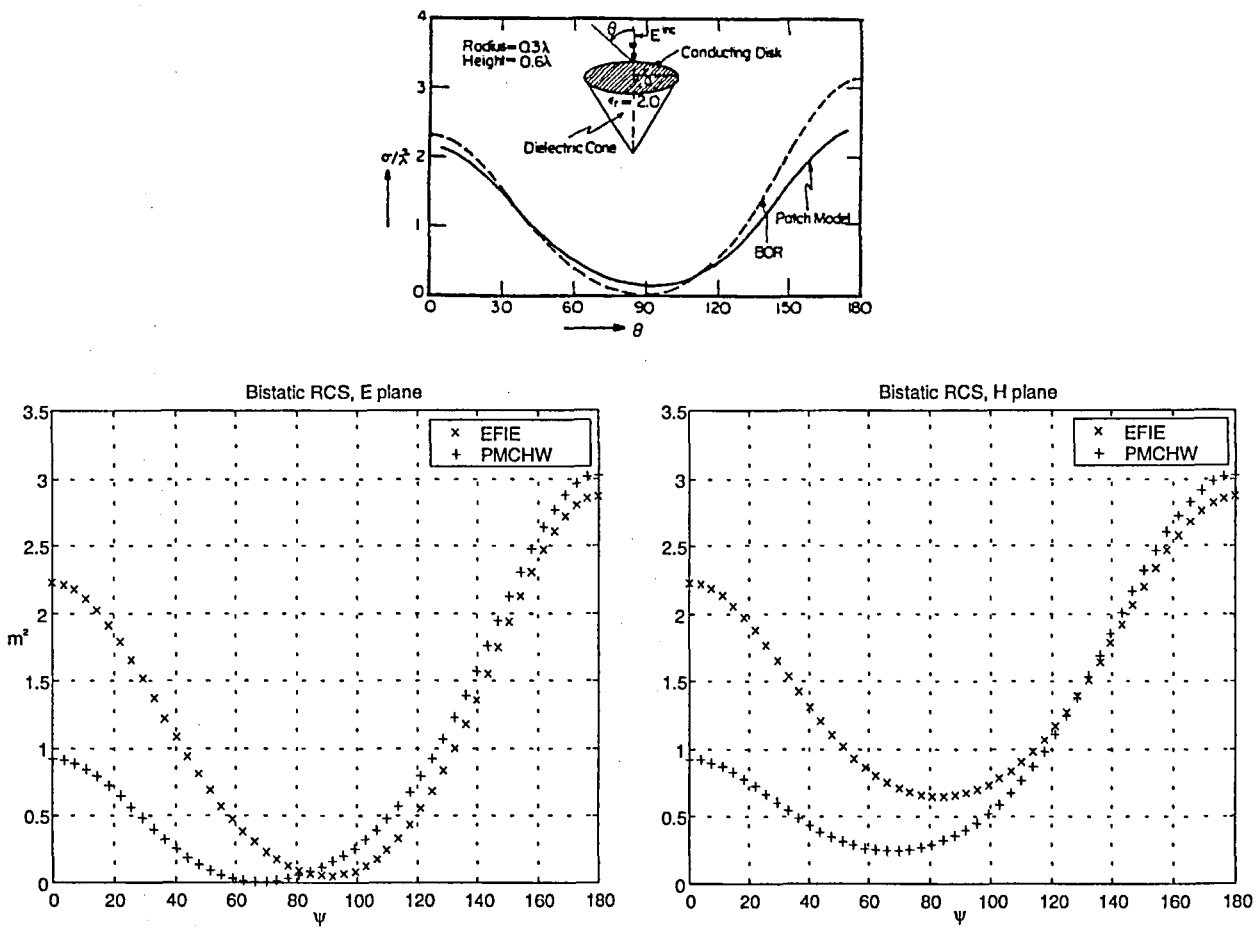

Fig. 8.38 RCS for a cone-disk composite structure -$\varepsilon_r = 2$, PeC- with 288 and 144 triangles each

8.4 CONCLUSIONS

The existence of the errors theoretically discussed in 8.1 associated to the dielectric operators EFIE-MFIE and PMCHW have been shown with examples.

The EFIE-MFIE misbehaviour is evident for problems with physical currents with a considerable high-order contribution. That is, electrically small penetrable bodies, where the influence of the physical edges is important. As the dimensions of the body increase, this error becomes decreasingly evident. Similarly, for problems with conducting regions this error diminishes because only one field condition -PeC-EFIE, PeC-MFIE- is required and thus the dual field condition can be ignored.

The PMCHW behaviour has shown to be more satisfactory for all the cases involving problems with two penetrable regions shaping the interface surfaces. This implies that in these cases the well defined PeC-EFIE(*RWG,RWG*) part is much more relevant than the PeC-MFIE(*RWG,RWG*) erroneous contribution. However, for groups of disjoint objects with a conducting and a dielectric region separated by a tiny distance, this error becomes remarkable.

In the PeC case, through the imposition $\vec{M} = 0$ one must only meet the continuity across the edges of the magnitudes in the same region and ignore the field continuity across the edges of the fields in the two media -see Fig. 8.39-. Indeed, the dielectric constants in the conducting region become superfluous because the electric and magnetic fields inside are zero. In the dielectric case, on the other hand, the continuity across the edges of the fields inside each region -as in the PeC case- and of the fields at each side of the surface -in both regions- must be ensured at the same time -see Fig. 8.39-.

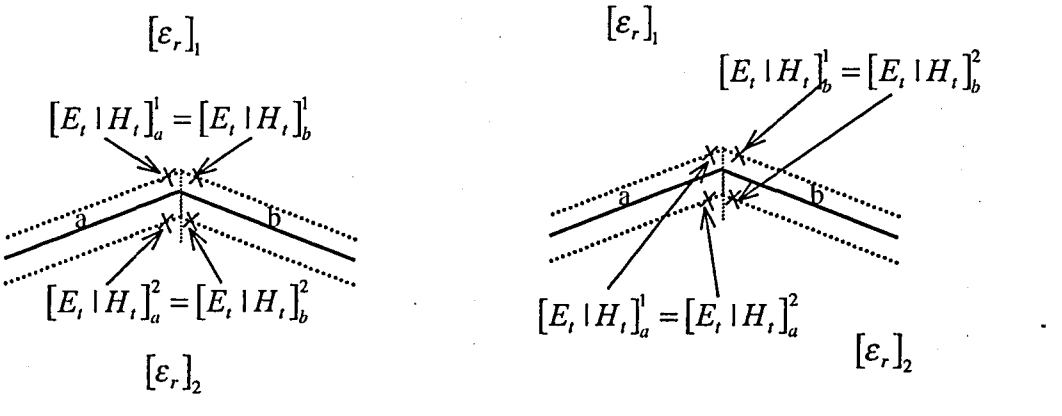

Field continuity in one region

Field continuity in two regions

Fig. 8.39 Continuity in the dielectric polyhedron

Note that the errors associated to EFIE-MFIE and PMCHW correspond to two possible strategies to overcome this difficulty. The EFIE-MFIE approaches enforce the continuity of the electric-magnetic field in one region -Fig. 8.39-. As the dual field requirement is ignored, they cannot satisfy the continuity of the fields across the edges through the two regions -unless the order of the current expansion is accurate enough-. The PMCHW, on the contrary, does ensure the interface continuity but, due to the discontinuity of the

tangential field component in each region, it has to assume an error -unimportant for problems with only penetrable regions[23]-.

Finally, the composite structures can be considered as a group of disjoint bodies with null distances of separation. The continuous transition from d increasingly small to d null can only be carried out by EFIE and MFIE. PMCHW cannot maintain the performance because PeC-MFIE(*RWG*,*RWG*) ignores the term due to the integration of the singularity, which is responsible for the continuous transition to d null.

[23] In Chapter 5, for the case of penetrable bodies with symmetry of revolution it was reasoned that the BoR-PMCHW, due to its balanced structure, excels as the dielectric operator that can best manage the BoR PeC-MFIE misbehaviour thanks to the well-behaving BoR PeC-EFIE. Now, in the 3D case, the PMCHW shows again this capacity.

Chapter 9 EFFICIENT METHODS

9.1 INTRODUCTION

The MoM is considered a brute-force method since the inversion of the resulting dense matrix requires excessive memory resources and computation time for electrically large problems. The LU decomposition -Gaussian elimination- calls for $o(N^3)$ operations and $o(N^2)$ memory storage -*N denotes the matrix dimensions-. Solutions for all the excitations* can be provided.

For such electrically large problems, it is thus recommended the use of iterative inverting techniques, such as the Conjugate Gradient -CG- or the Biconjugate Gradient -BiCG- methods. In this case, an approximation of the solution is obtained

$$I^{(k} \leftarrow [Z]I^{(k-1} \tag{9.1}$$

where $o(N^2)$ operations per iteration are required -the most costly step is the matrix-vector multiply-. CG guarantees monotonous convergence to error zero in N iterations. BiCG, in contrast, does not guarantee the convergence but usually requires less iterations for a reasonable error. The solution is supplied for only one excitation.

The recent phenomenal growth in computer technology, together with the development of fast algorithms with reduced computational complexity and memory requirements, have made a rigorous numerical solution of the problem of scattering from electrically large objects feasible [47]. In all these fast techniques the direct inversion is ignored since it is too demanding in computational terms.

One strategy to improve the computational efficiency is to reduce the number of iterations to achieve the solution. The preconditioning stands for the multiplication at both sides of the linear system -the solution is thus maintained- by a matrix dependent on the characteristics of $[Z]$. This matrix, so-called preconditioner -see 2.8.3.2-, resembles the inverse matrix of the original matrix, whereby the product of both becomes close to the identity matrix. This is very useful because it reduces the condition number of the system, which, as it is widely known, implies the decrease of the number of iterations to reach a given error.

Many researchers have also attempted to reduce the complexity of the MoM by reducing the computational requirements of the pertinent matrix-vector multiplies in the iterative methods. In this work, two strategies have been carried out, the PeC 3D IE-MEI [53] and the Fast Multipole Method -FMM-[45] and Multilevel FMM -MLFMM- [44][46][48][49] for dielectrics.

9.2 IE-MEI

The Measured Equation of Invariance -MEI- was carried out by K. Mei *et al.* [51]. This method adopts a formulation in finite differences to find efficiently the solution for a 2D PeC problem. Juan Manuel Rius extended this 2D procedure to an integral formulation -IE-MEI- [52].

The IE-MEI imposes a *measured equation* between the electric and magnetic fields over a set of adjacent weighing functions -Ω-.

$$\sum_{i\in\Omega} a_i \left\langle \vec{w}_{E,i}, \vec{E}^S_{PeC,i}\left(\vec{J}\right)\Big|_{\vec{r}_i\in S^-} \right\rangle + \sum_{i\in\Omega} b_i \left\langle \vec{w}_{H,i}, \vec{H}^S_{PeC,i}\left(\vec{J}\right)\Big|_{\vec{r}_i\in S^-} \right\rangle = 0 \tag{9.2}$$

Moreover, it is obligatory to expand the current with the same expanding set. In 3D problems, *RWG* is chosen -it is actually the only possible set because *unxRWG* is not allowed in the PeC-EFIE-. From the study in Chapter 6, the required weighting sets can only be: *RWG* for the PeC-EFIE and *unxRWG* for the PeC-MFIE. Therefore, (9.2) becomes

$$\begin{aligned} &\sum_{i\in\Omega} a_i \left\langle \vec{w}_i, \vec{E}\left(\vec{J}\right)\Big|_{\vec{r}_i\in S^-} \right\rangle + \sum_{i\in\Omega} b_i \left\langle \vec{w}_i\times\hat{n}_i^+, \vec{H}\left(\vec{J}\right)\Big|_{\vec{r}_i\in S^-} \right\rangle = \\ &\sum_{i\in\Omega} a_i \left\langle \vec{w}_i, \vec{E}^i\left(\vec{J}\right)\Big|_{\vec{r}_i\in S^-} \right\rangle + \sum_{i\in\Omega} b_i \left\langle \vec{w}_i\times\hat{n}_i^+, \vec{H}^i\left(\vec{J}\right)\Big|_{\vec{r}_i\in S^-} \right\rangle \end{aligned} \tag{9.3}$$

which, in accordance with the boundary conditions on the PeC surface, can be finally expressed as

$$\sum_{i\in\Omega} b_i \left\langle \vec{w}_i, \vec{J} \right\rangle = \sum_{i\in\Omega} a_i \left\langle \vec{w}_i, \vec{E}^i\left(\vec{J}\right)\Big|_{\vec{r}_i\in S^-} \right\rangle + \sum_{i\in\Omega} b_i \left\langle \vec{w}_i, \hat{n}_i^+\times\vec{H}^i\left(\vec{J}\right)\Big|_{\vec{r}_i\in S^-} \right\rangle \tag{9.4}$$

which stands for an alternative matrix integral expression for the traditional MoM impedance matrix

$$\begin{aligned} [B]\underline{J} &= [A]\underline{E}^i + [B]\underline{H}^i \\ \underline{J} &= [B]^{-1}[A]\underline{E}^i + \underline{H}^i \end{aligned} \tag{9.5}$$

The coefficients $\{a_i, b_i\}$ are obtained through the inversion of an overdetermined linear system locally defined over each set of weighting functions Ω.

$$[M][W]\begin{bmatrix}\underline{a}\\ \underline{b}\end{bmatrix} = 0 \tag{9.6}$$

where $[W]$ stands for the field impedance matrix over the subdomain spanned by Ω

$$W = \left[E^S_{PeC}\left(\vec{w}_{i(1)},:\right) \;..\; E^S_{PeC}\left(\vec{w}_{i(n)},:\right) \;\; H^S_{PeC}\left(\vec{w}_{i(1)},:\right) \;..\; H^S_{PeC}\left(\vec{w}_{i(n)},:\right) \right] \tag{9.7}$$

The matrix $[M]$ denotes the *metrons*, a set of vectors that allows for the enforcement of a specific property of the current coefficients. The efficient behaviour of the MEI method relies on the good choice of the set of *metrons*.

Note that the number of coefficients $\{a_i,b_i\}$ needs to be small enough in order to make the IE-MEI really efficient. Indeed, if the set of coefficients is reduced, $[A]$ and $[B]$ stand for sparse matrices and can thus compensate the unavoidable preliminary search of the coefficients by means of the later efficient matrix-vector multiply.

In 2D PeC structures, complex exponential functions are used as *metrons*. This choice enables a fast determination of the coefficients since the Fast Fourier Transform -FFT- is effectuated in (9.6). Moreover, a set of six local coefficients $\{a_i,b_i\}$ is enough in many problems. However, the generalization to 3D [53] lessens the 2D IE-MEI advantages because the exponential complex functions are not valid anymore and because more coefficients $\{a_i,b_i\}$ are needed, which yields comparatively fuller matrices.

9.2.1 Quasi-continuous metrons

In view of the well-behaving 2D harmonic *metrons* [51][52], this work has focused on the search of a good set of *metrons* for the 3D PeC-case relying on the use of the PeC-operators PeC-EFIE(*RWG,RWG*) and PeC-MFIE(*unxRWG,RWG*) -see (9.2)-.

Since the harmonic *metrons* have not worked for the 3D case, one has had to make do in principle with a trivial set of *metrons*: the identity matrix -so-called *delta metrons*-. The author of this dissertation Thesis has found a group of *metrons* that reduces the required number of coefficients $\{a_i,b_i\}$ -in comparison with the *delta metrons*- for the objects tested -spheres and cubes-. I have named this new set of *metrons*, a singular contribution of this work, *quasi-continuous*.

The full-expansion of the field space -MoM- guarantees the little discontinuity of the fields across the edges. Indeed, PeC-EFIE(*RWG,RWG*) and PeC-MFIE(*unxRWG,RWG*) ensure the continuity of one component -see 6.5-, respectively the normal and the tangential component. As the PeC-CFIE results from the linear combination of PeC-EFIE and PeC-MFIE, the little discontinuity of the field must be maintained for a given degree of discretization. The solution of the IE-MEI with a large set of coefficients $\{a_i,b_i\}$ approaches the PeC-CFIE solution and can thus fulfil the continuity requirements across the edges. However, in an implementation of the IE-MEI with a small set of coefficients $\{a_i,b_i\}$, the little discontinuity of the fields can not be ensured in principle over the reduced portion of the field space embraced by Ω. This implies that the little discontinuity for the current across the edges cannot be ensured either.

The *quasi-continuous metrons* enforce the little discontinuity of the current across the edges. This allows a better definition of the subdomain field space and therefore a smaller set of coefficients $\{a_i,b_i\}$ is required to achieve the same precision on the current solution. These *metrons* have been found heuristically by ensuring the continuity of the tangential component of the current at two points of each edge -the normal continuity is provided implicitly through the expansion in terms of *RWG*-. This obviously leads to an

overdetermined system of dimensions $2N \times N$. The set of *quasi-continuous metrons* forms thus a matrix - $\dim([M]) = N \times N$ - where each row is the least squares solution of the overdetermined system by compelling the current coefficient associated to the corresponding edge to one.

The relative current error -compared with the CFIE reference- for an increasing number of coefficients is shown for both sets of *metrons -delta* and *quasi-continuous-* for a cube of side 0.3λ and 192 triangles -Table 9.1- and a sphere of radius 0.25λ and 128 triangles -Table 9.2-.

$n_a = n_b$	*error (%) - Delta*	*error(%) - Quasi-continuous*
11	1e3	162
15	464	247
21	72	14
25	108	15
27	56	49
31	70	18
37	41	11
39	24	10
41	13	9
45	21	11
47	13	8
53	9	8

Table 9.1 Evolution of the IE-MEI error respect to CFIE, for a cube with side 0.3λ

$n_a = n_b$	*error (%) - Delta*	*error(%) - Quasi-continuous*
6	185	17
7	245	16
8	214	16
9	116	15
10	92	16
12	53	19
14	40	15
18	22	10
20	8.2	3.2
23	6.25	3.9
26	5.8	3.1
30	4.6	2.9
40	4.3	2.4

Table 9.2 Evolution of the IE-MEI error respect to CFIE, for a sphere with radius 0.25λ

In view of the results -Table 9.1 and Table 9.2- the improvement with the *quasi-continuous metrons* is remarkable since a reasonable error is reached with a smaller set of coefficients. However, this option is dismissed in practice because the matrix of *metrons* must be pre-computed for each specific case and because an extra full-matrix multiplication is required in (9.6).

9.3 FAST MULTIPOLE METHOD

The FMM is based on the division of the object in non-overlapping subdomains of expanding functions. For the sake of simplicity, cubical boxes are chosen -see Fig. 9.1 -. For PeC bodies, it is recommended a size of the box D of at least 0.25λ.

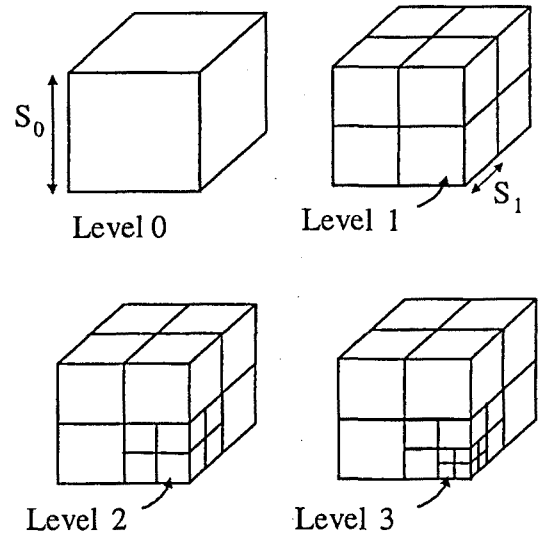

Fig. 9.1 Boxes enclosing the body in different levels

The FMM sorts out the electromagnetic interaction between the basis functions through the interaction of near field boxes and far field boxes -see Fig. 9.2-. The electromagnetic coupling between basis functions on the near field boxes embraces the influences with the same box or with touching boxes -see Fig. 9.2-.

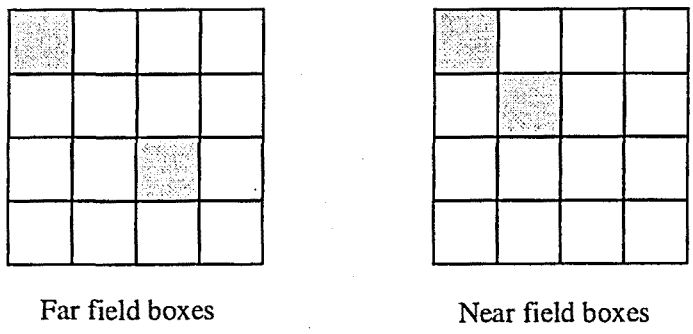

Fig. 9.2 Near and Far field boxes

The electromagnetic interactions between functions in the near field boxes are computed directly through MoM, which involves $N_m \cdot N_n$ operations. The electromagnetic influence between the functions in the far field boxes is computed through the FMM. This makes sense because such interactions have actually a number of degrees of freedom lower than the total combination of the possible interactions between the functions in both boxes - $N_m \cdot N_n$ -.

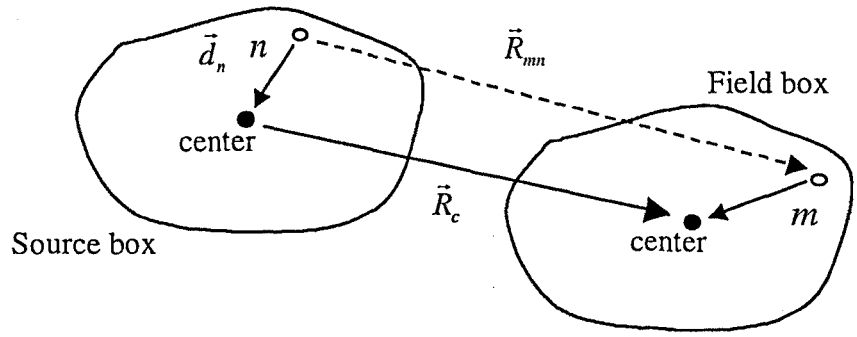

Fig. 9.3 Far box interaction

The far box interaction relies on the Plane Wave Expansion -PWE- of the free-space Green's funcion -see Fig. 9.3-

$$G\left(\left|\vec{R}_c+\vec{d}_n-\vec{d}_m\right|\right)=\frac{-jk_0}{4\pi}\int e^{-j\vec{k}\cdot\vec{d}_m}T(\hat{k},\vec{R}_c)e^{j\vec{k}\cdot\vec{d}_n}d^2\hat{k} \tag{9.8}$$

where

$$T(\hat{k},\vec{R}_c)=-\sum_{l=0}^{\infty} j^l(2l+1)h_l^{(2)}(kR_c)P_l(\hat{k}\cdot\vec{R}_c) \tag{9.9}$$

denotes the translation operator, which computes the field radiated by a plane wave of current. This field is also a plane wave.

The FMM relies on the truncation of the summation in (9.9) so that only the L+1 first terms in (9.9) are kept. L has been empirically estimated as

$$L=kD+P\log(kD+\pi) \tag{9.10}$$

where D stands for the box size and P denotes the precision parameter -it is very critical because it increases rapidly the CPU time-. L gives a measure of the minimum distance between boxes for the FMM to be valid -$R_{\min} = L / k$-. Likewise, L determines the number of directions K required in the discretization of the plane wave expansion; that is, -see (9.8)-

$$\int f\left(\vec{k}\right)\ e^{j\vec{k}\cdot\vec{r}}\ \ d^2\hat{k}=\sum_{i=1}^{K} f\left(\vec{k}_i\right)\ e^{j\vec{k}_i\cdot\vec{r}} \tag{9.11}$$

The K directions must be sufficient to give a quadrature rule that is exact for all spherical harmonics of order $l<2L$. A simple method to accomplish this is to pick polar angles θ that they are zeros of $P_L(\cos\theta)$, and azimuthal angles ϕ to be $2L$ equally spaced points, which leads to $K=2L^2$ [45].

The FMM implementation must compute the total electromagnetic interaction relying partially on (9.8), which affects actually only the Kernel. Therefore, the current in the source box is expanded

$$\vec{J}(\vec{r}) = \sum_{n=1}^{N_n} \vec{b}_n(\vec{r}) I_n \tag{9.12}$$

where N_n and I_n denote respectively the number of expanding functions in the source box and the current coefficients; $\{\vec{b}_n\}$ stands for the chosen set of expanding functions.

If we define

$$\vec{V}(\hat{k}_i) = \int \vec{b}_n(\vec{r}) \; e^{-j\vec{k}_i \cdot \vec{r}} d\vec{r} \tag{9.13}$$

the -electric or magnetic- field contribution $\vec{S}_m$ on the field box due to the source box become

$$\left[\vec{S}_m\right] = \sum_{i=1}^{K} \left[\vec{W}\right]^{+} T(\hat{k}_i, \vec{R}_c) \sum_{n=1}^{N_n} \left[\vec{V}\right] I_n \tag{9.14}$$

where $\left[\vec{W}\right]$ stands for the contribution due to the weighting procedure in the field box, which, in an analogous way as in (9.13), becomes

$$\vec{W}(\hat{k}_i) = \int \vec{t}_n(\vec{r}) \; e^{-j\vec{k}_i \cdot \vec{r}} d\vec{r} \tag{9.15}$$

where $\{\vec{t}_n\}$ stands for the weighting set.

According to the study developed in Chapters 6, 7 and 8, the relations between the expanding and weighting sets must be in agreement with the requirements of the operators. Since PeC-EFIE requires *RWG* for both sets, -see 6.1.1-

$$\vec{W}(\hat{k}_i) = \vec{V}(\hat{k}_i) = \int \vec{w}_n(\vec{r}) \; e^{-j\vec{k}_i \cdot \vec{r}} d\vec{r} \tag{9.16}$$

The chosen PeC-MFIE operator uses the *RWG* and *unxRWG* respectively as weighting and expanding sets and the -see 6.1.2-

$$\begin{aligned} \vec{V}(\hat{k}_i) &= \int (\vec{w} \times \hat{n})_n(\vec{r}) \; e^{-j\vec{k}_i \cdot \vec{r}} d\vec{r} \\ \vec{W}(\hat{k}_i) &= \int \vec{w}_n(\vec{r}) \; e^{-j\vec{k}_i \cdot \vec{r}} d\vec{r} \end{aligned} \tag{9.17}$$

Furthermore, the PeC-MFIE choice requires the modification of the translation operator in (9.14) in accordance with the Kernel in this case. Note that the combination of both PeC-operators enables a further development to the dielectric case.

Therefore, the collection of the near box and far box field contributions yields

$$[Z]=[W]^{+}[T][V]+[Z_{near}] \tag{9.18}$$

where all the matrices are very sparse and are pre-computed and stored in RAM memory or hard disk. In regard with the efficiency properties, it is optimum to subdivide the object with $\sqrt{N}$ boxes, which leads to $o(N^{3/2})$ operations per iteration.

9.3.1 MLFMM

The MLFMM is a refinement of FMM that takes advantage of the subdivision of boxes at L different levels -see Fig. 9.1- to yield a more efficient computation of the far field interactions

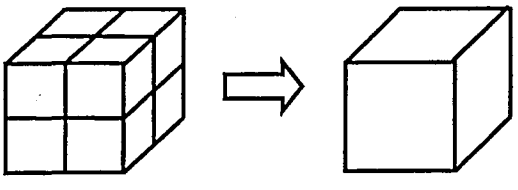

Fig. 9.4 Transition from level L to level L-1

First, the PWE of the expanding functions at level-L that are contained in the source box must be computed. The next step is the iterative computation of the PWE of the expanding functions at level L-1 from the PWE at the level L -see Fig. 9.4- which implies

1. to shift the PWE from the centers of the boxes in level-L to the centers of the boxes in level-L–1 -see Fig. 9.3-.

2. as the electrical dimensions of the box increase, the expansion in level-L–1 needs more plane wave directions -see (9.11), the value for K rises-. Therefore, the level-L PWE must be interpolated from the level-L-1 PWE.

Once the lowest level is reached, the PWE of the expanding functions must be translated from source box to field box to obtain the PWE of the field -see (9.8)-. Next, the iterative process must reversed to obtain the PWE of the field radiated by the source box at the finest level L in the field box.

It must be noted that the transition from a level to a lower level is only possible as long as the FMM conditions can be accomplished at the new level. Indeed, one must check, in accordance with the new box size value, if the distance between boxes at the new level is over $R_{min} = L / k$. The MLFMM excels as an improvement of the FMM that fastens the

computation of the far box field contributions. Indeed, the computational complexity per iteration can be reduced in practice to o(*N*log*(N)*).

In 9.3.2, some results are presented for the development of the MLFMM for penetrable bodies by using the *RWG* and *unxRWG* expanding sets.

9.3.2 MLFMM for penetrable bodies

According to the study in Chapter 8, the dielectric EFIE-MFIE operators have been chosen to develop the MLFMM. Indeed, since the low-order misbehaviour of EFIE-MFIE is evident for penetrable objects of electrically small dimensions, this misbehaviour must be unnoticeable for electrically large objects -those involved in the fast techniques-. Furthermore, EFIE-MFIE have shown a lower condition number than PMCHW for the same problem and discretization -see 8.2.1-. This is very advantageous when working with inverting techniques since less iteration steps are required to reach a certain bound of error. Finally, a PMCHW implementation would preclude any further development for PeC-dielectric composite structures.

Alex Heldring -who is pursuing the Doctorate in the department- has developed a MLFMM PeC-EFIE(*RWG,RWG*) and MLFMM PeC-MFIE(*unxRWG,RWG*) code. The author of this dissertation Thesis has adapted this work first to the operator PeC-MFIE(*RWG,unxRWG*), which is straightforward because the far field interactions are transposed -see Chapter 6-. After, he has developed the dual dielectric MLFMM EFIE-MFIE from the pertinent combination -see Chapter 8- of the MLFMM PeC-EFIE(*RWG,RWG*) and the MLFMM PeC-MFIE(*RWG,unxRWG*).

The MLFMM has been encoded together with the BiCG iterative method with preconditioning. The adopted preconditioner relies on the LU decomposition of a matrix that keeps the biggest impedance terms per row of the original matrix and sets the rest to zero. An incomplete LU decomposition is usually enough since no high accuracy for the preconditioner is required. This is advantageous since it fastens the pre-computation of the preconditioner.

The implementation of the MLFMM for a penetrable body is based on the application of the MLFMM on each region in accordance with the corresponding values of the dielectric constants -k_d , λ_d-. Therefore, the MLFMM provides different parameters for each region, which obviously results in a different distribution of boxes for the study of the electromagnetic interactions of the body in both regions.

Some penetrable spheres have been analysed with the MLFMM EFIE. Since the computer capabilities in the JRC allowed high memory storage but little hard disk space, the electrical dimensions undertaken have turned out slightly low for a MLFMM approach. X. Q. Shing *et al.* [44] recommend that the edge length of the finest cube is about half the wavelength in dielectrics. In this work, penetrable spheres with radius not over $0.7\lambda_d$ have been analysed; that is why it has not been possible to assess all the capabilities of the MLFMM performance.

In Fig. 9.5, Fig. 9.6 and Fig. 9.7, the bistatic RCS for spheres with respectively radius $0.3\lambda_0$ -$\varepsilon_r = 3$-, $0.5\lambda_0$-$\varepsilon_r = 2$- and $0.3\lambda_0$-$\varepsilon_r = 2$- are shown. The results are compared with the Mie solution of the sphere.

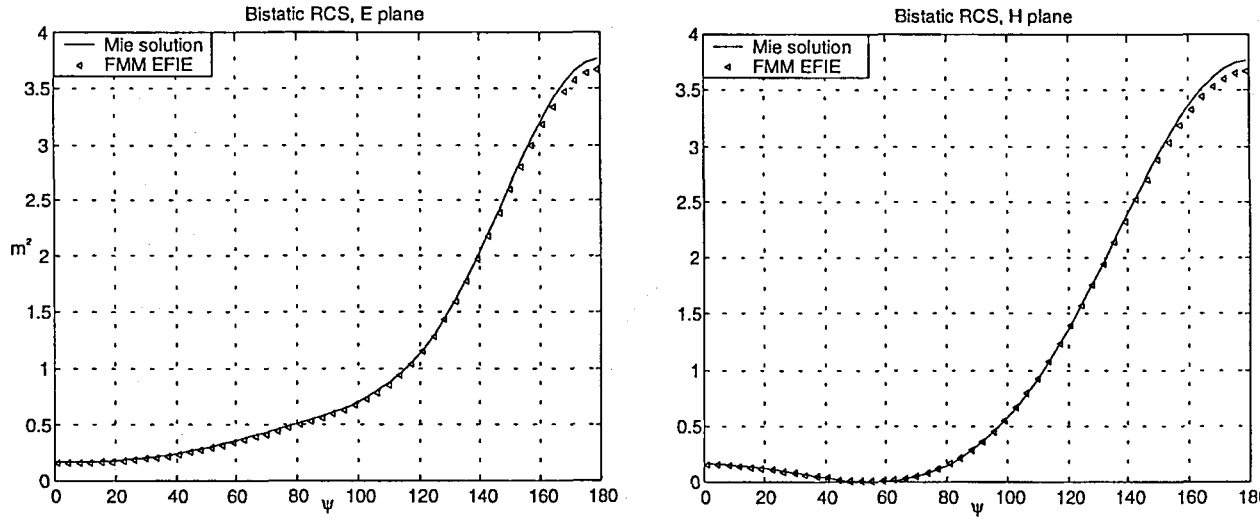

Fig. 9.5 Sphere with radius $0.3\lambda_0$ *-* $\varepsilon_r = 3$ *- and 26 boxes*

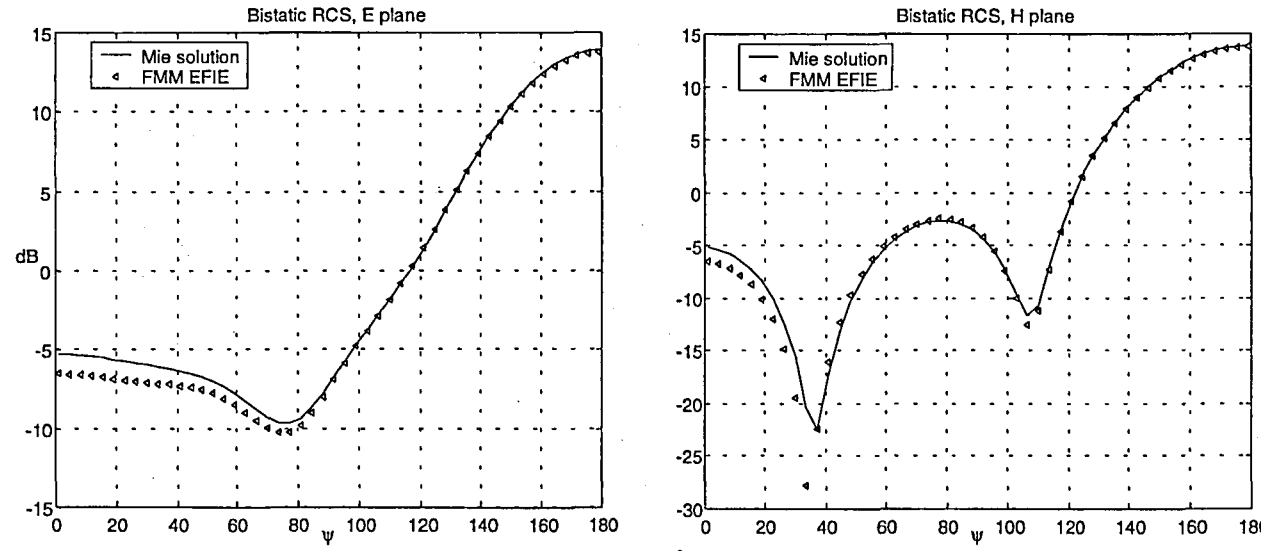

Fig. 9.6 Sphere with radius $0.5\lambda_0$ *-* $\varepsilon_r = 2$ *- and 20 boxes*

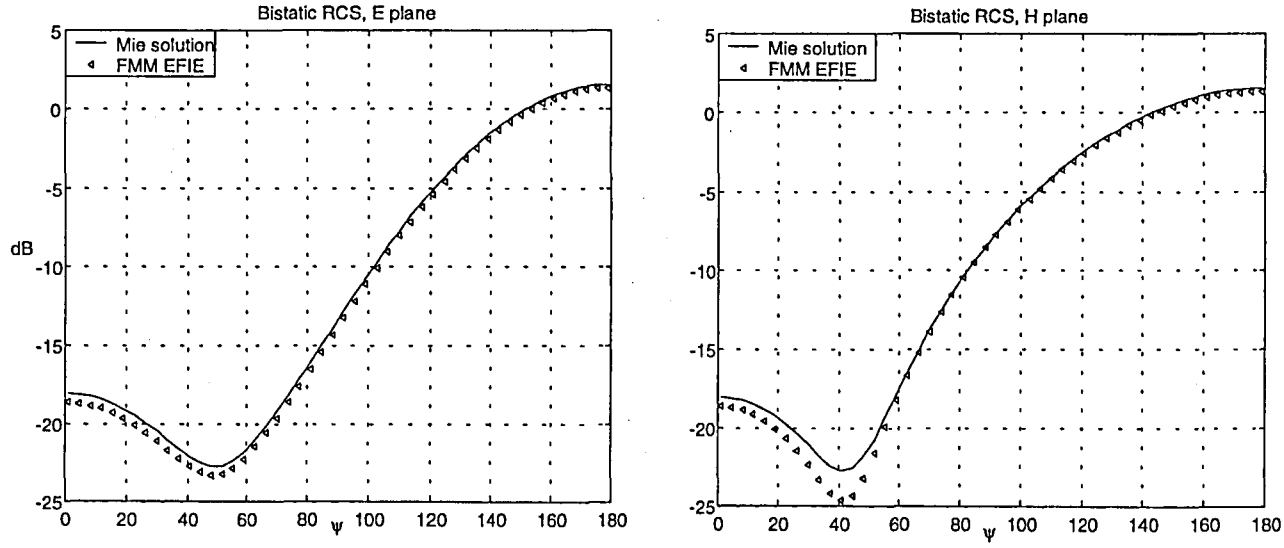

Fig. 9.7 Sphere with radius $0.3\lambda_0$ *-* $\varepsilon_r = 2$ *- and 26 boxes*

Some comments must be presented about the computation of the RCS for these spheres

1. It has turned out impossible to apply the FMM to both media -inside and outside- at the same time. The results in Fig. 9.5, Fig. 9.6 and Fig. 9.7 have been applied with FMM in the outer medium -the free-space-. The interactions in the inner medium are directly computed through MoM.

2. The size and the number of boxes for each case are $D=0.2\lambda_0$, 26 boxes -Fig. 9.5-, $D=0.48\lambda_0$, 20 boxes -Fig. 9.6 - and $D=0.2\lambda_0$, 26 boxes -Fig. 9.7-. The chosen values for D are the minimum that have enabled the convergence. Note that for Fig. 9.5 and in Fig. 9.7, the number of boxes is optimum in regard with to the computational time because $26\cong\sqrt{768}$.

3. For these cases, according to the not big enough electrical dimensions of the objects, the Multilevel implementation -MLFMM- could not be applied.

4. The parameters chosen are $P=1.5$ in all the cases and $K=16$ for Fig. 9.5 and Fig. 9.7 $K=56$ for Fig. 9.6, which makes sense because the box is comparatively bigger.

5. In comparison with the performance of FMM in the PeC cases, the pre-computation of the preconditioner has had to be done much more accurately. Indeed, the incomplete LU decomposition has required a drop tolerance much smaller -about 1e-5- and the number of elements per row chosen has not been lower than 300. This makes sense because the condition number of the original matrix is bigger in the dielectric case.

Chapter 10 CONCLUSIONS

The conclusions of this dissertation Thesis are presented in continuation for the main areas of study. The first half of this dissertation Thesis is based on the study of the bodies of revolution -BoR- -Chapters 3, 4 and 5-.

- **Bodies of revolution:**

  The PeC-EFIE operator -with the implementation of S. D. Gedney and R. Mittra [12]- has shown a much better performance than the PeC-MFIE operator, where the same ideas regarding the analytical recurrent formulation for the higher-order terms and the FFT transformation for the low-order terms have been adopted. This PeC-MFIE misbehaviour has to be attributed to the inaccurate computation of the electromagnetic interactions between the near annuli. This error becomes increasingly important as one heads for the low-frequency terms in the modal expansion of the current.

  Whenever the R^{-3}-dependent terms in PeC-MFIE are integrated differently so that an analytical equivalent expression relying on R^{-1}-dependent terms is employed, the PeC-MFIE performance improves. Two corrections regarding the R^{-3}-terms of the integrand dependent on $\partial()/\partial\phi$ and on $\sin\xi\partial()/\partial n$ enable the complete expression of the submatrices with ξ-odd behaviour -$[Z_{\phi,\phi}]$ and $[Z_{t,t}]$- in terms of R^{-1}-terms. However, the submatrices with ξ-even behaviour -$[Z_{\phi,t}]$ and $[Z_{t,\phi}]$- show still dependence on R^{-3}-terms that can only be partially corrected through the substitution of the $\sin\xi\partial()/\partial R$ terms. Therefore, an error remains in the PeC-MFIE operator but the improvement due to the corrections is noticeable in any case. One can well assess this in Chapter 4 for a sphere and a cylinder with generating arc of length $1\lambda_0$. This PeC-MFIE misbehaviour is present in the literature since no valid PeC-MFIE formulation has ever been published -to my knowledge-.

  The construction of a consistent BoR dielectric formulation from the PeC-EFIE and PeC-MFIE formulations is undertaken in Chapter 6. The unbalanced characteristics of the used expanding functions [13] only allow the use of the PMCHW dielectric approach. Indeed, the dielectric EFIE and MFIE yield a singular matrix for the mode zero. Furthermore, in view of the publications for dielectric BoR in literature either for a balanced set [19] [20] [31] or for an unbalanced set [13], the PMCHW operator seems to turn out more robust to the PeC-MFIE misbehaviour than the dielectric EFIE and MFIE. This has been attributed in this work to the formal structure of the PMCHW operator which, unlike EFIE and MFIE, distributes the influence of the well-behaving PeC-EFIE and of the erroneous PeC-MFIE to the two unknowns, the electric and the magnetic current. Some results show to some extent acceptable performance of PMCHW for this formulation.

The most outstanding contribution of this dissertation Thesis -Chapters 6, 7 and 8- is the study of the appropriate conditions to develop correctly the 3D-operators -PeC and dielectric- so as to yield accurate results for any structure. Since the discretization implies a break on the continuity properties of the physical magnitudes, the valid 3D-operators must ensure the physical electromagnetic requirements in the discretized surface. In mathematical terms, these requirements set the rank -field- and domain -current- spaces, which essentially require the enforcement of the continuity across the edges of either the tangential or the normal component of the expanded magnitudes.

The electromagnetic field requirements over the edges are the boundary conditions in the 2D case, derived from the Maxwell equations. The formulations that yield a compatible system -as many source conditions as field conditions- when ensuring the field requirements across the edges are well posed.

- **PeC 3D arbitrary bodies:**

  The operator PeC-EFIE(*RWG,RWG*) [28] enforces the continuity of the normal component of the electric field across the edges. This operator can only be defined as long as the *charge accumulation* across the edges is imposed to be null, which makes sense because it corresponds to the physical -continuous- performance. The normal continuity of the current across the edges -charge condition- stands for the source condition compatible with the field condition. Therefore, a suitable set of expanding and weighting functions is *RWG* or, in general, any divergence-conforming set.

  The linear charge density that appears in the electric field requirement across the edges shows that the system is undetermined. There must be hence some ambiguity in the solution for the current associated to the required imposition of null charge accumulation. When the degree of discretization is low, the ambiguity must be low because a small amount of edge conditions are incorporated. However, as the discretization becomes increasingly fine, the ambiguity must become more important. That is why the condition number of PeC-EFIE(*RWG,RWG*) accordingly grows when the discretization becomes finer for a given problem. In any case, in all the objects analysed in Chapter 7 -with pretty small electrical dimensions-, no evidence of ambiguity in the solution has been encountered.

  The operator PeC-MFIE(*RWG,unxRWG*) ensures the continuity of the normal component of the magnetic field across the edges. The tangential continuity of the current represents the corresponding compatible source condition. Therefore, the sets *RWG* and *unxRWG* -in general, any divergence-conforming and curl-conforming set- stand for appropriate weighting and expanding sets. The alternative operator PeC-MFIE(*unxRWG,RWG*) [11] ensures the continuity of the tangential component of the magnetic field across the edges. The corresponding compatible source condition comes now from enforcing the normal continuity of the current. Hence, the sets *RWG* and *unxRWG* -in general, any divergence or curl-conforming set- are accordingly fit as expanding and weighting sets. Both PeC-MFIE approaches, unlike the PeC-EFIE(*RWG,RWG*), are unambiguously posed. Therefore, their condition number turns out low and stable for any degree of discretization.

PeC-MFIE(*unxRWG,RWG*), unlike the other two operators, does not ensure a field condition that coincides with the required magnetic field condition -derived from the Maxwell equations-. Therefore, there must be some inherent error in the performance of PeC-MFIE(*unxRWG,RWG*). This error diminishes whenever the directions of the normal vectors at both sides of the edge approach. Indeed, only in case the normal vectors at both sides are parallel, the tangential continuity of the magnetic field across the edges coincides with the corresponding electromagnetic requirement.

The operators PeC-EFIE(*RWG,RWG*) and PeC-MFIE(*RWG,unxRWG*) have shown a better performance than PeC-MFIE(*unxRWG,RWG*) in any case. A heuristic procedure to improve the behaviour of PeC-MFIE(*unxRWG,RWG*) has been provided in Chapter 7 by defining a new solid angle value as the result of the weighted average of the solid angles on the edges shaping the triangle.

For physical polyhedrons, the operator PeC-EFIE(*RWG,RWG*) yields more accurate results for a lower degree of discretization. This implies a higher-order behaviour because it is more sensitive to the effect of the edges -particularly important on objects with electrically small dimensions-. The PeC-MFIE(*RWG,unxRWG*), on the other hand, requires a finer discretization to yield the same performance for the physical polyhedron, which means that its solution is of lower-order. In any case, for a sufficient degree of discretization the performances of both operators merge. This is reasonable because, as both operators are well posed in electromagnetic terms, they must lead to the complete solution of the physical polyhedron for a sufficient order of expansion.

Nevertheless, for entirely curved objects -mainly if coarsely meshed- the behaviour of PeC-MFIE(*RWG,unxRWG*) turns out more accurate than the PeC-EFIE(*RWG,RWG*). This must be due to the fact that it ignores more the effect of the edges -as explained in the previous paragraph-. Note that the edges associated to the discretization of a curved body are fictitious since they only appear because of the unavoidable planar modelling of the curvature. A correction is provided in Chapter 7 for the PeC-EFIE(*RWG,RWG*) behaviour in these cases by effectuating a parabolic interpolation of the current over the surface of the sphere, which is reasonable because the solution due to the PeC-EFIE(*RWG,RWG*) must be closer to the solution of the physical polyhedron derived from the coarse modelling of the curvature.

The accurate development of the presented operators PeC-EFIE(*RWG,RWG*), PeC-MFIE(*RWG,unxRWG*) and PeC-MFIE(*unxRWG,RWG*) relies on an analytical source-integration for the high-order terms [9] and on a numerical gauss quadrature rule for the source-low order terms and the testing. Since the PeC-EFIE operator supplies an integrand with a R^{-1}-dependence its performance varies less with the numerical parameters of integration.

- **Dielectric 3D arbitrary bodies**

In the PeC case, through the imposition of no magnetic sources, one must only meet the continuity across the edges of the magnitudes in the same region and ignore the field continuity across the edges of the fields in the two media. Indeed, the dielectric constants in the conducting region become superfluous because the electric and magnetic fields inside are null. In the dielectric case, however, the continuity across

the edges of the fields inside each region -as in the PeC case- and the continuity across the surface of the fields must be ensured at the same time.

This cannot be accomplished in general because one cannot ensure the two field requirements across the edges from four source conditions -the two PeC-conditions correct in electromagnetic terms for PeC-EFIE(*RWG,RWG*) and PeC-MFIE(*RWG,unxRWG*) become now four since they involve the two source magnitudes, the electric and the magnetic current-. All the dielectric operators relying on an integral formulation derived from the surface theorem of equivalence must show then an inherent misbehaviour when analysing penetrable objects.

The operators EFIE and MFIE stand for dual approaches to undertake the analysis of an arbitrary penetrable body. They enforce the continuity of the normal component, respectively, of the electric and the magnetic field in each region separately and ignore the field requirement for the dual magnitude, respectively, the magnetic and the electric field. The weighting sets of EFIE and MFIE must be *RWG* -or any divergence-conforming set- since the normal continuity is ensured. The sets *RWG* and *unxRWG* are used to expand the dual source magnitudes of each operator EFIE-MFIE; that is, respectively, the electric-magnetic current and the magnetic-electric current. Note that EFIE and MFIE rely on the combination of the well-behaving PeC-EFIE(*RWG,RWG*) and PeC-MFIE(*RWG,unxRWG*).

Only when the expansion of the source magnitudes is complete, the inherent ignorance in EFIE-MFIE of the dual field requirement can be actually assumed. Hence, the EFIE-MFIE misbehaviour is evident for problems with physical currents with a considerable high-order contribution -the low-order expansion in terms of *RWG* and *unxRWG* is not sufficient-. That is, for example, electrically small penetrable bodies, where the influence of the physical edges is important. As the dimensions of the penetrable body increase, this low-order misbehaviour becomes decreasingly evident. Similarly, for problems with conducting regions, the relevance of this error diminishes thanks to the fact that one field condition on the conducting interfaces is enough to pose correctly the problem -the dual field condition can be indeed ignored-.

The PMCHW operator ensures the normal continuity of the subtraction of the electric and magnetic fields at both sides of the surface. The source conditions compatible with these field conditions are the electric and magnetic charge conditions; that is, the enforcement of the normal continuity of the electric and the magnetic current. Therefore, *RWG* -or any divergence-conforming set- excels not only as a suitable weighting set but as an appropriate expanding set of both source magnitudes, the electric and the magnetic current. The PMCHW operator relies then in the combination of the well-behaving PeC-EFIE(*RWG,RWG*) and the badly defined PeC-MFIE(*RWG,RWG*). This implies that the normal continuity across the edges of the magnetic and the electric field separately on each region cannot be accomplished, which represents a less stringent field requirement than the requirements derived from the Maxwell equations.

However, the PMCHW behaviour has shown to be more satisfactory than the performance of EFIE-MFIE for all the problems involving problems with two penetrable regions shaping the interface surfaces. This implies that the badly defined PeC-MFIE(*RWG,RWG*) contribution becomes unimportant compared to the robust PeC-EFIE(*RWG,RWG*) term. Indeed, since the PeC-MFIE influence on the PMCHW

operator relies only on the principal value contribution, it is irrelevant that the weighting carried out by *RWG* cancels the integration of the singularity. Moreover, on single bodies, the PeC-MFIE interactions between near facets -the most relevant ones- become less important than the PeC-EFIE ones because these facets are co-planar or nearly co-planar. Note that, as mentioned for the BoR case, this is again a proof of the importance of the balanced structure of the PMCHW that puts stress on the well-behaving PeC-EFIE to compensate any presumable misbehaviour in PeC-MFIE.

Nonetheless, for groups of disjoint objects with a conducting and a dielectric region separated by a tiny distance, the PMCHW error becomes remarkable and the performance compared to EFIE-MFIE worsens considerably. This is reasonable because in this case the magnetic current over the dielectric interface tends to zero, whereby the PeC-EFIE contribution on the magnetic field becomes negligible in front of the badly defined PeC-MFIE contribution.

Note that the errors associated to EFIE-MFIE and PMCHW correspond to the two possible strategies to overcome the inherent difficulty of the surface equivalence theorem to set -at the same time- the surface continuity of the fields and the continuity across the edges separately at each region. Indeed, the EFIE-MFIE approaches enforce the continuity of the electric-magnetic field in each region. As the dual field requirement is ignored, they cannot satisfy the surface continuity -unless the order of the current expansion is accurate enough-. The PMCHW, on the contrary, does ensure the interface continuity but, because of the discontinuity of the tangential field component in each region, it has to assume an error -unimportant for problems with only penetrable regions-.

All the dielectric operators must provide the charge condition across the edges together with the field requirements. Meanwhile the dual EFIE and MFIE supply respectively the electric and magnetic charge condition, PMCHW has to provide both. This implies that the systems can only be posed for all the operators by imposing the charge accumulation null. Therefore, now, unlike the PeC-MFIE, EFIE, MFIE and PMCHW must assume some ambiguity in their solution -insignificant for a small degree of discretization-. In particular, the PMCHW operator shows a higher condition number than the dual EFIE-MFIE because it has to impose two magnitudes -the electric and the magnetic linear charge density- to zero, which yields a more undetermined system.

Finally, the composite structures can be considered as a group of disjoint bodies with null distances of separation -*d*-. The continuous transition from *d* increasingly small to *d* null can only be carried out by EFIE and MFIE, because they rely on the continuous basic operators PeC-EFIE(*RWG*,*RWG*) and PeC-MFIE(*RWG*,*unxRWG*). PMCHW, on the other hand, cannot maintain the performance for composite structures because PeC-MFIE(*RWG*,*RWG*) ignores the term due to the integration of the singularity, which is responsible for the continuous transition to a null distance of separation.

In Chapter 9, efficient methods -IE-MEI and MLFMM- relying on the 3D-operators of Chapters 6 and 8 are presented

- **Efficient methods:**

  The IE-MEI method [53] when applied on 3D PeC bodies cannot maintain the advantages present in the 2D case since the harmonic *metrons* are not valid in the 3D case. A new set of *metrons*, so-called *quasi-continuous* because they ensure little discontinuity of the current across the edges, is presented instead. This is advantageous because the little discontinuity of the magnitudes -field and current- cannot be ensured directly through a small amount of coefficients -over a small field subdomain-. It is shown with examples how the required amount of coefficients to attain a given error decreases with the *quasi-continuous metrons*. However, these *metrons* must be dismissed in practice since they must be pre-computed for each body and involve an extra multiplying matrix in the process of search of the coefficients.

  With regard to the dielectric MLFMM [45] implementation, the EFIE and MFIE are suitable operators since for electrically large dielectric bodies -involved in the fast techniques- the low-order misbehaviour disappears. Furthermore, EFIE-MFIE have shown a lower condition number than PMCHW for the same problem and discretization, which must enable a smaller time of convergence. Also, a PMCHW implementation would preclude any further development for PeC-dielectric composite structures. The dual dielectric EFIE-MFIE operators are developed from an existing PeC-MLFMM package. Some examples of penetrable spheres with moderate electrical dimensions have been shown, where it is remarked the required bigger precision to effectuate the incomplete LU decomposition in the preconditioning.

Chapter 11 APPENDICES

APPENDIX A

The elementary integrals I_α stand for

$$I_{\alpha(k,m)} = \int_0^{\pi/2} \frac{\cos^\alpha \varphi}{\left[1+\beta_1^2 \sin^2 \varphi\right]^{1/2}} d\varphi \tag{11.1}$$

The procedure developed by S. D. Gedney and R. Mittra yields I_α from the analytical results for I_0 and I_2 [1],

$$\begin{aligned} I_0 &= \int_0^{\pi/2} \frac{d\varphi}{\left[1+\beta_1^2 \sin^2 \varphi\right]^{1/2}} = \int_0^{\pi/2} \frac{d\varphi}{\left[1+\beta_1^2 (1-\cos^2 \varphi)\right]^{1/2}} \\ &= \frac{1}{\left[1+\beta_1^2\right]^{1/2}} \int_0^{\pi/2} \frac{d\varphi}{\left[1-\left(\beta_1^2/\left(1+\beta_1^2\right)\right)\cos^2 \varphi\right]^{1/2}} \\ &= \frac{1}{\left[1+\beta_1^2\right]^{1/2}} \int_0^{\pi/2} \frac{d\varphi}{\left[1-\left(\beta_1^2/\left(1+\beta_1^2\right)\right)\sin^2 \varphi\right]^{1/2}} \\ &= \frac{1}{\left[1+\beta_1^2\right]^{1/2}} K\left(\beta_1^2/\left(1+\beta_1^2\right)\right) \end{aligned} \tag{11.2}$$

$$\begin{aligned} I_2 &= \int_0^{\pi/2} \frac{\cos^2 \varphi d\varphi}{\left[1+\beta_1^2 \sin^2 \varphi\right]^{1/2}} = \int_0^{\pi/2} \frac{\cos^2 \varphi d\varphi}{\left[1+\beta_1^2 (1-\cos^2 \varphi)\right]^{1/2}} \\ &= \frac{1}{\left[1+\beta_1^2\right]^{1/2}} \int_0^{\pi/2} \frac{\cos^2 \varphi d\varphi}{\left[1-\left(\beta_1^2/\left(1+\beta_1^2\right)\right)\cos^2 \varphi\right]^{1/2}} \\ &= \frac{1}{\left[1+\beta_1^2\right]^{1/2}} \int_0^{\pi/2} \frac{\sin^2 \varphi d\varphi}{\left[1-\left(\beta_1^2/\left(1+\beta_1^2\right)\right)\sin^2 \varphi\right]^{1/2}} \\ &= \frac{1}{\left[1+\beta_1^2\right]^{1/2}} \int_0^{\pi/2} \frac{\left(1+\beta_1^{-2}\right) d\varphi}{\left[1-\left(\beta_1^2/\left(1+\beta_1^2\right)\right)\sin^2 \varphi\right]^{1/2}} \end{aligned}$$

$$
\begin{aligned}
&-\frac{1}{\left[1+\beta_1^2\right]^{1/2}}\int_0^{\pi/2}\frac{\left(1+\beta_1^{-2}-\sin^2\varphi\right)d\varphi}{\left[1-\left(\beta_1^2/\left(1+\beta_1^2\right)\right)\sin^2\varphi\right]^{1/2}}\\
&=\frac{\left[1+\beta_1^2\right]^{1/2}}{\beta_1^2}\int_0^{\pi/2}\frac{d\varphi}{\left[1-\left(\beta_1^2/\left(1+\beta_1^2\right)\right)\sin^2\varphi\right]^{1/2}}\\
&\quad-\frac{\left[1+\beta_1^2\right]^{1/2}}{\beta_1^2}\int_0^{\pi/2}\left[1-\left(\beta_1^2/\left(1+\beta_1^2\right)\right)\sin^2\varphi\right]^{1/2}d\varphi\\
&=\frac{\left[1+\beta_1^2\right]^{1/2}}{\beta_1^2}\left[K\left(\beta_1^2/\left(1+\beta_1^2\right)\right)-E\left(\beta^2{}_1/\left(1+\beta_1^2\right)\right)\right]
\end{aligned}
\tag{11.3}
$$

where $K(\ )$ and $E(\ )$ stand respectively for the widely known complete elliptic integrals of first and second kind.

I_α, for $\alpha \geq 4$, can be obtained by means of a recurrent relation. Starting from

$$
I_\alpha=\int_0^{\pi/2}\frac{\cos^\alpha\varphi d\varphi}{\left[1+\beta_1^2\sin^2\varphi\right]^{1/2}}=\int_0^{\pi/2}\frac{\cos^\alpha\varphi}{\left[1+\beta_1^2\sin^2\varphi\right]}\left[1+\beta_1^2\sin^2\varphi\right]^{1/2}d\varphi \tag{11.4}
$$

and according to

$$
\frac{\cos^\alpha\varphi}{\left[1+\beta_1^2\sin^2\varphi\right]}=\frac{\cos^\alpha\varphi}{\left[1+\beta_1^2-\beta_1^2\cos^2\varphi\right]}=-\frac{1}{\beta_1^2}\cos^{\alpha-2}\varphi+\frac{\left(1+\beta_1^2\right)}{\beta_1^2}\frac{\cos^{\alpha-2}\varphi}{\left[1+\beta_1^2\sin^2\varphi\right]} \tag{11.5}
$$

I_α becomes

$$
\begin{aligned}
I_\alpha&=-\frac{1}{\beta_1^2}\int_0^{\pi/2}\cos^{\alpha-2}\varphi\left[1+\beta_1^2\sin^2\varphi\right]^{1/2}d\varphi+\frac{\left(1+\beta_1^2\right)}{\beta_1^2}\int_0^{\pi/2}\frac{\cos^{\alpha-2}\varphi d\varphi}{\left[1+\beta_1^2\sin^2\varphi\right]^{1/2}}\\
&=-\frac{1}{\beta_1^2}R_{\alpha-2}+\frac{\left(1+\beta_1^2\right)}{\beta_1^2}I_{\alpha-2}
\end{aligned}
\tag{11.6}
$$

Still another definition

$$
F_\alpha(\varphi)=\int_0^\varphi\cos^\alpha\eta d\eta \tag{11.7}
$$

and the integration

$$R_\alpha = \int_0^{\pi/2} \cos^\alpha \varphi \left[1+\beta_1^2 \sin^2\varphi\right]^{1/2} d\varphi$$
$$= \left[1+\beta_1^2 \sin^2\varphi\right]^{1/2} F_\alpha(\varphi)\Big|_0^{\pi/2} - \int_0^{\pi/2} \frac{\beta_1^2 \sin\varphi\cos\varphi F_\alpha(\varphi)}{\left[1+\beta_1^2\sin^2\varphi\right]^{1/2}} d\varphi \tag{11.8}$$

let (11.6) expressible as

$$I_\alpha = -\frac{1}{\beta_1^2}\left[\left[1+\beta_1^2\right]^{1/2} F_{\alpha-2}(\pi/2) - \int_0^{\pi/2} \frac{\beta_1^2 \sin\varphi\cos\varphi F_{\alpha-2}(\varphi)}{\left[1+\beta_1^2\sin^2\varphi\right]^{1/2}} d\varphi\right] + \frac{\left(1+\beta_1^2\right)}{\beta_1^2} I_{\alpha-2} \tag{11.9}$$

Analogously, by replacing in (11.9) α by $\alpha-2$, one has

$$I_{\alpha-2} = -\frac{1}{\beta_1^2}\left[\left[1+\beta_1^2\right]^{1/2} F_{\alpha-4}(\pi/2) - \int_0^{\pi/2} \frac{\beta_1^2 \sin\varphi\cos\varphi F_{\alpha-4}(\varphi)}{\left[1+\beta_1^2\sin^2\varphi\right]^{1/2}} d\varphi\right] + \frac{\left(1+\beta_1^2\right)}{\beta_1^2} I_{\alpha-4} \tag{11.10}$$

The subtraction of $((\alpha-3)/(\alpha-2))I_{\alpha-2}$ to I_α entitles to

$$I_\alpha - \left(\frac{\alpha-3}{\alpha-2}\right) I_{\alpha-2} = -\frac{\left[1+\beta_1^2\right]^{1/2}}{\beta_1^2}\left(F_{\alpha-2}(\pi/2) - ((\alpha-3)/(\alpha-2))F_{\alpha-4}(\pi/2)\right)$$
$$+ \int_0^{\pi/2} \frac{\sin\varphi\cos\varphi\left(F_{\alpha-2}(\varphi) - ((\alpha-3)/(\alpha-2))F_{\alpha-4}(\varphi)\right)}{\left[1+\beta_1^2\sin^2\varphi\right]^{1/2}} d\varphi \tag{11.11}$$
$$+ \frac{\left(1+\beta_1^2\right)}{\beta_1^2}\left[I_{\alpha-2} - \left(\frac{\alpha-3}{\alpha-2}\right) I_{\alpha-4}\right]$$

Furthermore, taking into consideration that α is always even for this formulation, $F_\alpha(\varphi)$ can be set as

$$F_\alpha(\varphi) = \int_0^\varphi \cos^\alpha \eta d\eta = \frac{\cos^{\alpha-1}\eta \sin\eta}{\pi}\Big|_0^\varphi + \frac{\alpha-1}{\alpha}\int_0^\varphi \cos^{\alpha-2}\eta d\eta$$
$$= \frac{\cos^{\alpha-1}\eta\sin\eta}{\alpha}\Big|_0^\varphi + \frac{\alpha-1}{\alpha} F_{\alpha-2}(\varphi) \tag{11.12}$$

and particularly for $\varphi = \pi/2$,

$$F_\alpha(\pi/2) = \frac{\alpha-1}{\alpha} F_{\alpha-2}(\pi/2) \tag{11.13}$$

Back in (11.11) and allowing for (11.12) and (11.13),

$$I_\alpha - \left(\frac{\alpha-3}{\alpha-2}\right)I_{\alpha-2} = \frac{1}{\alpha-2}\int_0^{\pi/2}\frac{\cos^{\alpha-2}\varphi\sin^2\varphi}{\left[1+\beta_1^2\sin^2\varphi\right]^{1/2}}d\varphi + \frac{\left(1+\beta_1^2\right)}{\beta_1^2}\left[I_{\alpha-2} - \left(\frac{\alpha-3}{\alpha-2}\right)I_{\alpha-4}\right]$$

$$= \frac{1}{\alpha-2}\int_0^{\pi/2}\frac{\cos^{\alpha-2}\varphi - \cos^{\alpha}\varphi}{\left[1+\beta_1^2\sin^2\varphi\right]^{1/2}}d\varphi + \frac{\left(1+\beta_1^2\right)}{\beta_1^2}\left[I_{\alpha-2} - \left(\frac{\alpha-3}{\alpha-2}\right)I_{\alpha-4}\right] \tag{11.14}$$

$$= \frac{1}{\alpha-2}\left[I_{\alpha-2} - I_\alpha\right] + \frac{\left(1+\beta_1^2\right)}{\beta_1^2}\left[I_{\alpha-2} - \left(\frac{\alpha-3}{\alpha-2}\right)I_{\alpha-4}\right]$$

Finally,

$$I_\alpha = \left(\frac{\alpha-2}{\alpha-1}\right)\left(\beta_1^{-2}+2\right)I_{\alpha-2} - \left(\beta_1^{-2}+1\right)\left(\frac{\alpha-3}{\alpha-1}\right)I_{\alpha-4} \tag{11.15}$$

which is a recurrent relation for the integration along $\xi = \phi - \phi'$ $\forall\alpha \geq 4$.

APPENDIX B

The elementary integrals N_α stand for

$$N_{\alpha(k,m)} = \int_0^{\pi/2}\frac{\cos^{\alpha}\varphi}{\left[1+\beta_1^2\sin^2\varphi\right]^{3/2}}d\varphi \tag{11.16}$$

The starting expressions for the recurrent formula are [1]

$$N_0 = \int_0^{\pi/2}\frac{1}{\left[1+\beta_1^2\sin^2\varphi\right]^{3/2}}d\varphi$$

$$= \frac{1}{\left(1+\beta_1^2\right)^{3/2}}\int_0^{\pi/2}\frac{1}{\left[1-\beta_1^2/(1+\beta_1^2)\cos^2\varphi\right]^{3/2}}d\varphi$$

$$= \frac{1}{\left(1+\beta_1^2\right)^{3/2}}\int_0^{\pi/2}\frac{1}{\left[1-\beta_1^2/(1+\beta_1^2)\sin^2\varphi\right]^{3/2}}d\varphi$$

$$= \frac{\left(1+\beta_1^2\right)}{\left(1+\beta_1^2\right)^{3/2}}E(\beta_1^2/(1+\beta_1^2)) = \frac{1}{\left(1+\beta_1^2\right)^{1/2}}E(\beta_1^2/(1+\beta_1^2)) \tag{11.17}$$

and

$$N_2 = \int_0^{\pi/2}\frac{\cos^2\varphi d\varphi}{\left[1+\beta_1^2\sin^2\varphi\right]^{3/2}} = \int_0^{\pi/2}\frac{\cos^2\varphi}{\left[1+\beta_1^2-\beta_1^2\cos^2\varphi\right]^{1/2}\left[1+\beta_1^2\sin^2\varphi\right]^{1/2}}d\varphi$$

$$= \int_0^{\pi/2}\frac{1}{\left[1-\beta_1^2/(1+\beta_1^2)\cos^2\varphi\right]^{3/2}}d\varphi$$

$$
\begin{aligned}
&= \int_0^{\pi/2} \left[-\frac{1}{\beta_1^2} + \frac{(1+\beta_1^2)}{\beta_1^2} \frac{1}{\left[1+\beta_1^2 \sin^2\varphi\right]} \right] \frac{1}{\left[1+\beta_1^2 \sin^2\varphi\right]^{1/2}} d\varphi \\
&= -\frac{1}{\beta_1^2} \int_0^{\pi/2} \frac{d\varphi}{\left[1+\beta_1^2 \sin^2\varphi\right]^{1/2}} + \frac{(1+\beta_1^2)}{\beta_1^2} \int_0^{\pi/2} \frac{d\varphi}{\left[1+\beta_1^2 \sin^2\varphi\right]^{3/2}} \\
&= -\frac{1}{\beta_1^2 (1+\beta_1^2)^{1/2}} K\left(\beta_1^2/(1+\beta_1^2)\right) + \frac{(1+\beta_1^2)^{1/2}}{\beta_1^2} E\left(\beta_1^2/(1+\beta_1^2)\right)
\end{aligned} \tag{11.18}
$$

where $K(\ )$ and $E(\ )$ are respectively the widely known complete elliptic integrals of first and second kind.

N_α, for $\alpha \geq 4$, can be obtained by means of a recurrent relation. Starting from

$$
N_\alpha = \int_0^{\pi/2} \frac{\cos^\alpha \varphi d\varphi}{\left[1+\beta_1^2 \sin^2\varphi\right]^{3/2}} = \int_0^{\pi/2} \frac{\cos^\alpha \varphi}{\left[1+\beta_1^2 \sin^2\varphi\right]} \frac{1}{\left[1+\beta_1^2 \sin^2\varphi\right]^{1/2}} d\varphi \tag{11.19}
$$

and according to

$$
\frac{\cos^\alpha \varphi}{\left[1+\beta_1^2 \sin^2\varphi\right]} = \frac{\cos^\alpha \varphi}{\left[1+\beta_1^2 - \beta_1^2 \cos^2\varphi\right]} = -\frac{1}{\beta_1^2} \cos^{\alpha-2}\varphi + \frac{(1+\beta_1^2)}{\beta_1^2} \frac{\cos^{\alpha-2}\varphi}{\left[1+\beta_1^2 \sin^2\varphi\right]} \tag{11.20}
$$

N_α becomes

$$
\begin{aligned}
N_\alpha &= -\frac{1}{\beta_1^2} \int_0^{\pi/2} \frac{\cos^{\alpha-2}\varphi}{\left[1+\beta_1^2 \sin^2\varphi\right]^{1/2}} d\varphi + \frac{(1+\beta_1^2)}{\beta_1^2} \int_0^{\pi/2} \frac{\cos^{\alpha-2}\varphi d\varphi}{\left[1+\beta_1^2 \sin^2\varphi\right]^{3/2}} \\
&= -\frac{1}{\beta_1^2} S_{\alpha-2} + \frac{(1+\beta_1^2)}{\beta_1^2} N_{\alpha-2}
\end{aligned} \tag{11.21}
$$

By resorting to $F_\alpha(\varphi)$ in (11.7) along with the partial integration

$$
\begin{aligned}
S_\alpha &= \int_0^{\pi/2} \frac{\cos^\alpha \varphi}{\left[1+\beta_1^2 \sin^2\varphi\right]^{1/2}} d\varphi \\
&= \frac{F_\alpha(\varphi)}{\left[1+\beta_1^2 \sin^2\varphi\right]^{1/2}} \Bigg|_0^{\pi/2} + \int_0^{\pi/2} \frac{\beta_1^2 \sin\varphi \cos\varphi F_\alpha(\varphi)}{\left[1+\beta_1^2 \sin^2\varphi\right]^{3/2}} d\varphi
\end{aligned} \tag{11.22}
$$

allow (11.21) to be expressible as

$$
N_\alpha = -\frac{1}{\beta_1^2} \left[\frac{F_{\alpha-2}(\pi/2)}{\left[1+\beta_1^2\right]^{1/2}} + \int_0^{\pi/2} \frac{\beta_1^2 \sin\varphi \cos\varphi F_{\alpha-2}(\varphi)}{\left[1+\beta_1^2 \sin^2\varphi\right]^{1/2}} d\varphi \right] + \frac{(1+\beta_1^2)}{\beta_1^2} N_{\alpha-2} \tag{11.23}
$$

Analogously, by substituting α by $\alpha - 2$ in (11.23), one has

$$N_{\alpha-2}=-\frac{1}{\beta_1^2}\left[\frac{F_{\alpha-4}(\pi/2)}{\left[1+\beta_1^2\right]^{1/2}}+\int_0^{\pi/2}\frac{\beta_1^2\sin\varphi\cos\varphi F_{\alpha-4}(\varphi)}{\left[1+\beta_1^2\sin^2\varphi\right]^{1/2}}d\varphi\right]+\frac{\left(1+\beta_1^2\right)}{\beta_1^2}N_{\alpha-4} \tag{11.24}$$

The subtraction of $((\alpha-3)/(\alpha-2))N_{\alpha-2}$ to N_α entitles to

$$\begin{aligned}N_\alpha-\left(\frac{\alpha-3}{\alpha-2}\right)N_{\alpha-2}=&-\frac{1}{\beta_1^2\left[1+\beta_1^2\right]^{1/2}}(F_{\alpha-2}(\pi/2)-((\alpha-3)/(\alpha-2))F_{\alpha-4}(\pi/2))\\&-\int_0^{\pi/2}\frac{\sin\varphi\cos\varphi(F_{\alpha-2}(\varphi)-((\alpha-3)/(\alpha-2))F_{\alpha-4}(\varphi))}{\left[1+\beta_1^2\sin^2\varphi\right]^{1/2}}d\varphi\\&+\frac{\left(1+\beta_1^2\right)}{\beta_1^2}\left[N_{\alpha-2}-\left(\frac{\alpha-3}{\alpha-2}\right)N_{\alpha-4}\right]\end{aligned} \tag{11.25}$$

which, in accordance with the equalities in (11.12) and (11.13), yields

$$\begin{aligned}N_\alpha-\left(\frac{\alpha-3}{\alpha-2}\right)N_{\alpha-2}&=\frac{1}{\alpha-2}\int_0^{\pi/2}\frac{\cos^{\alpha-2}\varphi\sin^2\varphi}{\left[1+\beta_1^2\sin^2\varphi\right]^{3/2}}d\varphi+\frac{\left(1+\beta_1^2\right)}{\beta_1^2}\left[N_{\alpha-2}-\left(\frac{\alpha-3}{\alpha-2}\right)N_{\alpha-4}\right]\\&=-\frac{1}{\alpha-2}\int_0^{\pi/2}\frac{\cos^{\alpha-2}\varphi-\cos^{\alpha}\varphi}{\left[1+\beta_1^2\sin^2\varphi\right]^{3/2}}d\varphi+\frac{\left(1+\beta_1^2\right)}{\beta_1^2}\left[N_{\alpha-2}-\left(\frac{\alpha-3}{\alpha-2}\right)N_{\alpha-4}\right]\\&=-\frac{1}{\alpha-2}\left[N_{\alpha-2}-N_\alpha\right]+\frac{\left(1+\beta_1^2\right)}{\beta_1^2}\left[N_{\alpha-2}-\left(\frac{\alpha-3}{\alpha-2}\right)N_{\alpha-4}\right]\end{aligned} \tag{11.26}$$

Finally,

$$N_\alpha=\left(\frac{\alpha-2}{\alpha-3}\right)\left(\frac{\alpha-4}{\alpha-2}+\beta_1^{-2}+1\right)N_{\alpha-2}-\left(\beta_1^{-2}+1\right)N_{\alpha-4} \tag{11.27}$$

which is a recurrent relation for the analytical integration along $\xi=\phi-\phi'\ \forall\alpha\geq 4$.

BIBLIOGRAPHY

[1] M. Abramowitz and I. A. Stegun, "Handbook of Mathematical Functions", Dover Publications, New York.

[2] C. A. Balanis, "Antenna Theory, Analysis and Design", Harper & Row, New York.

[3] R. F. Harrington, "Field Computations by Moment Methods", MacMillan, New York, 1968.

[4] Morita, N. Kumagai, J. R. Mautz, "Integral Equation Methods for Electromagnetics", Artech House, 1990.

[5] Ángel Cardama Aznar, Lluís Jofre Roca, Juan Manuel Rius Casals, Jordi Romeu Robert, Sebastián Blanch Boris, "Antenes", Edicions UPC, Barcelona, 1998

[6] Nuria Duffo Úbeda, "Análisis de problemas electromagnéticos mediante elementos de contorno", Dissertation Thesis, Universitat Politècnica de Catalunya, december 1995

[7] A. J. Poggio and E. K. Miller, "Integral equation solutions of three dimensional scattering problems", *Computer Tecniques for Electromagnetics,* Oxford. U.K.: Pergamon, 1973, Chap. 4.

[8] Y. Chang and R. F. Harrington, "A surface formulation for characteristic modes of material bodies", *IEEE Transactions on Antennas and Propagation*, vol. AP-25, pp. 789-795

[9] D. R. Wilton, S. M. Rao, A. W. Glisson, D. H. Schaubert, O. M. Al-Bundak and C. M. Butler, "Potential Integrals for Uniform and Linear Source Distributions on Polygonal and Polyhedral Domains", *IEEE Transactions on Antennas and Propagation*, vol. AP-32, No. 3, pp. 276-281, March 1984.

[10] D. A. Dunavant, "High Degree efficient symmetrical gaussian quadrature rules for the triangle", *International Journal for Numerical Methods in Engineering,* vol. 21, pp. 1129-1148, 1985.

[11] R. E. Hodges and Y. Rahmat-Samii, "The evaluation of MFIE integrals with the use of vector triangle basis functions", *Microwave and Optical Technology letters,* vol. 14, No. 1, pp. 9-14, January 1997.

[12] S. D. Gedney and R. Mittra, "The Use of the FFT for the Efficient Solution of the Problem of Electromagnetic Scattering by a Body of Revolution", *IEEE Transactions on Antennas and Propagation,* vol. 38, No. 5, pp. 313-322, March 1990.

[13] A. W. Glisson and D. R. Wilton, "Simple and Efficient Numerical Methods for Problems of Electromagnetic Radiation and Scattering from Surfaces", *IEEE Transactions on Antennas and Propagation,* vol. AP-28, No. 5, pp. 593-603, September 1980.

[14] B. M. Kolundzija, B. D. Popovic, "Entire-domain Galerkin method for analysis of metallic antennas and scatterers", *IEE Proceedings-H,* vol. 140, No. 1, February 1993.

[15] T. K. Sarkar, S. M. Rao and A. R. Djordjevic, "Electromagnetic Scattering and Radiation from Finite Microstrip Structures", *IEEE Transactions on Microwave Theory and Techniques,* vol. 38, No. 11, pp. 1568-1575, November 1990.

[16] T. K. Sarkar, E. R. Arvas and S. Ponnapalli, "Electromagnetic Scattering from Dielectric Bodies", *IEEE Transactions on Antennas and Propagation,* vol. 37, No. 5, pp. 673-676, May 1989.

[17] A. A. Kishk and L. Shafai, "Different Formulations for Numerical Solution of Single or Multibodies of Revolution with Mixed Boundary Conditions", *IEEE Transactions on Antennas and Propagation,* vol. AP-34, No. 5, pp. 666-673, May 1986.

[18] J. R. Mautz and R. F. Harrington, "Radiation and scattering from Bodies of revolution", *Applied Science Research,* vol. 20, pp. 405-435, June 1969.

[19] L. N. Medgyesi-Mitschang and C. Eftimiu, "Scattering from Axisymmetric Obstacles Embedded in Axisymmetric Dielectrics: The Method of Moments Solution", *Applied Physics,* 19, pp. 275-285, February 1979.

[20] L. N. Medgyesi-Mitchsang and J. Putnam, "Electromagnetic Scattering from Axially Inhomogeneous Bodies of Revolution", *IEEE Transactions on Antennas and Propagation,* vol. AP-32, No. 8, pp. 797-806, August 1984.

[21] S. Ström and W. Zheng, "The Null field Approach to Electromagnetic Scattering from Composite Objects", *IEEE Transactions on Antennas and Propagation,* vol. 36, No. 3, pp.376-382, March 1988.

[22] M. S. Ingber and R. H. Ott, "An Application of the Boundary Element Method to the Magnetic Field Integral Equation", *IEEE Transactions on Antennas and Propagation,* vol. 39, No. 5, pp. 606-611, May 1991.

[23] T. K. Sarkar and E. R. Arvas, "Scattering Cross Section of Composite Conducting and Lossy Dielectric Bodies", *Proceedings of the IEEE,* vol. 77, No. 5, pp. 788-795, May 1989.

[24] P. Barber and C. Yeh, "Scattering of electromagnetic waves by arbitrarily shaped dielectric bodies", *Applied Optics,* vol. 14, No. 12, pp. 1864-2872, December 1975.

[25] K. Umashankar, A. Taflove and S. M. Rao, "Electromagnetic Scattering by Arbitrary Shaped Three-Dimensional Homogeneous Lossy Dielectric Objects", *IEEE Transactions on Antennas and Propagation,* vol. AP-34, No. 6, pp. 758-766, June 1986.

[26] T. K. Sarkar and E. Arvas, "An Integral Equation Approach to the Analysis of Finite Microstrip Antennas: Volume/Surface Formulation", *IEEE Transactions on Antennas and Propagation,* vol. 38, No. 3, pp. 305-312, March 1990.

[27] P. A. Raviart and J. M. Thomas, "A mixed finite element method for 2^{nd} order elliptic problems", in *Mathematical Aspects of Finite Elements Methods*, A. Dold and B. Eckmann, Eds. New York: Springer-Verlag, 1977.

[28] S. M. Rao, D. R. Wilton and A. W. Glisson, "Electromagnetic Scattering by surfaces of Arbitrary Shape", *IEEE Transactions on Antennas and Propagation,* vol. AP-30, No. 3, pp. 409-418, May 1982.

[29] D. H. Schaubert, D. R. Wilton, and W. Glisson, "A tetrahedral modeling method for electromagnetic scattering by arbitrarily shaped inhomogeneous dielectric bodies", *IEEE Transactions on Antennas and Propagation,* vol. AP-32, pp. 77-85, January 1984.

[30] S. M. Rao, T. K. Sarkar, P. Midya and A. R. Djordevic, "Electromagnetic Radiation and Scattering from Finite Conducting and Dielectric Structures: Surface/Surface Formulation", *IEEE Transactions on Antennas and Propagation,* vol. 39, No. 7, July 1991.

[31] Te-Kao Wu and L. L. Tsai, "Scattering form arbitrarily-shaped lossy dielectric bodies of revolution", *Radio Science,* vol. 12, No. 5, pp. 709-718, September-October 1977.

[32] J. C. Nedelec, "Mixed finite elements in R^3", *Numer. Mathem.,* vol.35, pp. 315-341, 1980.

[33] R. D. Graglia, D. R. Wilton and A. F. Peterson, "Higher Order Interpolatory Vector Bases for Computational Electromagnetics", *IEEE Transactions on Antennas and Propagation,* vol. 45, No. 3, pp. 329-342, March 1997.

[34] L. S. Andersen and J. L.Volakis, "Development and Application of a Novel Class of Hierarchical Tangential Vector Finite Elements for Electromagnetics", *IEEE Transactions on Antennas and Propagation,* vol. 47, No.1, pp.112-120, January 1999.

[35] M. L. Barton and Z. J. Cendes, "New vector Finite Elements for three-dimensional Magnetic Field Computation", *Journal on Applied Physics,* vol. 61, No. 8, pp. 3919-3921, April 1987.

[36] J. J. H. Wang, "Generalised moment methods in electromagnetics", *IEE Proceedings,* vol. 137, Pt. H, No. 2, pp. 127-132, April 1990.

[37] T. K. Sarkar, "A Note on the Choice of Weighting functions in the Method of Moments", *IEE Transactions on Antennas and Propagation,* vol. Ap-33, No. 4, pp. 436-441, April 1985.

[38] T. K. Sarkar, A. R. Djordjevic and E. Arvas, "On the Choice of Expansion and Weighting Functions in the Numerical Solution of Operator Equations", *IEEE transactions on Antennas and Propagation,* vol. AP-33, No. 9, pp. 988-996, September 1985.

[39] J. H. Richmond, "On the Variational Aspects of the Moment Method", *IEEE Transactions on Antennas and Propagation,* vol. 39, No. 4, pp. 473-479, April 1991.

[40] S. Wandzura, "Optimality of Galerkin Method for Scattering Computations", *Microwave and Optical Technology letters*, vol. , No. 5, pp. 199-200, April 1991.

[41] A. F. Peterson, D. R. Wilton and R. E. Jorgenson, "Variational Nature of Galerkin and Non-Galerkin Moment Method Solutions", *IEEE Transactions on Atnennas and Propagation,* vol. 44, No. 4, pp. 500-503, April 1996.

[42] A. Bossavit and J.C. Vérité, "A mixed FEM-BIEM method to solve 3D eddy curent problems", *IEEE Trans. Magn.*, vol. MAG-18, pp. 431-435, March 1982.

[43] M.Hano, "Finite-element analysis of dielectric-loaded waveguides", *IEEE Trans. Microwave Theory Tech.*, vol. MTT-32, pp. 1275-1279, October 1984.

[44] X. Q. Sheng, J. Jin, J. Song W. C. Chew and C. Lew, "Solution of Combined-Field Integral Equation Using Multilevel Fast Multipole Algorithm for Scattering by homogeneous Bodies", *IEEE transactions on Antennas and Propagation,* vol. 46, No. 11, pp. 1718-1726, November 1998.

[45] R. Coiffman, V. Rokhlin and S. Wandzura, "The Fast Multipole Method for the Wave Equation: A Pedestrian Prescription", *IEEE Antennas and Propagation Magazine,* vol. 35, No. 3, pp. 7-12, June 1993.

[46] J. Song, C. Lu and W. C. Chew, "Multilevel Fast Multipole Algorithm for Electromagnetic Scattering by Large Complex Objects", *IEEE Transactions on Antennas and Propagation,* vol. 45, No. 10, pp. 1488-1493, October 1997.

[47] W. C. Chew, J. Jin C. Lu, E. Michielssen and J. M. Song, "Fast Solutions Methods in Electromagnetics", *IEEE Transactions on Antennas and Propagation,* vol. 45, No. 3, pp. 533-543, March 1997.

[48] C. Lu and W. C. Chew, "A Multilevel Algorithm for Solving a Boundary Integral Equation of Wave Scattering", *Microwave and Optical Technology Letters,* vol. 7, No. 10, pp. 466-470, July 1994.

[49] J. M. song and W. C. Chew, "Multilevel Fast-Multipole Algorithm for solving Combined Field Integral Equations of Electromagnetic Scattering", *Microwave and Optical Technology Letters,* vol. 10, No. 1, pp. 14-19, September 1995

[50] S. Wandzura, "Electric Current Basis functions for Curved Surfaces", *Electromagnetics*, vol. 12, pp.77-91, 1992

[51] Kenneth K. Mei, Rafael Pous, Zhaoqing Chen, Yao-Wu Liu and Mark D. Prouty, "Measured Equation of Invariance: A New concept in Field Computations", *IEEE Transactions on Antennas and Propagation*, vol. 46, No. 11, pp.1718-1726, March 1994.

[52] J. M. Rius, R. Pous, A. Cardama, "Integral Formulation of the Measured Equation of Invariance: A Novel Sparse Matrix Boundary Element Method", *IEEE Trans. on Magn.* , vol. 32, No. 3, pp. 962-967, May 1996.

[53] J. M. Rius, J. Parrón, E. Úbeda, J. R. Mosig, "The integral Equation MEI applied on three-dimensional arbitrary surfaces", *IEE Electronic Letters,* vol. 33, No. 24, pp. 2029-2031, November 1997.